University of Venda
Creating Future Leaders

ANALYSIS OF THE SOLAR RADIATION DATA AND THE DETERMINATION OF REGRESSION COEFFICIENTS FOR VHEMBE REGION, LIMPOPO PROVINCE

A Dissertation Submitted to the Department of Physics

For the fulfilment of a M.Sc Degree

By

MULAUDZI TSHIMANGADZO SOPHIE

STUDENT NUMBER: 11553991

In the School of Mathematical and Natural Sciences,

University of Venda,

THOHOYANDOU, LIMPOPO PROVINCE

Supervisor : Prof. V. Sankaran, UNIVEN

Co-supervisor : Dr. M. D. Lysko, CSIR

MARCH 2011

DECLARATION

I, TSHIMANGADZO SOPHIE MULAUDZI, hereby declare that the dissertation for the M.Sc. degree at University of Venda hereby submitted by me has not previously been submitted for a degree at this or any other university and that is my own work in design and execution and all the reference materials contained therein has been duly acknowledged.

Signature: .... Date: 01/08/2011

ACKNOWLEDGEMENT

I would like to express my deep sense of gratitude to my supervisor, Prof. V. Sankaran (University of Venda) for his guidance from the start to the completion of this work. He has always been providing positive criticisms, support and words of encouragement.

I wish to thank Dr. M.D. Lysko (DPSS unit, CSIR) for her role as the co-supervisor. She has always been giving the entire support and guidance throughout the course of this study. Her expertise has assisted me to learn a lot of information about solar radiation and measurements.

I also wish to thank:

(i) The Defence, Peace, Safety and Security (DPSS) unit, CSIR, for allowing me to use their facilities as well as the support to obtain hands-on training which I received at Deutscher Wetterdienste Observatorium (DWD) in Germany, for indoor calibration of diffuse direct solar radiometer (D2SR).

(ii) NRF that has contributed financially through the bilateral agreement of CSIR and DWD.

(iii) DWD (Germany) for hosting us during the indoor calibration of D2SR. A special thanks to the staff, who constantly helped us during the entire process of calibration.

(iv) University of Venda (UNIVEN), for the financial support given to me in order to attend the eleventh International Pyrheliometer Comparison (IPC-xi) held at Davos, Switzerland – where I gained knowledge of calibration of radiometer using reference radiometer.

(v) The Agricultural Research Council (ARC) for providing the meteorological parameter data for the north eastern region of South Africa.

(vi) The South African Weather Services (SAWS) for supplying the actual sunshine data closest to the ARC sites in this study.

(vii) Mr K Sankaran for assisting me to develop the programme for the computation of solar radiation parameters in this study.

(viii) Dr Kirui, HOD, Department of Physics at UNIVEN and all staff members for their assistance and constant support during my research study.

(ix) The support, understanding and encouragement that I received constantly from my husband, my children and friends.

Above all, I thank God, who through His grace, made it possible for me to continue tirelessly with this work up to the end.

I wish to add that if there are any inadvertent errors or omissions in the printed text, I accept the full responsibility.

ABSTRACT

An attempt has been made to determine the regression coefficients from sunshine hours for the Vhembe Region, Limpopo Province. Parameters such as horizontal average daily extraterrestrial solar radiation (H_o) and daily possible sunshine hours (N) were computed. Horizontal average daily global radiation data and daily actual sunshine hour data for the five stations in this study were obtained from Agricultural Research Council (ARC) and South African Weather Services (SAWS).

The plots of monthly average daily relative sunshine hours ($\frac{N_0}{N}$) versus clearness index ($\frac{H}{H_0}$) were drawn to determine the values of a and b of Angstrom – Prescott linear equation (where N_o and H represent the actual sunshine hours (in hours) and global solar radiation on the horizontal surface (in MJ) respectively. The variables a and b are the regression coefficients. The results obtained are discussed. From the computations, the values of a and b for Vhembe Region are calculated and the results obtained are compared with the regression coefficients for different countries.

The regression coefficients from a station with the best correlation of the coefficients were used to compute the estimated average monthly horizontal global solar radiation for the other four stations and the results compare favourably with our data.

TABLE OF CONTENTS

Chapter 1

Background to the research problem — Page

1.1 Introduction — 1
1.2 Renewable and non renewable energies — 2
1.3 Need for renewable energy — 2
1.4 Energy poverty in South Africa — 4
1.5 Solar Energy — 5
1.6 Advantages and disadvantages of renewable energies — 9
1.7 Summary — 10

Chapter 2

Literature review

2.1 Introduction — 12
2.2 The sun as the source of radiation — 12
2.3 The earth and solar constant — 14
2.4 Spectral distribution of extraterrestrial radiation — 15
2.5 Variation of the horizontal extraterrestrial radiation — 16
2.6 Solar geometry — 18
2.7 Solar time and equation of time — 21
2.8 Solar radiation at the earth's surface — 23
2.9 Solar radiation on an inclined and horizontal surfaces — 27
2.10 Solar radiometers — 30

Chapter 3

Study area in Vhembe Region

3.1 Overview — 35
3.2 Univen's Vuwani site — 39
3.3 Agricultural Research Council sites in the Vhembe Region — 40

Chapter 4

Methodology

4.1	Introduction	46
4.2	Regression models	46
4.3	Computation of solar variables	47

Chapter 5

Data Assimilation

5.1	Introduction	51
5.2	Daily possible sunshine hours (*N*)	51
5.3	Actual sunshine hours, (N_o)	60
5.4	Extraterrestrial solar radiation (H_0) on horizontal surface	62
5.5	Daily global solar radiation (H)	69
5.6	Comparison of global radiation between stations	72

Chapter 6

Regression Coefficients

6.1	Monthly average best fit lines	75
6.2	Thohoyandou Mutale station	75
6.3	Malamulele Mhinga station	78
6.4	Makhado Rabali station	81
6.5	Makhado Mulima station	84
6.6	Makhado Alldays station	88
6.7	Vuwani station – Univen site	91
6.8	Annual regression coefficients	91
6.9	Seasonal trends	92
6.10	Representative regression coefficients for Vhembe Region	93
6.11	Statistical tests	94
6.12	Summary	97

Chapter 7

Calibration of Solar Radiometers

7.1 Introduction 99

7.2 The importance of calibrating measuring instruments. 99

7.3 Terms involved in calibration of radiometers 100

7.4 World radiometric reference (WRR) 101

7.5 Calibration factor 101

7.6 Hierarchy of calibration of pyrheliometers 102

7.7 Absolute cavity pyrheliometer (ahf 31117) 103

7.8 Calibration of AHF31117 pyrheliometer 104

Chapter 8

Summary and Conclusions

8.1 Summary 108

8.2 Conclusions 110

8.3 References 111

CHAPTER 1

BACKGROUND TO THE RESEARCH PROBLEM

1.1 INTRODUCTION

This research is geared towards the collection and analysis of solar radiation data and hence to compute the global solar radiation (H) and extraterrestrial solar radiation (H_0). The daily and monthly average values will be used to compute the values of regression coefficients for the North-Eastern region of the Limpopo province, i.e. Vhembe Region. These values will be compared with the values available in the literature for other countries. In fact, these values will be of great use in the design and installation of solar energy devices in this region.

Global solar radiation is required in many applications due to its essential role. Global solar radiation data helps the manufacturers when designing the solar panels to be installed in a particular area. Architects and engineers need daily global radiation data too.It acts as a driving input to agronomic, ecological, hydrological and soil-vegetation processes. Agriculturists depend on daily global solar radiation for the vegetation they grow. The level of education and literacy in regions within South Africa is low, for example within Limpopo Province. Thus the standard of living is very low. For the survival of their families, the food givers depend on farming such as cattle rearing as well as growing vegetables. Farming needs energy.

The use of energy is probably the most fundamental requirement for the human existence. Renewable fuels and bio-fuels have been widely used by human beings for many centuries. Energy usage has grown more rapidly than the population because of the simultaneously rising standards of living and continuous change to more energy intensive methods of providing that standard of living. According to the world assessment, energy services are indispensable for human survival and development and consequently play a critical role in all development activities [1].

However, the majority of the rural population in South Africa have never had the opportunity to experience a high standard of living since their basic energy needs are not met [2]. There is a dire need to intensify the renewable energy research with specific relevance to rural needs and also to create awareness among the rural communities and science students to fully harness the freely available energy [2]. In the present study an attempt will be made to study the solar radiation data of the Vhembe region. This is of great importance because the fossil fuels are depleting and hence we have to resort to different types of small-scale energy production for the rural communities from the raw materials that are available in the communities.

1.2 RENEWABLE AND NON RENEWABLE ENERGIES

Energy can be classified under two broad categories; they are renewable and non-renewable energy. Energy from sources which replenish as energy is released is termed renewable energy sources and the reverse is the case for non-renewable energy sources. Hydropower, wind-power and solar energies are forms of renewable energy sources, while energy from nuclear reaction and fossil fuel are from non-renewable sources. Exploration and exploitation of non-renewable energy sources has some negative effect on the environment. Pollution and radioactive emission are some of the effects. On the contrary, renewable energy generated from solar radiation, hydropower stations or wind-power stations is clean and environmentally friendly. This is important since air quality has become a serious issue in many countries because it is linked to health [2]. The use of wind as an energy source dates back ages. At one time wind was a major source of energy for transportation (sailing), grinding grains and for pumping water. Other forms of renewable energy like biomass, hydropower and ocean thermal energy have also contributed in meeting energy needs of the society.

1.3 NEED FOR RENEWABLE ENERGY

The recent rapid growth of interest in renewable energy applications may be partly attributed to concern over dwindling supplies of fossil fuels. Considerable amount of research is going on all over the world to make the best use of the freely available renewable energy. It is important to realize that the earth is a system with limited supplies of land, air, water, vegetation and minerals. Because our present energy supplies are both finite and non-renewable, our energy splurge appears to be coming to an end. In fact, it is the energy of sunlight assimilated by biological organisms over millions of years that has made possible the industrial growth. Most of the other renewable means of power generation also depend on the sun as the primary source [3].

Presently, the world is turning to renewable energy sources for responsible energy use, which would be a footstool for sustainable development and a sustainable future [4]. The premise for the search for a sustainable option was predicated by the political events, beginning with the oil crises of 1973 and continuing through the Iranian revolution in 1979. This created awareness on how crucial energy is to the daily functioning of modern society. The energy crises of the 1970s were almost forgotten in the 1980s. However, that decade brought an increased awareness of the environment. Concerns about global warming, acid rain and radioactive fall-out are still with us today a reminder that each of these topics is a consequence of energy use [5].

In 1987, Brunt Land [2] defined sustainable development as "development that meets the needs of the present generation without compromising the ability of the future generation to meet their own needs". Africa needs not be an exception in embracing renewable energy option as a way forward. Presently, African states are encountering various problems ranging from economic, food production, socio-political and above all energy generation. Poverty also runs high in most of these states and the worst hit areas are the rural communities. Here absence of energy carriers and poverty culminate and tackling these problems is of great priority to African policy makers.

Among the three billion people living in rural areas in developing countries today, about two billion neither have access to, nor can afford to pay for modern energy carrier, such as electricity, liquid or gaseous fuel [1]. This will consequently affect the income opportunities and quality of life of these rural people. Population growth is another factor that has defied efforts made to provide these energy carriers; hence access to every service is virtually stable since 1980. The problem is worse-off in sub-Saharan Africa, which hosts thirty of the forty nine least developed countries. Although 800 million people benefited from the rural electrification schemes during 1970-1990, only 20 million gained electricity access in sub-Saharan Africa [1].

1.4 ENERGY POVERTY IN SOUTH AFRICA

Access to electricity and other modern energy sources are necessities, though not a sufficient requirement for economic and social development. Poverty alleviation among other factors like clean water, adequate sanitation, effective health service, good educational system and culminating all these, an inexpensive and available energy is indispensable.

Poverty is generally characterized by the inability of individual households or an entire community to command sufficient resources to satisfy a socially acceptable minimum standard of living [6]. It is necessary to consider whether poverty is a residual problem of uneven development or rational problem arising from structural characteristics of the society and the relationships they give rise to [7]. The understanding of trends of poverty is important since it deeply influences the design of policies and other interventions to address the problem like access to energy carriers. As observed in Table 1.1, poverty rate in rural areas is very high. Renewable energy can address this problem by reducing the need of monthly payments of electricity bills through installation of solar panels and solar water heaters.

	Population share in %	Poverty share in %	Poverty rate in %
Rural	50.4	71.6	70.9
Urban	49.6	28.4	28.9
All	100	100	40.9

Table 1.1: The distribution of poor individuals by rural/urban classification in South Africa. [11].

In 1995, a survey made based on a pre-adult equivalent line of payment of R352 per month, estimated that 61% of Africans, 38% of Coloreds, 5% of Indians and 1% of Whites were poor in South Africa [8]. Another dimension to these estimates is the geographical distribution of poverty based on the same data set 72% of all poor people live in the rural areas and 71% of all rural people were poor [9]. Kwazulu-Natal, Limpopo and Eastern Cape, the most populous former homelands, record the highest figures of the rural poor [10].

The energy poor could be referred to the population that cannot afford the basic standard energy carrier, such as electricity, kerosene, LPG etc. In South Africa, the dominant feature of poor households is a tendency to use multiple energy sources to meet their energy need. This behavioural pattern is linked to inaccessibility to modern energy forms, which offer little opportunities for making improvements in their economic well being. Efforts so far made in the power industry toward providing power to rural communities seem inadequate and would require new peak capacity in 2006 since about 30% of households have no access to electricity [11].

Solar energy technology implementation in rural areas could be the sustainable energy source in this regard considering its diverse application. Furthermore, the availability of solar radiation, affordability of the technology in medium to long term and the applicable cultural preference will put solar energy technology development at the centre stage of sustainable energy provision for indigent rural communities and could chart a new course for poverty alleviation.

1.5 SOLAR ENERGY

Solar energy harnessed with appropriate technologies could provide the much-needed sustainable development largely due to its diverse application and environmental benefits. In the USA, Cohen [5] found that solar energy is being utilized by businesses every day. Research revealed that businesses could save 40-80% on electricity or fuel bills by replacing conventional water heater systems with solar water heaters. Also at the summer Olympics games in Atlanta, a solar heating system were used to maintain the temperature of the swimming pool [5].

For the protection of life and the environment, Wal-Mart stores in California integrated photovoltaic systems into its operation and will be able to reduce atmospheric pollution that causes smog by three tons and global warming by seven hundred and twenty tons and will save four hundred and twenty tons of coal, one thousand three hundred barrel of oil [5]. In South Korea, the twenty four storey Jae office building in Seoul met over eighty five percent of its daily hot water needs with a solar hot water system. Installed in 1984, the efficiency of the system has exceeded its design specification and provides ten to twenty percent of the annual space heating [5].

Because of the growing demand for energy, combined with the depletion of fossil resources, global warming and its associated climate change, there is an urgent need for environmentally sustainable energy technologies. Among all the renewable energy technologies, such as wind turbine, hydropower, wave and tidal power, solar cells, solar thermal, biomass-derived liquid fuels and biomass-fired electricity generation, photovoltaic technology utilizing solar energy is considered as the most promising one. Fortunately the supply of energy from the Sun to the Earth is gigantic, which is in the order of 3 x10^{24} J / year [3, 12].

South Africa's supply of energy mainly depends on water and coal for electricity. Several interests have motivated the development of alternative energy sources, including those related to economical and political questions, as well as those related to health and environmental concerns e.g. for decreasing air pollution and carbon dioxide emission [2,12]. In view of such concerns, solar energy can be considered the most important energy source. The great demand for petrochemical energy has also led to the development of alternative power sources, such as solar cells in recent years and is expected to be a clean energy source of the future. Solar radiation is abundant, clean, and safe and allows energy generation in remote areas [14].

Nowadays there are many commercial applications for which solar power is already cost effective [14, 15]. Solar cells operate by converting sunlight directly into electricity using electronic properties of a class of materials known as semiconductors. This concept is one of the most promising of renewable energy options to have emerged in the past few decades. Solar cells depend upon the photovoltaic effect for their operation. Application of solar cells initially was in space vehicles but now the big potential area is in terrestrial applications [15].

In South Africa most of the households lack modern energy services and the government is working towards extensive electrification. The biggest challenge is the distant remote rural areas where there is no grid line. Experience has demonstrated that renewable energy and energy efficiency technologies are proven, commercially available and affordable by the majority of the unserved population. Energy production and use are key factors in the economic and social development, water management and the preservation of natural resources and climate change [2, 13, and 16].

The fundamental problem of South Africa's energy sector involves the interaction of several factors, such as [13]:

(i) The lack of access to modern energy by the vast majority of South African households.

(ii) Reduction in the availability of traditional fuels.

(iii) Global and environmental impacts of both current energy practice and the potential adoption of the energy models of the industrialized world.

South African's present electricity generation is dominated by fossil fuel use. The role of traditional fuels is of major concern, as the environmental and health impacts of the traditional fuel usage are well documented and retards future development.

The conventional silicon based solar cell is used worldwide to produce more than hundred million watts of electricity each year [17]. Due to the cost of producing such high purity silicon, as well as the fact that energy conversion efficiency for this type of cell remained neither a practical nor an economically viable, replacement of fossil fuels energy sources [17, 18, and 19]. Development of solar cells from silicon-based devises to a new dye-sensitized type, which are called dye-sensitized solar cells (DSC), is a great step forwardin the area of solar energy. It utilizes a simple fabrication technique and reduces cost [12, 20, 21, and 22].

Titanium solar cell technology is a promising advancement for specific application in photovoltaic (PV) solar cells. It is a completely different technology from that used in the production of silicon solar cells. The cells are made by assembling layers of the semiconductor titanium dioxide (TiO_2), a light-sensitive dye, an electrolyte and a catalyst between two transparent conductive glass plates. When light shines on the cell, the dye is energized and releases an electron that is picked up by the (TiO_2). The electrolyte regenerates the dye after it gives off its charge, while the catalyst supplies the electron to the electrolyte [23, 24, and 25].

Clean and economically sound energy projects that reach rural as well as urban population are needed, with a focus on the following [2, 13]:

(i) Photovoltaic (PV) solar home system in rural areas that displaces kerosene and candles.

(ii) Solar water pumping systems that supply clean, reliable water for household use and irrigation, displacing diesel-powered pumps.

(iii) Energy efficient upgrades of commercial and industrial buildings in urban centres that reduce the amount of electricity consumed.

All of these approaches to energy production and use, have been demonstrated on a commercial basis outside of Africa. The goal is to now seize the opportunity and harness them to the benefit of the South African population.

The call for the implementation of solar energy technology in rural African communities has been welcomed by "Core International", describing solar power (solar technology) as a "practical alternative to extending power distribution to remote and low density population" [26]. Solar energy has been widely used in rural communities around the world for electricity (PV) generation, crop processing and preservation, irrigation (using solar water pumps), heating and cooling homes etc. This has greatly reduced incurred cost, pollution and global warming as against conventional energy use. With better energy policies by government of African states in solar energy technology will be easily accessible and hence the attainment of the government's goal for better living standards of its populace could be achieved and also sustainable development accelerated much faster than through conventional rural electrification programmes [27].

Knowledge of the resource loading is a key to any renewable energy system. Solar resource maps have been developed for countries such as the United States of America [28], Germany [29] and Australia [30]. Unfortunately, South Africa lacks any accurate resource map, which is a serious disadvantage for renewable energy researchers and developers.

1.6 ADVANTAGES AND DISADVANTAGES OF RENEWABLE ENERGIES

1.6.1 Advantages

After the initial investment has been recovered, energy from the sun is practically free. The recovery/ payback period for this investment can be very short depending on the resource and how much electricity the household uses. In South Africa financial incentives are available from the government that can reduce cost. If one can develop a system that produces more energy than what is used, the utility company can buy it and that will be building up a credit on the account. This nifty little scheme is called "net-metering". Solar energy does not require any fuel. It's not affected by the supply and demand of fuel and is therefore not subjected to the ever-increasing price of gasoline [31]. The savings are immediate and for many years to come. The use of solar energy indirectly reduces health costs.

Solar energy is clean, renewable (unlike gas, oil and coal) and sustainable, helping to protect our environment. It does not pollute air by releasing carbon dioxide, nitrogen oxide, sulphur dioxide or mercury into the atmosphere like many traditional forms of electrical generation does. Therefore solar energy does not contribute to global warming, acid rain or smog. It actively contributes to the decrease of harmful green house gas emissions. It's generated where it is needed. By not using any fuel, solar energy does not contribute to the cost and problems of the recovery and transportation of fuel or the storage of radioactive waste.

Solar energy can be utilized to offset utility-supplied energy consumption. It does not only reduce the electricity bill, but also continues to supply a home/ business with electricity in the event of a power outage. A solar energy system can operate entirely independently, not requiring a connection to a power or gas grid at all. Systems can therefore be installed in remote locations, making it more practical and cost-effective than the supply of utility electricity to a new site. The use of solar energy reduces the people's dependence on foreign and/or centralized sources of energy free from influenced by natural disasters or international events and so contributes to a sustainable future. Solar energy supports local job and wealth creation, fuelling local economies.

Solar energy systems are virtually maintenance free and will last for decades. Once installed, there are no recurring costs. They operate silently, have no moving parts, do not release offensive smells and do not require one to add any fuel. More solar panels can easily be added in the future when a household's energy demand grows.

1.6.2 Disadvantages

The initial cost is one of the main disadvantages of installing a solar energy system, largely as a result of the high expense of the semi-conducting materials used in building one. As energy shortages are becoming more common, solar energy is becoming more price-competitive. Solar panels require quite a large area for installation to achieve a good level of applicability [31]. The efficiency of the system also relies on the location of the sun, although this problem can be overcome with the installation of certain components such as solar panels. The production of solar energy is influenced by the presence of clouds or pollution in the air. Similarly, no solar energy will be produced during night time although a battery backup system and/or net metering can solve this problem. As far as solar powered cars go, their slower speed might not appeal to everyone caught up in today's rat race.

As one can see, there are many advantages of solar energy. Disadvantages can be found in any product or system, but it is important to know that they can be managed in this case.

1.7 SUMMARY

This study consists of eight chapters. Chapter 1 discusses the background of the research study and the need for renewable energy in South Africa. Chapter 2 gives a description of solar radiation, i.e. extraterrestrial solar radiation and terrestrial solar radiation. Description of different types of solar radiometers has been discussed as well. The descriptions of the selected stations used in this study together with their Google maps are given in Chapter 3. The methods used to compute the regression coefficients for the Vhembe Region have been explained in detail in Chapter 4. Chapter 5 gives the results on calculation of meteorological parameters and analysis of the horizontal global solar radiation while Chapter 6 describes the computation of the regression coefficients. The science of measurement, including measurement of solar irradiance, demands the calibrated instrumentation to ensure data quality. Towards this end, work done during the International Pyrheliometer Comparison of 2010 is described in chapter 7. Results for South Africa's primary radiometer are given. Chapter 8 gives the summary of this study.

CHAPTER 2

LITERATURE REVIEW

2.1 INTRODUCTION

All substances, at temperatures above the absolute zero, emit energy in the form of electromagnetic waves. This energy is called radiation. During this process (radiation), no intervention of medium is required for its transmission. The most important sources of radiation to the living organisms on the surface Earth is that emitted by the Sun, the Earth and the atmosphere lying within the ultraviolet, visible and infrared spectral regions. The radiation of importance to solar energy users fall between 0.15 and 0.3 micrometre [32]. This chapter deals with solar radiation and its geometry on the Earth's surface.

2.2 THE SUN AS THE SOURCE OF RADIATION

The Sun is a sphere of intensely hot gaseous matter with a diameter of 1.39×10^{9} m and is about 1.5×10^{11} m away from the Earth. It generates heat by thermo-nuclear fusion reactions, where four hydrogen atoms combine to form one helium atom whose mass is less than that of the four protons, some mass having been lost in the reaction and converted to energy. The amount of energy is released in accordance with the following reaction [33]:

$$4H^{1} \rightarrow 2He^{4} \qquad E = +26.7\ \text{MeV} \qquad 2.1$$

The nuclear reaction represented by equation 2.1 results from the fact that the four protons of hydrogen have a total of uncombined mass of 4.0304 atomic mass unit (amu) and mass of helium nucleus is 4.0027 amu. Thus 0.0277 amu of matter are converted into energy in accordance with the energy (E) and mass (m) relation $E = mc^{2}$, given by Einstein, where c is velocity of light [33].

The Sun radiates energy in every direction as seen from figure 2.1. This radiant energy moves outward through space as electromagnetic waves that have a wide range of frequencies. In free space, radiation would travel a distance equal to the Sun's radius in a little more than two seconds, but absorption is so strong inside the sun that it takes a million or two million years for the radiation to make its way out. A radiation zone reaches out from the core for about 70% of the Sun's radius. Core radiation slowly diffuses through this region until it reaches the boundary of the convection zone, where the temperature has fallen and made the gas highly opaque. Warm gases move from the interior to the outer layers, causing a transfer of energy, eventually carrying the flow of energy all the way to the sun's visible surface [34].

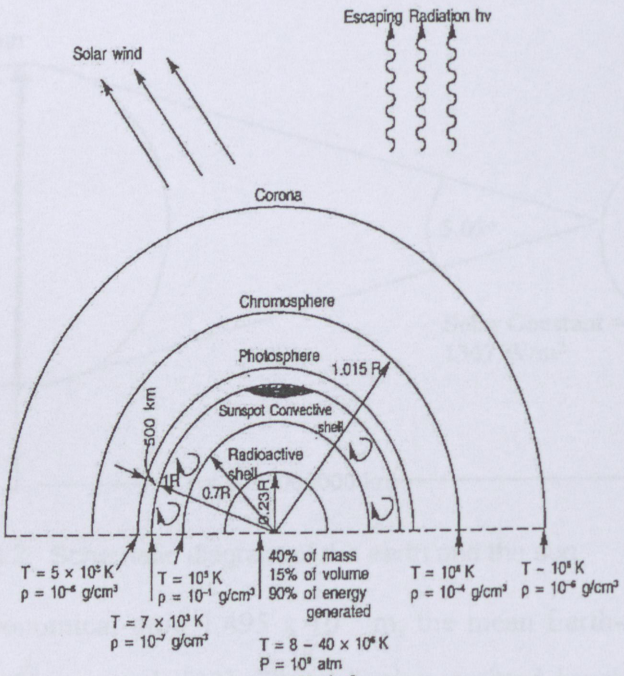

Figure 2.1 The structure of the sun

The Sun's surface appears to be composed of irregular convection cells. Other features of the solar surface are sunspots which vary in size, photosphere (meaning sphere of light) which is the source of most of solar radiation, chromospheres (meaning sphere of colour) which is made up of fiery red clouds of gases which sometimes shoot as far as a 1 609 344 km out into the space and corona with very low density and very high temperature (10^6 K) [35].

2.3 THE EARTH AND SOLAR CONSTANT

The Earth is considered to be a sphere with a diameter of approximately 12, 800 km. It makes one rotation about its axis every 24 hours and completes a revolution about the Sun in a period of approximately 365.25 days [35, 36]. Its mean density is about 5.517 g/cm^3 and its central core is about 2,560 km in diameter which is more rigid than steel. Beyond the central core is a mantle which forms about 70% of the Earth's mass.

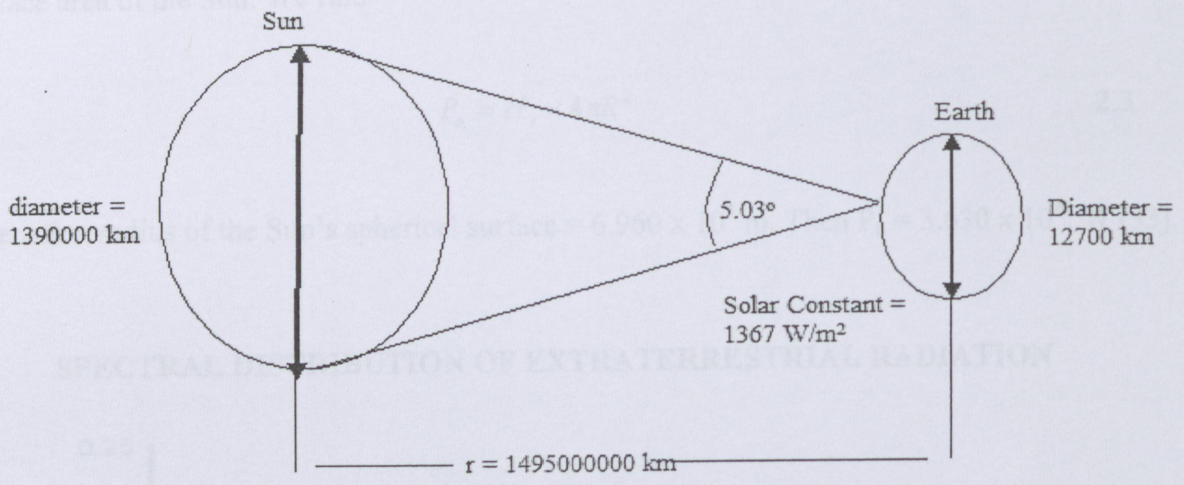

Figure 2.2 Schematic diagram of the earth and the sun

At a distance of one astronomical unit, 1.495×10^{11} m, the mean Earth-Sun distance, the Sun subtends an angle of 5.03^0 on earth [32]. The radiation emitted by the Sun and its spatial relationship to the Earth result in a nearly fixed intensity of solar radiation outside the Earth's atmosphere. H_s in equation 2.2 represents the energy from the Sun per unit time, received on a unit area of surface perpendicular to the direction of propagation of the radiation at the Earth's mean distance from the Sun outside the atmosphere. The World Meteorological Organization (WMO) has adopted a value of 1367 W/m^2 as the solar constant with uncertainty of the order of 1% for solar constant. The value of the solar constant is not actually a constant, but varies with season and somewhat with solar activity [37].

Solar radiation intensity leaving the surface of the Sun is given by Stephan-Boltzman's law as:

$$H_s = \sigma T_o^4 \quad (2.2)$$

where σ = Stefan-Boltzman constant = 5.670 x 10^{-8}W/m^2-K^4 and

T_o = Average temperature on surface = 5762^{o}K

Now using equation 2.2, H_s = 5.961 x 10^7 W/m^2.

Total radiant power P_o, emitted from the Sun is obtained by multiplying equation 2.2 by the surface area of the Sun. We find

$$P_o = H_s \times 4\pi R^2 \quad (2.3)$$

where R = radius of the Sun's spherical surface = 6.960 x 10^8 m. Then P_o = 3.630 x 10^{26} W [33].

2.4 SPECTRAL DISTRIBUTION OF EXTRATERRESTRIAL RADIATION

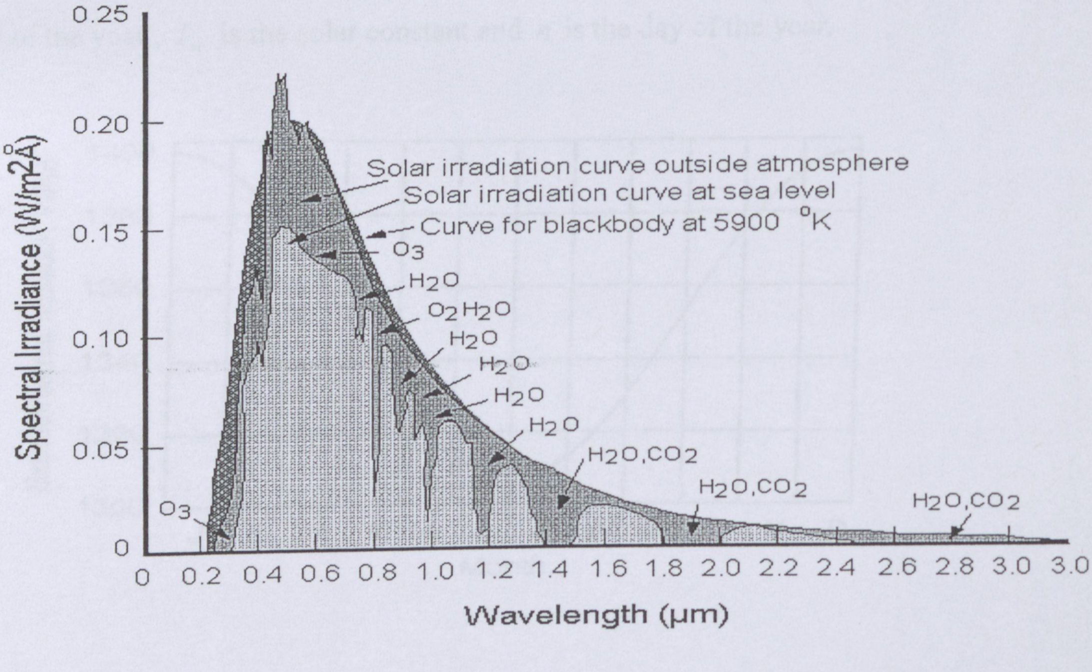

Figure 2.3 The spectral distribution of the sun's radiation and its absorption by atmospheric gases

It is useful to know the spectral distribution to the extraterrestrial radiation that would be received in the absence of the atmosphere. A standard spectral irradiance curve has been compiled, based on high-altitude and space measurements. The WRC standard spectrum is shown in Figure 2.3 [37].

2.5 VARIATION OF THE EXTRATERRESTRIAL RADIATION ON THE HORIZONTAL SURFACE

There are two causes of variation in extraterrestrial radiation that have to be considered. The first is the variation in the radiation emitted by the sun. The second cause, variation of the Earth-Sun distance, however, does lead to variation of extraterrestrial radiation flux. The dependence of the extraterrestrial radiation on the time of year is indicated by Equation 2.4 and Figure 2.4 [32]

$$I_{on} = I_{sc}\left[1 + 0.033\cos\left(\frac{360\,n}{365}\right)\right] \qquad 2.4$$

where I_{on} is the extraterrestrial radiation, measured on the plane normal to the radiation on the n^{th} day of the year , I_{sc} is the solar constant and n is the day of the year.

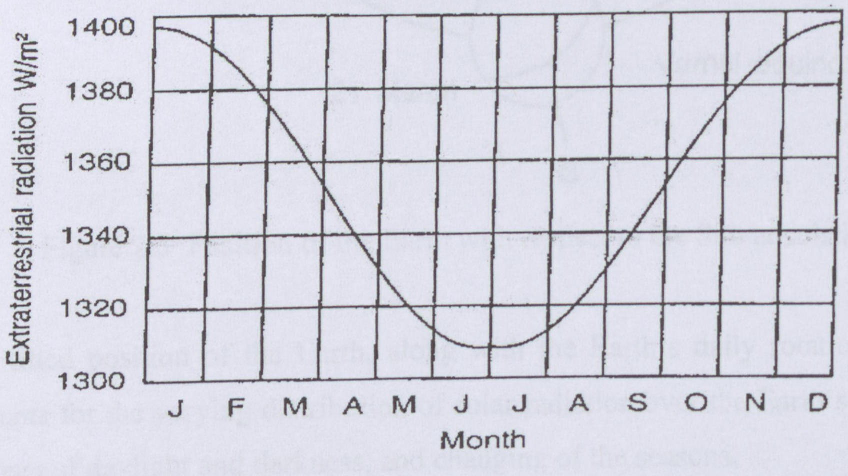

Figure 2.4 Variation of extraterrestrial solar radiation with time of the year

The extraterrestrial radiation on horizontal surface, H_o is given by equation 2.5.

$$H_o = I_{sc}\left(1 + 0.033\cos\frac{360\,n}{365}\right)\cos\theta_z \qquad 2.5$$

where θ_z is the solar zenith angle [35].

The Earth's axis of rotation is tilted 23.45° with respect to its orbit about the Sun. In its orbital movement the Earth keeps its axis oriented in the same direction as observed in Figure 2.5.

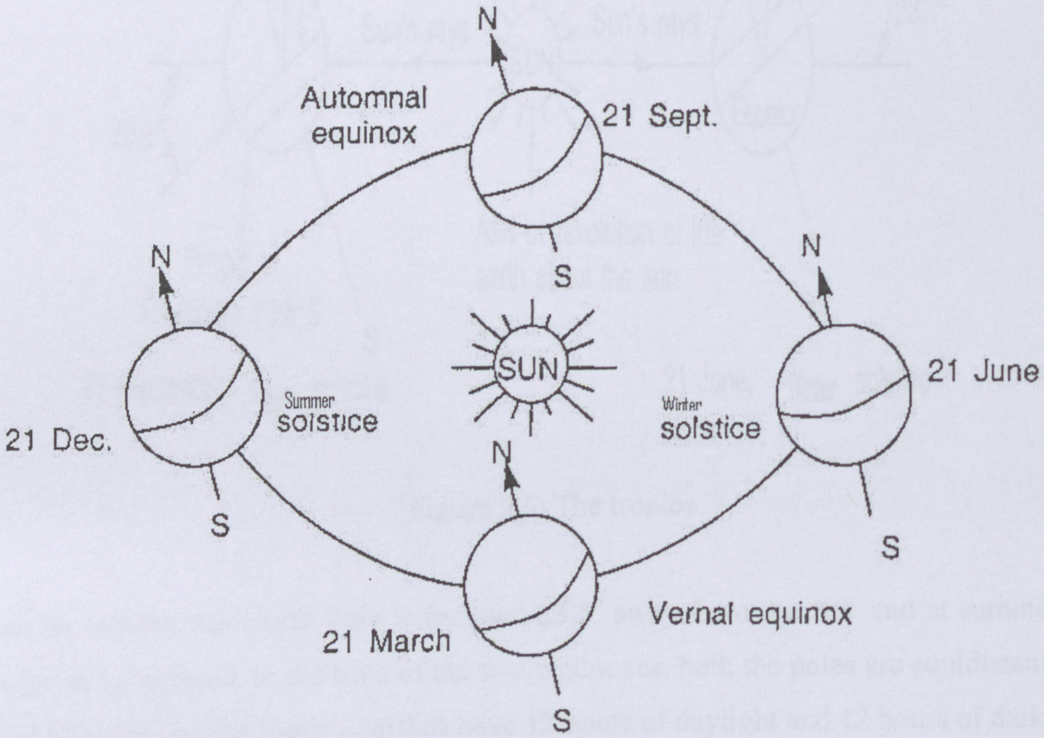

Figure 2.5 Position of the Earth with respect to the Sun at solstice and equinoxes

This tilted position of the Earth, along with the Earth's daily rotation and yearly revolution, accounts for the varying distribution of solar radiation over the Earth's surface, changing length of hours of daylight and darkness, and changing of the seasons.

In South Africa, the day length hours in summer season are longer compared to winter. The average day length in summer is approximately thirteen hours and about ten and half hours in winter. Figure 2.6 below is a diagram of the earth's orbit around the sun [32].

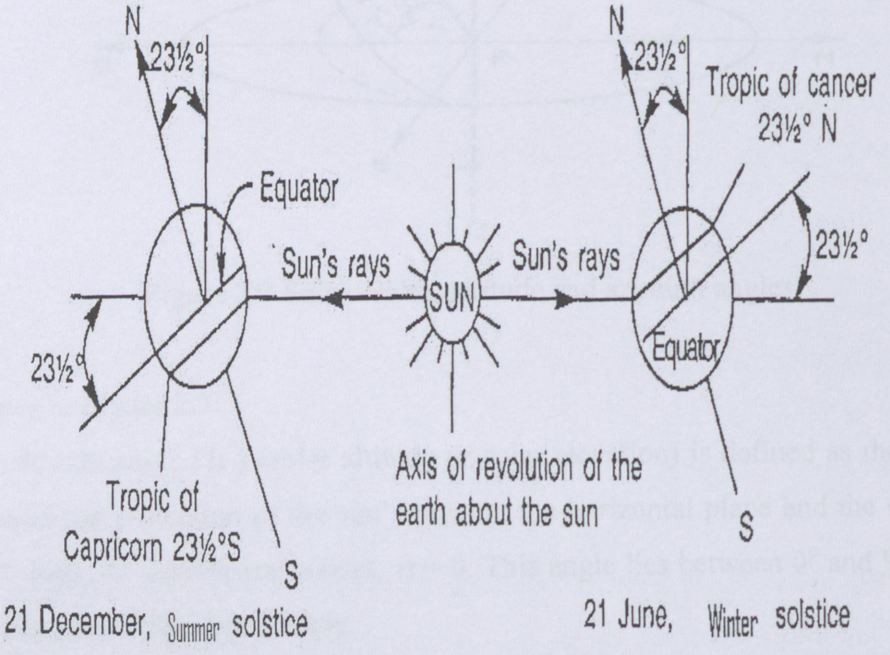

Figure 2.6 The tropics

At winter solstice the North Pole is inclined 23.5° away from the Sun and at summer solstice the situation is reversed, at the time of the two equinoxes, both the poles are equidistant from the Sun and all points on the Earth's surface have 12 hours of daylight and 12 hours of darkness.

2.6 SOLAR GEOMETRY

In order to calculate the solar radiation reaching the horizontal surface on the Earth, it is necessary to indicate the trigonometric relationships between the solar position in the sky and the surface coordinates on the Earth. The knowledge of the Sun's path in the sky on various days in a year at a particular place is of a fundamental pre-requisite since this helps in designing solar devices [32].

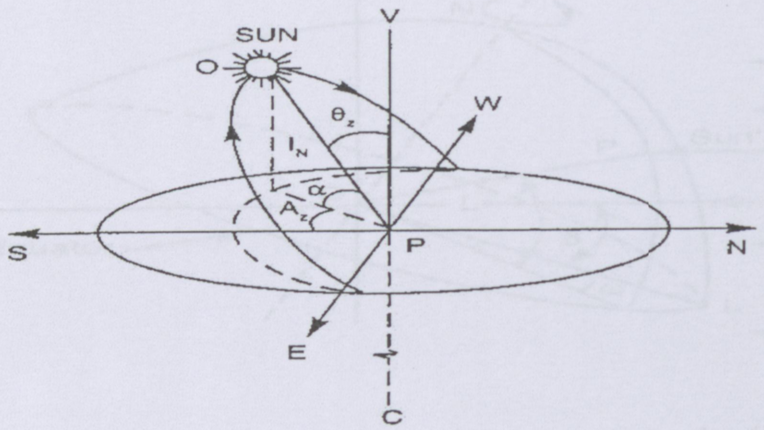

Figure 2.7 Solar zenith, altitude and azimuth angles

With reference to Figure 2.7:

- The altitude angle (α) (solar altitude or solar elevation) is defined as the vertical angle between the projection of the sun's rays on the horizontal plane and the direction of the Sun's rays. At sunrise and sunset, $\alpha = 0$. This angle lies between 0^o and 90^o and it is the complement of the zenith angle.
- The solar zenith angle (θ_Z) is the complementary angle of the Sun's altitude angle. It is a vertical angle between the sun's ray and a line perpendicular to the horizontal plane at point P [33]. That is

$$\theta_z = \frac{\pi}{2} - \alpha \qquad 2.6(a)$$

And it follows that

$$\cos\theta_z = \sin\alpha = \cos\delta \cdot \cos\phi \cdot \cos\omega + \sin\phi \cdot \sin\delta \qquad 2.6(b)$$

Solar zenith angle increases steadily from sunrise to sunset. When the solar zenith angle reaches 90^o, the Sun's rays are parallel to the Earth's surface. The time of sunrise and sunset depends on the terrain and on which point of the solar disc it is taken as the characteristic of the Sun [32, 39].

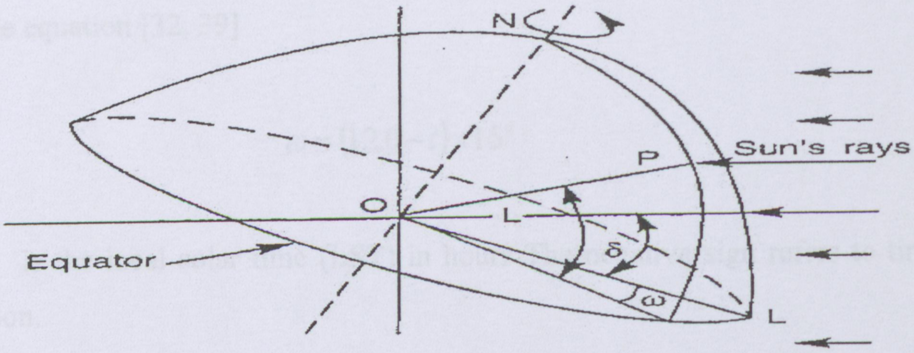

Fig.2.8 Latitude (∅), hour angle (ω) and sun's declination (δ)

- Azimuth angle A_z (solar azimuth angle) is the angle in the horizontal plane measured from the south (northern hemisphere) to the horizontal projection of the Sun's rays.
- Latitude is the angle between the line drawn from a point on the Earth's surface to the centre of the Earth, and the Earth's equatorial plane.
- Solar declination (δ) is defined as the angle between the line joining the centres of the Sun and the Earth and its projection on the equatorial plane. Declination is due to the rotation of the Earth about an axis which makes an angle of 66.5 percent with the plane of its rotation around the Sun. The declination varies from a maximum value of 23.45° on June 21 to a minimum of -23.45° on December 21. The declination can be calculated from the relation (Cooper's equation, 1969) [40, 41 and 60]:

$$\delta = 23.45^{o} \sin\left[\frac{360}{365}(284 + n)\right] \qquad 2.7$$

where n is the day of the solar year (n ∈ [1; 365])

- Hour angle (ω) is the angle through which the Earth must be rotated to bring the meridian of the plane directly under the sun. It may be referred to as the displacement of the sun east or west of the local meridian due to rotation of the Earth on its axis at 15° per hour. The hour angle is zero at solar noon. The hourly variation of the hour angle takes it from negative values before noon to positive values after solar noon. It can be computed using the equation [32, 39]

$$\omega = (12.0 - t) \times 15^o \qquad 2.8$$

where t is the local solar time (LST) in hours The negative sign refers to time before solar noon.

➤ The sunset (sunrise) hour angles (ω_S): This angle indicates the length of the day and can be expressed according to the relation [39]:

$$\cos\omega_s = -\tan\phi \cdot \tan\delta \qquad 2.9$$

The sunset (sunrise) hour angle is directly related to the number of hours from solar noon to sunset (sunrise). The day length or possible sunshine hours, *N*, is given by [38]

$$N = \left(\frac{2}{15}\right)\omega_s \qquad 2.10$$

The possible sunshine hours depend on the location, i.e. latitude and the day of the year.

2.7 SOLAR TIME AND EQUATION OF TIME

It is desirable to convert clock time into solar time in solar energy problems. Solar time is measured with respect to solar noon which is the time when the Sun is crossing the observer's meridian. Solar time is converted to standard time by the equation [32, 39]:

$$\text{Solar time (t)} = \text{Standard time} \pm 4(L_{st} - L_{loc}) + E \qquad 2.11$$

where E is the correction arising out of the variation in the length of the solar day through the year. Thi is called equation of time. The second term arises due to the difference in observer's longitude (L_{st}) and longitude on which the local time (L_{loc}) is based; the sun traverses each degree of longitude in 4 minutes.

$$E = 9.87 \sin 2B - 7.53 \cos B - 1.5 \sin B \qquad 2.12$$

where

$$B = \frac{360\,(n-1)}{364} \qquad 2.13$$

and n = day of the year, $1 \leq n \leq 365$

Solar day varies throughout the year in a somewhat irregular manner [33, 39]. The mean value of solar day taken over the year is exactly 24 hours. The solar day has a maximum length of 24 hr + 30 sec near the winter solstice and a minimum length of 24 hr – 19 sec shortly before autumnal equinox. A secondary maximum occurs near the summer solstice, whereas secondary minimum occurs near the vernal equinox. The solar noon at a place can be determined from the following equation:

Local solar noon = 12 – equation of time in hours on that day

$$\pm \frac{\text{longitude of reference meridian} - \text{observer's longitude}}{15} \qquad 2.14$$

Solar noon occurs when the Sun crosses an imaginary line in the sky extending from the North Pole to the South Pole and passing directly over an observer's head [39]. The times between two successive solar noon (solar day) is very nearly constant throughout the year, This means that if an observer observes solar noon at say, 11:55 AM local time, the next solar noon can be observed at no more than 19 seconds before or 30 seconds after 11:55 AM on the following day .

2.8 SOLAR RADIATION AT THE EARTH'S SURFACE (TERRESTRIAL RADIATION)

From the point of view of utilization of solar energy, the energy received at the earth's surface is of vital importance. Solar radiation received in the Earth is in the form of direct radiation (also referred to as beam radiation) and diffuse radiation.

2.8.1 Beam and diffuse solar radiation

That portion of the incident solar radiation which comes from the apparent solar disc without reflection from other objects is called direct or beam radiation [33]. These radiations are received from the Sun without change in direction.

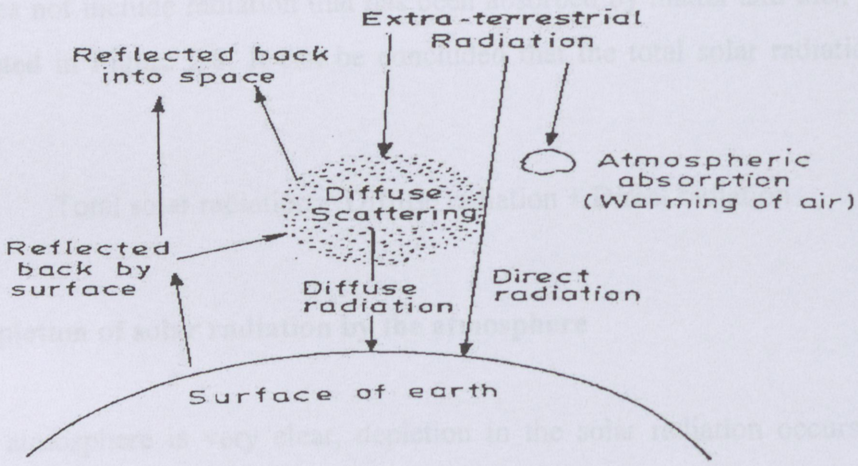

Figure 2.9 Direct, diffuse and total solar radiation [33]

With reference to Figure 2.9 diffuse radiation is observed as that solar radiation received from the Sn after its direction has been changed by reflection and scattering by the atmosphere. Clouds have a far greater effect on the variation of solar radiation. A cloud between the observer and the Sun blocks the direct radiation, clouds elsewhere in the sky increase diffuse radiation. Effects on solar radiation due to aerosols, water vapour and atmospheric pollution are smaller and normally treated for clear-sky conditions. The intensity of diffuse radiation seen by the observer on a clear day varies as a function of latitude, time of the year, time of the day, atmospheric content and other factors[32,33].

If the latitude of the Sun is small, the length traversed by the beam is long. On the other hand, if the Sun is at zenith (overhead), the solar beam traverses a vertical path, the shortest path through the atmosphere.

2.8.2 Global solar radiation

The total solar radiation or global solar radiation reaching the surface of the Earth is all solar radiation incident on a surface, including scattered, reflected, and direct (where scattered and reflected is referred to as diffuse solar radiation. The total solar radiation that reaches the Earth surface does not include radiation that has been absorbed by matter and then re-emitted. This is also indicated in Figure 2.8. It can be concluded that the total solar radiation is given by the equation:

$$\text{Total solar radiation} = \text{Diffuse radiation} + \text{Direct radiation} \tag{2.15}$$

2.8.3 Depletion of solar radiation by the atmosphere

When the atmosphere is very clear, depletion in the solar radiation occurs via three distinct physical processes [32]:

(i) Selective absorption
(ii) Rayleigh scattering by molecules and dust particles
(iii) Mie scattering

These processes occur when the atmosphere is very clear. In a cloudy atmosphere, considerable depletion of the direct solar radiation takes place. A major part of solar radiation is reflected back into space by the clouds. The fraction of the total solar radiant energy reflected back to space by the clouds, scattering by the atmospheric gases and dust particles, and by reflection at the Earth's surface is called albedo of the Earth atmosphere system [32].The path length of the beam through the atmosphere is accounted for in air mass (m).

$$m = \sec\theta_z \qquad 2.16$$

Air mass is the ratio of the path of the sun's rays through the atmosphere to the length of path when the Sun is at the zenith.

$m = 0$ Outside the earth's atmosphere

$m = 1$ When the sun is at zenith, i.e. directly overhead

$m = 2$ When the zenith angle is 60^{o}.

2.8.3.1 Selective absorption

The transmittances for absorption $\tau_{\lambda(abs)}$ are to be combined in the same manner as those for scattering$\tau_{\lambda(s)}$, the resulting monochromatic transmittance for beam radiation may be written as [33]

$$\tau_{\lambda} = \tau_{\lambda(s)} \times \tau_{\lambda(abs)} \qquad 2.17$$

where τ_{λ} = monochromatic atmospheric transmittance considering scattering and absorption (at wavelength λ)

$\tau_{\lambda(s)}$ = monochromatic atmospheric transmittance considering scattering only

$\tau_{\lambda(abs)}$ = monochromatic atmospheric transmittance considering absorption only.

2.8.3.2 Rayleigh scattering

Rayleigh scattering of sunlight in clear atmosphere is the main reason why sky is blue. A portion of the light from the sun scatters off due to other molecules and particles in the atmosphere. The sky appears blue because air scatters short-wavelength light more than longer wavelengths. Since blue light is at the short wavelength end of the visible spectrum, it is more strongly scattered in the atmosphere than long wavelength red light. The result is that the human eye perceives blue when looking toward parts of the sky other than the sun. Rayleigh's scattering formula is given as:

$$\sigma \,\alpha\, f^4 \qquad 2.18$$

where σ is the amount of the scattered light and f is the frequency of light.
f^4 indicates the fast increase with frequency.

This type of scattered light gives the sky its brightness and its colour. During the day, the sky is seen as blue due to the Rayleigh scattering which is inversely proportional to the fourth power of wavelength, so that the shorter wavelength violet and blue light will scatter more than the longer wavelengths (yellow and especially red light).So, Rayleigh scattering is wavelength dependent. This scattering occurs through light's interaction with air molecules.

2.8.3.3 Mie Scattering

Mie scattering is responsible for white appearance of clouds. This type of scattering is caused by pollen, dust, smoke, water droplets, and other particles found in the lower atmosphere. Clouds, ice and deserts have high albedos (i.e. the fraction of solar energy that is reflected back to space). Clouds reflect more shortwave radiation back to space than the surface would in the absence of the cloud thus leaving less solar energy available to heat the surface and atmosphere.

It is of vital importance that we study scattering in this research since it is the main factor responsible for the variation of the coefficient of clearness index in the form of cloudiness, dust, ozone, etc. Of all these factors cloudiness is the most influential and also exhibits the largest variation from day to day as was pointed out by Liu and Jordan [42]. Increasing daily cloudiness decreases the clearness index.

2.9 SOLAR RADIATION ON INCLINED AND HORIZONTAL SURFACES

2.9.1 Average daily diffuse radiation

Liu and Jordan [42] showed that there is a positive correlation between the ratio of average daily diffuse radiation, H_d to average daily global radiation, H, $\left(\frac{H_d}{H}\right)$ and the ratio of daily global radiation to average daily extraterrestrial radiation, $\frac{H_o}{H}$ known as the cloudiness index K_T. Several researchers in different countries compared Liu and Jordan correlation and observed some discrepancy. The differences could be due to instrumental error or seasonal effects.

2.9.2 Hourly total irradiance on a horizontal plane

The hourly solar radiation on a horizontal surface is dependent on the sunset hour angle (ω_s). The ratio of hourly total to daily total solar radiation is given by Equation 2.19 [38].

$$\frac{I_{tot}}{H_h} = \frac{\pi}{24}\left[a + b\cos\omega\left(\frac{\cos\omega - \cos\omega_s}{\sin\omega_s - \left(\frac{2\pi\omega_s}{360}\cos\omega_s\right)}\right)\right] \quad 2.19$$

where I_{tot} is the hourly total radiation on horizontal surface in mega joules per meter square (MJ/m^2) and a and b are the regression coefficients. These regression coefficients are to be determined for the Vhembe region terrain province in this study. See also Chapter 4, Equation 4.1.

2.9.3 Hourly diffuse radiation components on a horizontal plane

The ratio of hourly diffuse solar radiation $\frac{I_d}{H_d}$ had been developed by Liu and Jordan [42] in 1960. This ratio is given by Equation 2.20.

$$\frac{I_d}{H_d} = \frac{\pi}{24}\left[\frac{\cos\omega - \cos\omega_s}{\sin\omega_s - \left(\frac{2\pi\omega_s}{360}\right)\cos\omega_s}\right] \quad 2.20$$

where I_d and H_d are the hourly and daily diffuse solar radiation on horizontal surface respectively in mega joules per meter square.

2.9.4 Hourly beam and diffuse radiation components on an inclined plane

Any plane oriented towards the Sun is making an angle with the incident solar beam. The angle between the solar beam and the normal to the surface is called the angle of incidence, θ_i, and can be expressed as [32, 39]

$$\cos\theta_i = \sin\delta\sin\emptyset\cos\beta - \sin\delta\cos\emptyset\sin\beta\cos\gamma + \cos\delta\cos\emptyset\cos\omega + \cos\delta\sin\emptyset\sin\beta\cos\omega\cos\gamma + \cos\delta\sin\beta\sin\omega\sin\gamma \quad 2.21$$

where δ = declination angle,

β = tilt angle,

$\emptyset$ = latitude angle and

γ = the angle by which the collector is diverted from south.

If the plane is a horizontal one then the angle of incidence is equivalent to the sum zenith angle, θ_z. In most of the applications where the solar collectors are fixed, the collectors are sloped towards the equator, in this case $\gamma = 0^\circ$ and the expression for θ_i can now be given by

$$\cos\theta_i = \cos(\phi - \beta)\cdot\cos\beta\cdot\cos\omega + \sin(\phi - \beta)\cdot\sin\delta \quad 2.22$$

At the time of solar noon, the altitude of the sun, α_n, can be determined from the following equations:

$$\cos\theta_z = \cos\delta \cdot \cos\phi \cos w + \sin\phi \cdot \sin\delta \qquad 2.23$$

and $\alpha = 90^o - \theta_z$ on a horizontal surface, then

$$\alpha_n = 90^0 - (\phi - \delta) \qquad 2.24$$

Figure 2.10 below depicts various angles discussed above, where O is the centre of the Earth and P is an observer on the Earth. I_N is the direct solar radiation. Sunrise hour angle or sunset hour angle, ω_s is determined using the following equation $\cos\omega_s = -\tan\phi \cdot \tan\delta$ (from Eq. 2.9).

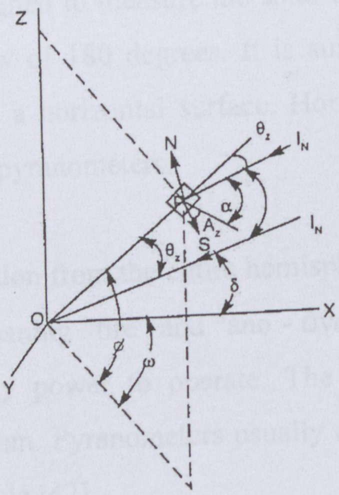

Fig 2.10 Direction of beam radiation

For inclined plane,

$$\cos\omega_s' = -\tan(\phi - \beta)\tan\delta \qquad 2.25$$

where ω_s' is the sunrise or sunset hour angle for an inclined plane.

2.10 SOLAR RADIOMETERS

Experimental determination of energy transferred to a surface by solar radiation requires instruments which measure the heating effect of direct, diffuse solar radiation and global solar radiation. It is important to know the specific instruments (as explained in 2.10.1 – 2.10.4) that are suitable for the measurement of diffuse, direct or global solar radiation although there is one that can measure diffuse and direct or direct and global radiation simultaneously. Some of these instruments are listed in this section.

2.10.1 Pyranometer

A pyranometer is a type of radiometer used to measure broadband solar irradiance on a planar surface and is a sensor that is designed to measure the solar radiation flux density (in watts per meter square) from a field of view of 180 degrees. It is suitable for the measurement of the global or sky radiation usually on a horizontal surface. Horizontal global solar radiation data used in this study are measured by pyranometers.

A Pyranometer is sensible to radiation from the entire hemisphere. The name of the pyranometer stems from Greek, "pyr – πῦρ" meaning "fire" and "ano - ἄνω" meaning "above sky". A typical pyranometer does not require any power to operate. The solar radiation spectrum extends approximately from 300 to 2,800 nm. Pyranometers usually cover that spectrum with a spectral sensitivity that is as “flat” as possible [42].

For an irradiance measurement it is required by definition that the response to “beam” radiation varies with the cosine of the angle of incidence; i.e. full response when the solar radiation hits the sensor perpendicularly (normal to the surface, sun at zenith, 0 degrees angle of incidence), zero response when the sun is at the horizon (90 degrees angle of incidence, 90 degrees zenith angle), and 0.5 at 60 degrees angle of incidence. It follows from the definition that a pyranometer should have a so-called “directional response” or “cosine response” that is close to the ideal cosine characteristic.

A pyranometer's main components are:

- A thermopile sensor with a black coating. This sensor absorbs all solar radiation, has a flat spectrum covering the 300 to 50,000 nanometer range, and has a near-perfect cosine response.
- A glass dome. This dome limits the spectral response from 300 to 2,800 nanometers (cutting off the part above 2,800 nm), while preserving the 180 degrees field of view. Another function of the dome is that it shields the thermopile sensor from convection.

The black coating on the thermopile sensor absorbs the solar radiation. This radiation is converted to heat. The heat flows through the sensor to the pyranometer housing. The thermopile sensor generates a voltage output signal that is proportional to the solar radiation. Pyranometers are frequently used in meteorology, climatology, solar energy studies and physics of buildings. They can be seen in many meteorological stations - typically installed horizontally and next to solar panels - typically mounted with the sensor surface in the plane of the panel.

2.10.2 Pryheliometers

A pyrheliometer is an instrument for direct measurement of solar irradiance at normal incidence. Sunlight enters the instrument through a window and is directed onto a thermopile which converts heat to an electrical signal that can be recorded. The pyrheliometer is used with used with a solar tracking system to keep the instrument aimed at the sun [44]. Every five years, The World Solar Group (WSG) organises International Pyrheliometer comparisons at Davos. Calibrated pyrheliometer instruments that participated during these comparisons are considered as reference pyrheliometers and they can be used to calibrate other solar radiometer instruments such as pyranometer through shade and unshade methods. This is discussed in chapter 6 in this study.

In order to find the global solar radiation data, one can measure direct solar radiation and diffuse solar radiation since the sum of direct and diffuse gives global solar radiation. Computation of global solar radiation has to specify whether it is horizontal or on an incline surface.

2.10.3 Pyrgeometer

A pyrgeometer is a device that measures the atmospheric infra-red radiation spectrum that extends approximately from 4.5 μm to 100 μm. It measures the terrestrial solar radiation only [44].

A pyrgeometer consists of the following major components:

- A thermopile sensor which is sensitive to radiation in a broad range from 200 nm to 100 μm
- A silicon dome or window with a solar blind filter coating. It has a transmittance between 4.5 μm and 50 μm that eliminates solar shortwave radiation.

The Figure 2.11 shows the components of a pyrgeometer .

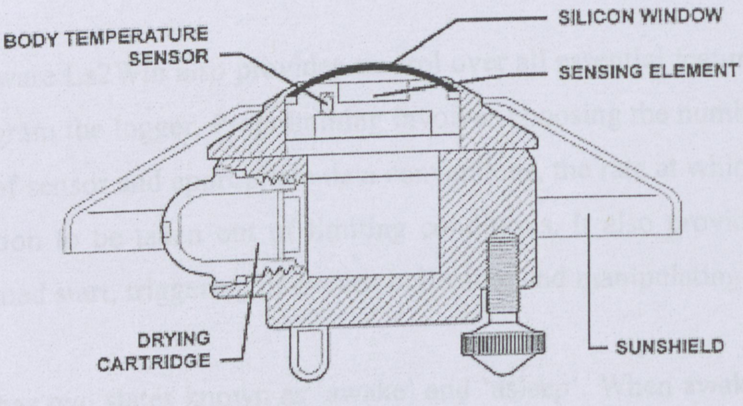

Figure 2.11 A pyrgeometer components

- A temperature sensor to measure the body temperature of the instrument.
- A sun shield to minimize heating of the instrument due to solar radiation.

2.10.4 Sun-Shine Recorder

It is also desirable to have the duration of bright sunshine in a day. Sun-shine recorder is an instrument used to measure the duration in hours of bright sun shine during the course of the day.

It consists of a glass sphere mounted in a section of spherical brass bowl with grooves for holding the recorder cards. The sphere burns a trace being a direct measure of the duration of bright sunshine.

2.10.5 Univen's system at Vuwani

A special discussion is given here on the University of Venda's system at Vuwani. The system is a pyranometer, which consists of the data logger unit (DL2) containing all the hardware required for capturing and storing data from a wide variety of sensors under most environmental conditions [45]. DL2 runs an internal logging program as set by the user and records the data. There are features such as starting and stopping the logger, displaying current readings, providing status reports, and outputting logged data to a local printer.

The windows software Ls2Win also provides control over all essential features mentioned above and is used to program the logger. Programming involves choosing the number of channels to be logged, the types of sensor and appropriate data conversions, the rate at which each channel is to be logged and action to be taken out of limiting conditions. It also provides a range of other features such as timed start, triggering of events, collecting and manipulating logged data.

The DL2e logger has two states known as 'awake' and 'asleep'. When awake all of the logger's circuitry is powered up and all its functions are active. The logger is awake during a LOG, WARM-UO or EVENT while communicating via its RS232 port or performing any of the tasks controlled from its keypad. When one is logging or carrying out one of the priority tasks, the logger flashes up a message on its display to indicate that the other logger functions are temporarily suspended. When asleep a minimum number of components are powered up, notably the clock, memory and circuitry which enables the logger to be woken. The logger's display is always blank when the logger is asleep.

2.10.5.1 Sensor status

The current status of all channels programmed as sensors are displayed on the user's PC in the sensors panel of the DL2 control panel using the keypad READ function. The DL2 Control panel displays a single value of each channel. This information is independent of logging, and can be obtained before or while logging with no interference to logged data. The READ panel or Sensor panel gives an error message if appropriate. Error status are categorized as battery failure, memory full, sensor malfunctions and over-run errors [45].

2.10.5.2 Collecting logged data

Data can be collected from the logger at any time during logging. There is no need to stop logging. Data output from the logger is controlled from the PC. In order to create space the data, data that have been collected can be erased from the logger's memory. Data is transferred to the PC for processing as required [45].

CHAPTER 3

STUDY AREA IN VHEMBE REGION

3.1 OVERVIEW

The study area is Vhembe Region in Limpopo Province South Africa. South Africa is the southernmost part of the African continent. The latitude stretches across 22° to 35° S, and from 17° to 33° E, longitude. Its surface area is 1 219 090 km^2 [58]. South Africa is divided into nine provinces, namely, Gauteng, Mpumalanga, North West, Kwazulu-Natal, Eastern Cape, Northern Cape, Western Cape, Free State and Limpopo.

South Africa is a subtropical location. The temperature conditions are mainly defined by the Benguela (or Mozambique) ocean currents and the altitude of the interior plateau [43]. It is famous for its sunshine. It's a relatively a dry country, with an average annual rainfall of about 464mm (compared to a world average of about 860mm).

Over much of South Africa, summer (mid-October to mid-February) is characterised by hot, sunny weather - often with afternoon thunderstorms that clear quickly, leaving a warm, earthy, uniquely African smell in the air. Autumn (fall) in South Africa (mid-February to April) offers in some ways the best weather [43]. Very little rain falls over the whole country, and it is warm but not too hot, getting colder as the season progresses. Winter in South Africa (May to July) is characterised in the higher-lying areas of the interior plateau by dry, sunny, crisp days and cold nights. The climate of Mpumalanga and Limpopo provinces, offer fantastic winter weather with sunny, warmish days and virtually no wind or rain. Spring is in August to mid-October.

The subtropical location on either side of 30°S accounts for the warm temperature conditions so typical of South Africa. South Africa is dry with abundant sunshine. Temperature conditions in South Africa are characterised by three main features. Firstly, temperature tends to be lower than in other regions at similar latitudes, for example, Australia. Secondly despite a latitudinal span of 13 degrees, average annual temperatures are remarkably uniform throughout the country.

Temperatures above 32°C are fairly common in summer, and frequently exceed 38°C in Limpopo Province. In September, the temperatures may sometimes reach the maximum of 42°C.

Figure.3.1 Map of South Africa

Figure 3.1 is the South African map with Vhembe Region marked in red colour. Although Makhado Alldays is slightly out of the Vhembe region, it is included so as to make a comparison. Limpopo is South Africa's northernmost province, which has a strong rural basis. Limpopo's surface area is 123 910 km^2 wherein more than 5.2 million people live. The northern and eastern parts of Limpopo are subtropical with hot, humid summers [58]. Limpopo is sub-divided into regions, namely Capricorn, Waterberg, Sekhukhune and Vhembe.

Figure 3.2 Demarcation of Vhembe Region

The image of Figure 3.2 gives the elevation profile for the perimeter of the Vhembe Region.

Aside from the station at Vuwani, all the stations illustrated in Figure 3.3 are managed by the Agricultural Research Council (ARC). The ARC has provided daily global solar irradiance data for their stations. The South African Weather services have provided the required data for sunshine duration from their stations closest to the ARC stations used in this study.

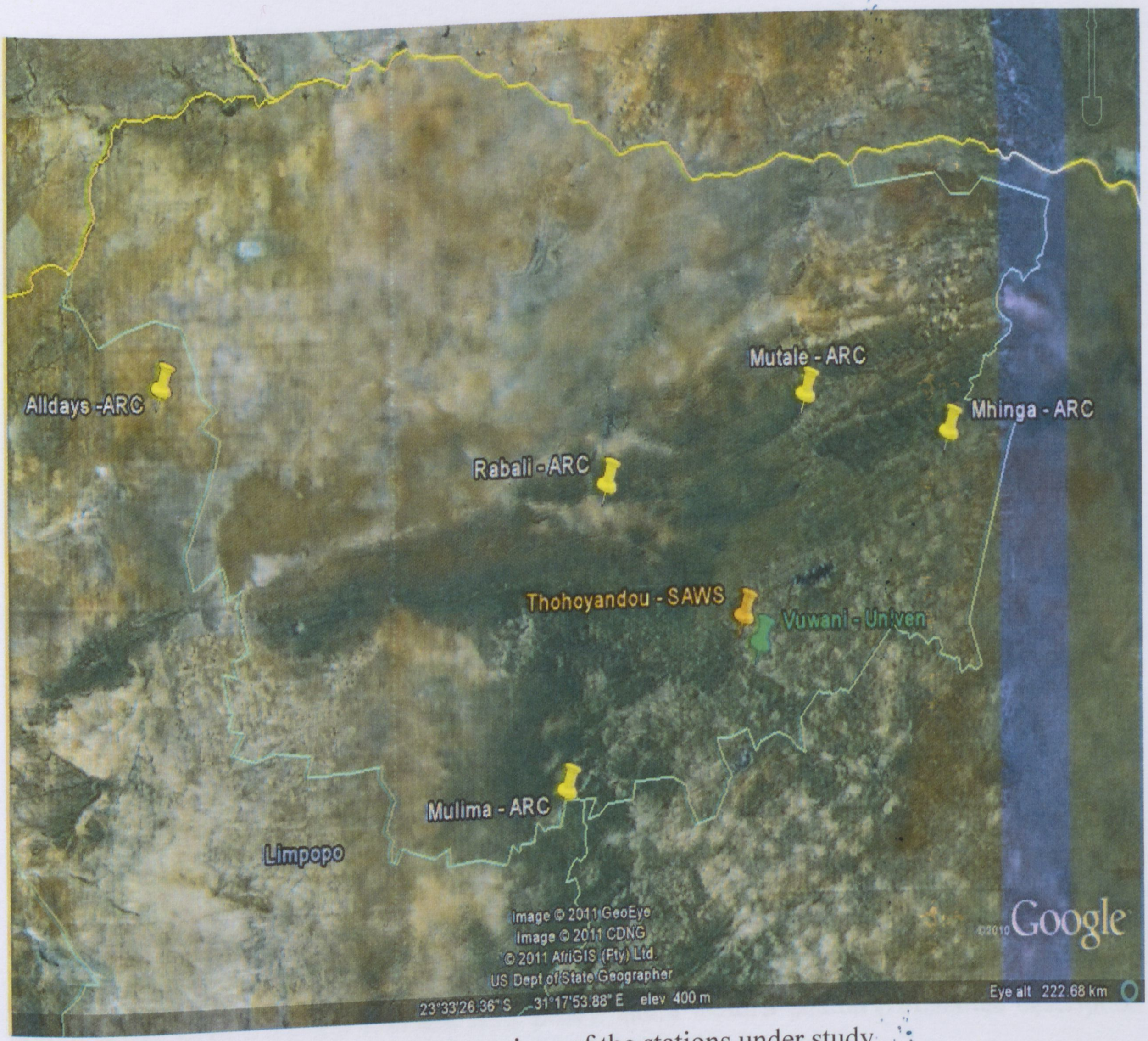

Figure 3.3 Locations of the stations under study.

The stations that were selected for this study along with their latitude, longitude, altitude and the number of years in which horizontal global solar radiation was measured by the ARC are presented in Table 3.1. These values were obtained from ARC.

Station	Latitude	Longitude	Altitude	Availability of data
Vuwani	23.13030°S	30.41980°E	480 m	none
Makhado Alldays	22.68264°S	29.10466°E	842 m	2006 – now
Thohoyandou Mutale	22.73461°S	30.52188°E	550 m	2006 – now
Malamulele Mhinga	22.79675°S	30.84219°E	460 m	2006 – now
Makhado Rabali	22.87038°S	30.08112°E	720 m	2006 – now
Makhado Mulima	23.35612°S	29.98923°E	1032 m	2006 - now

Table 3.1 Geographical locations of the selected stations.

3.2 UNIVEN'S VUWANI SITE

Figure 3.4 indicates where Vuwani site is situated. There are tarred and dusty roads. The buildings and trees are at a distance of about one kilometre from the station. Instruments are installed at the northern side of one of the buildings at the centre. These are a Cmp-6 pryranometer from Kipp and Zonnen, solar panels and a weather station (A detailed description is given in section 2.10.5).

Figure 3.4 Vuwani Site

3.3 AGRICULTURAL RESEARCH COUNCIL SITES IN THE VHEMBE REGION

The Agricultural Research Council (ARC) collects meteorological data from many stations in the northern region of the Limpopo province. For the present investigations five stations were identified in the Vhembe region. Some of the meteorological parameters that were recorded by the ARC are average daily global horizontal radiation data in MJ/m^2 horizontal global solar radiation, the maximum and minimum daily average temperatures; amount of rainfall; wind speed and humidity. It is also indicated from the received data that these meteorological parameters were recorded from August 2006. Some of the above parameters are essential for the computation of regression coefficients. In the present study the horizontal daily global solar radiation data (H) was used together with the computed values of possible sunshine hours (N) and extraterrestrial solar radiation (H_0) on the horizontal surface were used.

3.3.1 MAKHADO ALLDAYS SITE

As shown in Figure 3.5, Makhado Alldays station is situated in a dusty area and a street nearby is gravel. The trees and buildings are on the northern and southern side of the station. This location is classified as sub-Sahara area. Although the area looks dry and brownish in colour, trees can grow high.

Figure 3.5 Makhado Alldays Station

3.3.2 THOHOYANDOU MUTALE SITE

As observed from Figure 3.6, Thohoyandou Mutale station is situated at the foot of Mutale mountain range and surrounded by buildings. There are industrials centres towards southern part of the station.

Figure 3.6 Thohoyandou Mutale Station

3.3.3 MALAMULELE MHINGA SITE

Malamulele-Mhinga station is in the midst of trees and there is a river on its north-eastern part. The roads are dusty too. It is noticed that the station is surrounded by cultivated area. This location looks greenish during summer season and changes with seasons of the year. The 3D-buildings are far away from the station.

Figure 3.7 Malamulele Mhinga Station

3.3.5 MAKHADO RABALI SITE

With reference to Figure 3.8, Makhado Rabali station is situated at the hill facing northwards. The buildings are far away from the station. The ground is rocky which can attribute to an increase of global radiation due to back-scattering depending on the season of the year.

Figure 3.8 Makhado Rabali Station

3.3. 6 MAKHADO MULIMA SITE

Referring to Figure 3.9, it is observed from that Makhado Mulima station is situated closer to the gravel road and surrounded by 3D-buildings. Radiometers that are used to record data in this station need great care in order to eliminate errors.

Figure 3.9 Makhado Mulima Station

An overall observation indicates that there are gravel road near all the stations and in general the region under study is sub-Saharan with forests nearby. Along the rivers, there are concentrated tall trees. Regular calibration of the solar energy measuring instruments in this area may improve the accuracy of the readings recorded.

CHAPTER 4

METHODOLOGY

4.1 INTRODUCTION

In this chapter, the methodology followed to compute the regression coefficients using the Angstrom's first order model for the five different stations selected in Vhembe Region is described. Although one regression model has been employed, three more Angstrom's equations are discussed. The method used to calculate solar variables that are found in Angstrom's linear equation such as extraterrestrial solar radiation on the horizontal surface and possible sunshine hours are explained as well.

4.2 REGRESSION MODELS

A linear relation proposed by Angstrom and modified by Prescott [41, 46], for computation of the average daily global radiation on a horizontal surface is given by (Refer to equation 2.19):

$$\frac{\overline{H}}{\overline{H_0}} = a + b\frac{\overline{N_0}}{\overline{N}} \qquad 4.1$$

where $\overline{H}$ = average of the daily global radiation on a horizontal surface, $\overline{H}_o$ = average of the daily global radiation on a horizontal surface on clear days at the same location, $\overline{N}_0$= daily average of duration of actual sunshine hours, $\overline{N}$ = daily average of duration of possible sunshine hours, and a and b are the revised empirical constants/regression coefficients.

Although Equation 4.1 is the only model that will be used in this study for parameterisation, other models that use actual sun shine hours and daily global solar radiation for the determination of the regression coefficients exist.

For instance, models given by Equations 4.2, 4.3 and 4.4.

Quadratic [46]: $$\frac{\overline{H}}{\overline{H_0}} = a + b\left(\frac{\overline{N_0}}{\overline{N}}\right) + c\left(\frac{\overline{N_0}}{\overline{N}}\right)^2 \tag{4.2}$$

Third degree [47]: $$\frac{\overline{H}}{\overline{H_0}} = a + b\left(\frac{\overline{N_0}}{\overline{N}}\right) + c\left(\frac{\overline{N_0}}{\overline{N}}\right)^2 + d\left(\frac{\overline{N_0}}{\overline{N}}\right)^3 \tag{4.3}$$

Logarithmic [48]: $$\frac{\overline{H}}{\overline{H_0}} = a + b\log\left(\frac{\overline{N_0}}{\overline{N}}\right) \tag{4.4}$$

4.3 COMPUTATION OF SOLAR VARIABLES

With reference to the model in Equation 4.1, $\overline{H}$ is measured as average of an hourly daily global solar radiation recorded at the geographical location of the selected stations in MJ/m^2/day. The other parameters computed in order to find the regression coefficients a and b, are (i) the daily average extraterrestrial solar radiation on the horizontal surface, $\overline{H_o}$ in MJ/m^2/day and (ii) the daily possible sunshine hours, $\overline{N}$.

4.3.1 The extraterrestrial global radiation ($\overline{H}_o$)

The daily extraterrestrial radiation on a horizontal surface, H_0, is calculated as a function of the solar constant *(*I_{sc}*)*, the latitude of the site on study(ϕ), the eccentricity correction factor of the Earth's orbit (E_o), the solar declination $(\delta)$and the mean sunrise hour angle (ω_s) using Equation 4.5 [32, 33].

$$\overline{H_0} = \frac{24}{\pi} I_{sc} E_o\left(\cos\delta \cdot \cos\phi \cdot \sin\omega_s + \frac{\pi w_s}{180}\sin\phi \cdot \sin\omega_s\right) \tag{4.5}$$

where $E_o = 1 + 0.033\cos\frac{360n}{365}$

where I_{sc} is the solar constant defined as the amount of energy received at the top of the Earth's atmosphere measured at an average distance between the Earth and the Sun on a surface oriented perpendicular to the Sun. The generally accepted solar constant has been approximated as 1367 Wm^{-2} by the World Meteorological Organization (WMO),

n = the day of the year, $1 \leq n \leq 365$,

δ = solar declination angle, (as in Equation 2.7) which can be expressed as follows [37, 58]:

$$\delta = 23.45^0 \sin\left[\frac{360}{365}(284+n)\right], \qquad 4.6$$

where, ϕ = latitude of the solar radiation station or site of study and ω_s = mean sunrise hour angle, (as in Equation 2.9) in degrees and is expressed as [60]:

$$\cos w_s = -\tan\phi \cdot \tan\delta \qquad 4.7$$

Sunset hour angle depends on the solar declination angle and latitude of the geographical study area.

4.3.2 Actual sunshine hours (N_o)

Actual sunshine hours are measured at large stations in almost all countries of the world using Campbell Stokes sunshine recorder. In the present study the daily actual sunshine data (in hours) obtained from the South African Weather Services (SAWS) has been used.

4.3.3 Possible sunshine hours (N)

The daily possible sunshine hours depend on the location and day of the year and can be computed using the equation given in the subsequence page [32]:

$$N = \frac{2\omega_s}{15}\cos^{-1}(-\tan\phi \cdot \tan\delta) \qquad 4.9$$

In the northern and southern hemispheres, the shortest day lengths are observed during winter season irrespective of the latitude.

4.3.4 The regression coefficients *a* and *b*

The possible sunshine hours or day length *N*, horizontal daily extraterrestrial solar radiation H_o, horizontal daily global solar radiation *H* and actual sunshine duration N_o are the parameters that determine the regression coefficients of a particular location. The daily averages of each of the parameters mentioned above are used to determine the monthly and annual average regression coefficients. The daily clearness index $\frac{\overline{H}}{\overline{H_0}}$ and relative sunshine hours $\frac{\overline{N_0}}{\overline{N}}$ for each station are computed in order to draw the best fit lines. Regression coefficients *a* and *b* are read from the equation given on each graph, *b* represents the gradient while *a* is for the y-intercept of the graph. The averages of the monthly and annual regression coefficients of each station are calculated. The annual values of *a* and *b* are compared.

The Angstrom-Prescott linear equation was used to calculate the horizontal global solar radiation also called estimated global solar radiation. The following parameters are substituted in place of parameters make reading as complete as possible: N_o, *N*, H_o and average monthly regression coefficients *a* and *b* are determined. *N* and H_o are computed , *N* is the data received from SAWS while *a* and *b* are the monthly regression coefficients of the station whose correlation coefficients are the best, i.e. above 90% for all the months of study. The accuracy of the estimated values was later tested by calculating the correlation coefficient of regression, the root mean square error and the mean bias error.

The R-squared statistic (R^2) or correlation of coefficient (*CC*) indicates the percentage of variability of the dependent variable as it is fitted in the full model [40, 50 and 51]. The standard error of the estimate shows the value for the standard deviation of the residuals, estimated by the square root of the mean squared error. The mean absolute error is a measure of the forecast accuracy, calculated by summing the absolute errors and dividing by the number of observations.

The square root of the mean squared error (RMSE) and the mean absolute error are the fundamental measures of accuracy. It is given by

$$RMSE = \sqrt{\frac{1}{n}\left(\sum_{i}^{n} d_i^{\ 2}\right)} \qquad 4.10$$

The mean bias error (MBE) is given by

$$MBE = \frac{1}{n}\sum_{i}^{n} d_i \qquad 4.11$$

where n is the number of data pairs observed, d_i is the difference between the i th estimated and the i th measured horizontal global radiation.

The number of data pairs depends on the number of days used in a month during computation of the respective regression coefficients per station. The t-statistic is given by the equation [63]:

$$t = \sqrt{\frac{(n-1)\cdot MBE^{\ 2}}{RMSE^{\ 2} - MBE^{\ 2}}} \qquad 4.12$$

The t-statistic is a statistical indicator that allows models to be compared and at the same time indicates whether or not the model's estimates are statistically significant at a particular confidence interval [64]. Torgul verified that the t-statistic used in addition to RMSE and MBE gave more reliable and explanatory results [63]. The smaller the value of t-statistic calculated the better is the model's performance. In order to determine whether the model's estimates are statistically significant, t-critical value must be obtained from the standard statistical tables, i.e. $t_{\frac{\alpha}{2}}$ at α level of confidence and (n-1) degree of freedom. The model's estimate is statistically significance if t-calculated is less than t-critical.

CHAPTER 5

DATA ASSIMILATION

5.1 INTRODUCTION

The main objective of this research was to determine the regression coefficients a and b for the selected stations in the Vhembe Region, in Limpopo South Africa. In chapter 3 a detailed description of the methods for the computation of the regression coefficients of a and b was presented. According to the initial plans of this study, the data logger was used to record the horizontal global solar radiation data at Vuwani Science Resource Centre whose coordinates are as follows: Latitude: 23.1303^0 S, Longitude: 30.4198^o E. However due to some technical problems data was collected for a period of six months. The data collected during those six months will be compared with the data obtained from the Agricultural council (ARC) and we will then explore the possibility of calibration for future use.

As given in Chapter 4, the Angstrom-Prescott linear equation [4.1] is used for the computation of the regression coefficients a and b. The equation is rewritten here [41, 46]:

$$\frac{\overline{H}}{\overline{H_o}} = a + b\frac{\overline{N_o}}{\overline{N}} \qquad 5.1$$

To determine the values of a and b, it is necessary to compute or measure the values of the parameters N, N_o, H_o and H for the area under study.

5.2 DAILY POSSIBLE SUNSHINE HOURS (N)

The daily possible sunshine hours N for the selected stations are calculated using relation 4.9 [29]. The daily possible sunshine hours are solar sunrise hour angle dependant while sunrise hour angle changes with day number, n, of the year.

5.2.1 Solar declination (δ)

The results of solar declination angles computed using Equation 4.6 is displayed graphically in Figure 5.1

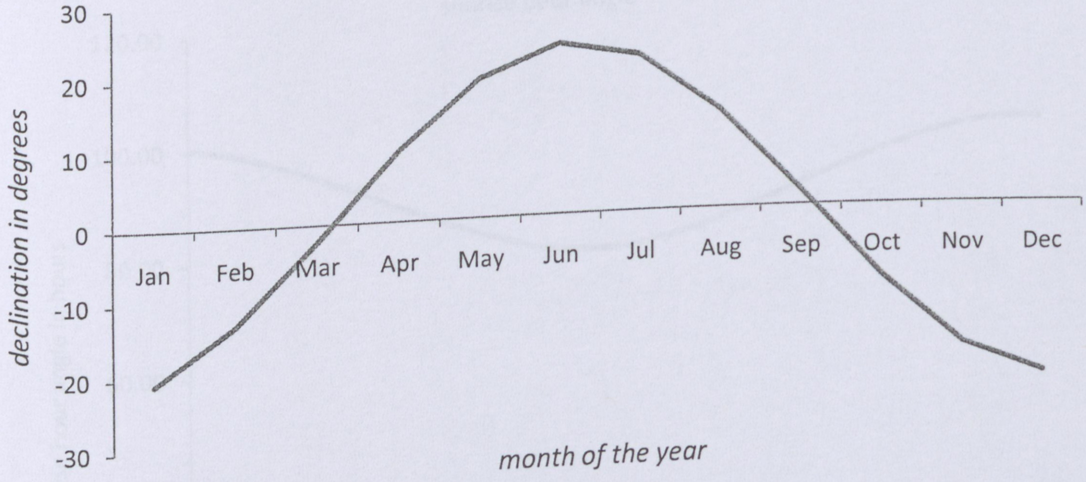

Figure. 5.1 Variation of solar declination angles in a year

The monthly average of daily solar declination angle in the northern hemisphere is comparably the same as in the southern hemisphere [41]. The variation of solar declination angles depends on the day number and independent of the altitude or longitude of the geographical site of study. It is noticed from Figure 5.1 that the solar declination angle is zero on March the 21st as well as on September 22nd as expected. These days are referred to as vernal and autumnal equinoxes and have a value of approximately $+23.5^0$ at winter and about - 23.5^0 at summer in the Southern hemisphere which opposes the Northern hemisphere due to seasons that differ.

5.2.2 Daily sunrise hour angle (ω_s)

The daily sunrise hour angles for each of the selected stations are computed using Equation 4.7. For illustration, Malamulele Mhinga station's results are presented graphically in Figure 5.2. All stations in the study ought to have the closely matched daily sunset/rise hour angle given the proximity of their latitudes. At low solar declination angle, the respective sunrise hour angles are is high.

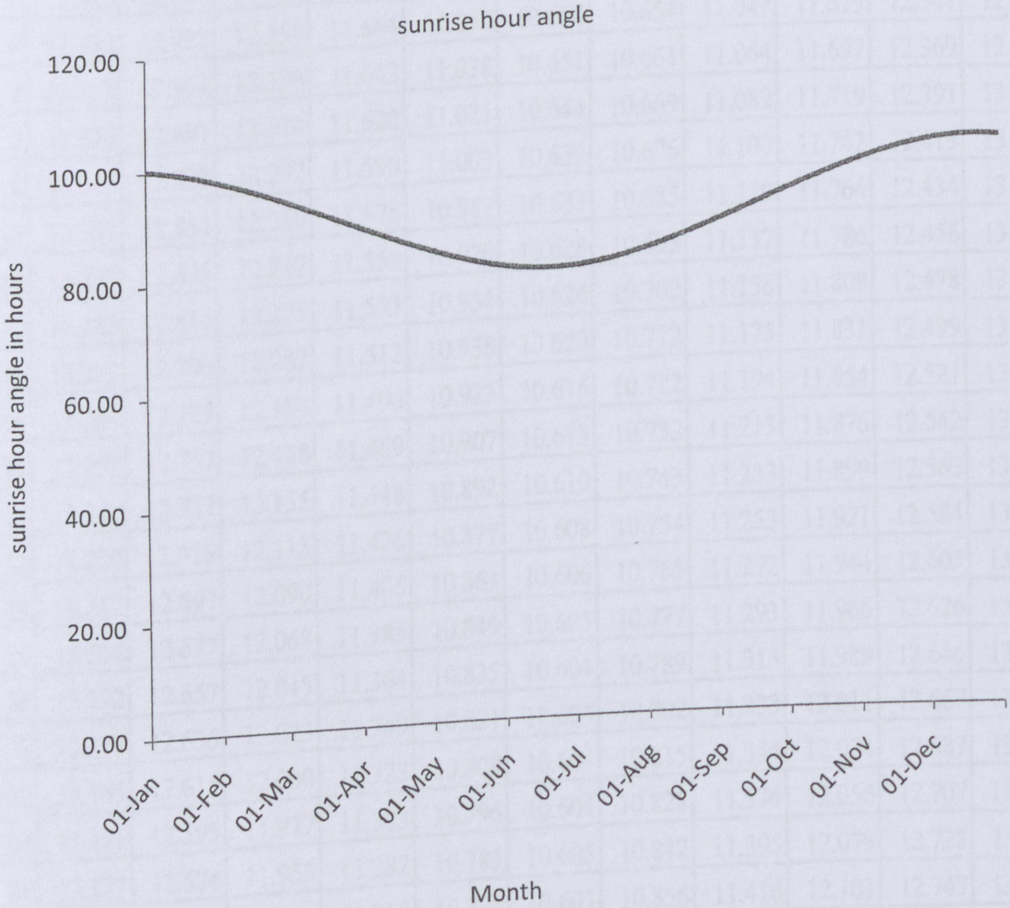

Figure.5.2 Daily sunrise hour angles (ω_s) of Malamulele Mhinga Station (22.79675^0 S; 30.842190 E)

5.2.3 Computed daily possible sunshine hours for the selected stations.

The daily possible sunshine hour values, calculated from Equation 4.9, and using the above inputs are presented in Tables 5.1 – 5.5 below.

n	Jan	Feb	Mar	Apr	May	Jun	Jul	Aug	Sep	Oct	Nov	Dec
1	13.367	13.013	12.467	11.775	11.146	10.698	10.626	10.962	11.566	12.236	12.881	13.307
2	13.361	12.997	12.445	11.753	11.128	10.689	10.631	10.978	11.587	12.258	12.900	13.315
3	13.356	12.979	12.424	11.731	11.109	10.680	10.636	10.995	11.609	12.281	12.918	13.324
4	13.349	12.962	12.402	11.708	11.091	10.672	10.641	11.012	11.631	12.303	12.936	13.331
5	13.342	12.945	12.380	11.686	11.073	10.665	10.648	11.029	11.653	12.325	12.953	13.339
6	13.335	12.927	12.358	11.664	11.055	10.658	10.654	11.047	11.675	12.347	12.971	13.346
7	13.328	12.909	12.336	11.642	11.038	10.651	10.661	11.064	11.697	12.369	12.988	13.352
8	13.320	12.891	12.314	11.620	11.021	10.644	10.669	11.082	11.719	12.391	13.005	13.359
9	13.311	12.872	12.292	11.598	11.003	10.639	10.676	11.100	11.742	12.413	13.022	13.364
10	13.302	12.854	12.269	11.576	10.987	10.633	10.685	11.119	11.764	12.434	13.038	13.369
11	13.293	12.835	12.247	11.555	10.970	10.628	10.693	11.137	11.786	12.456	13.054	13.374
12	13.283	12.816	12.225	11.533	10.954	10.624	10.702	11.156	11.809	12.478	13.070	13.378
13	13.273	12.796	12.202	11.512	10.938	10.620	10.712	11.175	11.831	12.499	13.085	13.382
14	13.263	12.777	12.180	11.490	10.922	10.616	10.722	11.194	11.854	12.521	13.101	13.386
15	13.252	12.757	12.158	11.469	10.907	10.613	10.732	11.213	11.876	12.542	13.115	13.389
16	13.240	12.737	12.135	11.448	10.892	10.610	10.743	11.233	11.899	12.563	13.130	13.391
17	13.229	12.718	12.113	11.426	10.877	10.608	10.754	11.253	11.921	12.584	13.144	13.393
18	13.217	12.697	12.090	11.405	10.863	10.606	10.765	11.272	11.944	12.605	13.158	13.395
19	13.204	12.677	12.068	11.385	10.849	10.605	10.777	11.293	11.966	12.626	13.172	13.396
20	13.192	12.657	12.045	11.364	10.835	10.604	10.789	11.313	11.989	12.646	13.185	13.396
21	13.179	12.636	12.023	11.343	10.821	10.604	10.802	11.333	12.011	12.667	13.198	13.396
22	13.165	12.615	12.000	11.323	10.808	10.604	10.815	11.354	12.034	12.687	13.211	13.396
23	13.151	12.595	11.977	11.303	10.796	10.604	10.828	11.374	12.056	12.707	13.223	13.395
24	13.137	12.574	11.955	11.282	10.783	10.605	10.842	11.395	12.079	12.728	13.235	13.394
25	13.123	12.552	11.932	11.263	10.771	10.607	10.856	11.416	12.101	12.747	13.246	13.392
26	13.108	12.531	11.910	11.243	10.760	10.609	10.870	11.437	12.124	12.767	13.257	13.390
27	13.093	12.510	11.887	11.223	10.748	10.611	10.885	11.458	12.146	12.787	13.268	13.387
28	13.078	12.488	11.865	11.204	10.737	10.614	10.899	11.479	12.169	12.806	13.278	13.384
29	13.062		11.842	11.184	10.727	10.618	10.915	11.501	12.191	12.825	13.288	13.380
30	13.046		11.820	11.165	10.717	10.622	10.930	11.522	12.214	12.844	13.298	13.376
31	13.030		11.798		10.707		10.946	11.544		12.863		13.372
Averag	13.225	12.761	12.134	11.462	10.904	10.629	10.758	11.240	11.888	12.558	13.111	13.373

Table 5.1 Possible sunshine hours for Thohoyandou Mutale station

n	Jan	Feb	Mar	Apr	May	Jun	Jul	Aug	Sep	Oct	Nov	Dec
1	13.371	13.016	12.468	11.774	11.144	10.694	10.622	10.959	11.564	12.237	12.884	13.311
2	13.366	13.000	12.447	11.752	11.125	10.685	10.626	10.975	11.586	12.259	12.903	13.319
3	13.360	12.982	12.425	11.730	11.107	10.676	10.632	10.992	11.608	12.281	12.921	13.328
4	13.353	12.965	12.403	11.707	11.088	10.668	10.637	11.009	11.630	12.304	12.939	13.336
5	13.347	12.948	12.381	11.685	11.070	10.661	10.643	11.026	11.652	12.326	12.956	13.343
6	13.339	12.930	12.359	11.663	11.052	10.653	10.650	11.044	11.674	12.348	12.974	13.350
7	13.332	12.912	12.337	11.641	11.035	10.647	10.657	11.061	11.696	12.370	12.991	13.357
8	13.324	12.893	12.315	11.619	11.018	10.640	10.664	11.079	11.719	12.392	13.008	13.363
9	13.315	12.875	12.293	11.597	11.000	10.634	10.672	11.097	11.741	12.414	13.025	13.368
10	13.306	12.856	12.270	11.575	10.984	10.629	10.681	11.116	11.763	12.436	13.041	13.374
11	13.297	12.837	12.248	11.553	10.967	10.624	10.689	11.134	11.786	12.458	13.057	13.378
12	13.287	12.818	12.226	11.532	10.951	10.619	10.698	11.153	11.808	12.479	13.073	13.383
13	13.277	12.799	12.203	11.510	10.935	10.615	10.708	11.172	11.831	12.501	13.089	13.387
14	13.266	12.779	12.181	11.489	10.919	10.612	10.718	11.192	11.853	12.522	13.104	13.390
15	13.256	12.760	12.158	11.467	10.904	10.609	10.728	11.211	11.876	12.543	13.119	13.393
16	13.244	12.740	12.136	11.446	10.889	10.606	10.739	11.231	11.898	12.565	13.133	13.395
17	13.233	12.720	12.113	11.425	10.874	10.604	10.750	11.250	11.921	12.586	13.148	13.397
18	13.220	12.700	12.090	11.404	10.859	10.602	10.762	11.270	11.943	12.607	13.162	13.399
19	13.208	12.679	12.068	11.383	10.845	10.601	10.773	11.290	11.966	12.628	13.175	13.400
20	13.195	12.659	12.045	11.362	10.831	10.600	10.786	11.311	11.989	12.648	13.189	13.400
21	13.182	12.638	12.023	11.341	10.818	10.599	10.798	11.331	12.011	12.669	13.202	13.401
22	13.169	12.617	12.000	11.321	10.805	10.600	10.811	11.352	12.034	12.689	13.214	13.400
23	13.155	12.596	11.977	11.300	10.792	10.600	10.825	11.372	12.057	12.710	13.227	13.399
24	13.141	12.575	11.955	11.280	10.780	10.601	10.838	11.393	12.079	12.730	13.238	13.398
25	13.126	12.554	11.932	11.260	10.767	10.603	10.852	11.414	12.102	12.750	13.250	13.396
26	13.111	12.533	11.910	11.240	10.756	10.605	10.867	11.435	12.124	12.769	13.261	13.394
27	13.096	12.511	11.887	11.221	10.744	10.607	10.881	11.457	12.147	12.789	13.272	13.391
28	13.081	12.490	11.864	11.201	10.734	10.610	10.896	11.478	12.169	12.808	13.282	13.388
29	13.065		11.842	11.182	10.723	10.613	10.911	11.499	12.192	12.828	13.292	13.385

Table 5.2 Possible sunshine hours for Malamulele Mhinga station

n	Jan	Feb	Mar	Apr	May	Jun	Jul	Aug	Sep	Oct	Nov	Dec
1	13.371	13.016	12.468	11.774	11.144	10.694	10.622	10.959	11.564	12.237	12.884	13.311
2	13.366	13.000	12.447	11.752	11.125	10.685	10.626	10.975	11.586	12.259	12.903	13.319
3	13.360	12.982	12.425	11.730	11.107	10.676	10.632	10.992	11.608	12.281	12.921	13.328
4	13.353	12.965	12.403	11.707	11.088	10.668	10.637	11.009	11.630	12.304	12.939	13.336
5	13.347	12.948	12.381	11.685	11.070	10.661	10.643	11.026	11.652	12.326	12.956	13.343
6	13.339	12.930	12.359	11.663	11.052	10.653	10.650	11.044	11.674	12.348	12.974	13.350
7	13.332	12.912	12.337	11.641	11.035	10.647	10.657	11.061	11.696	12.370	12.991	13.357
8	13.324	12.893	12.315	11.619	11.018	10.640	10.664	11.079	11.719	12.392	13.008	13.363
9	13.315	12.875	12.293	11.597	11.000	10.634	10.672	11.097	11.741	12.414	13.025	13.368
10	13.306	12.856	12.270	11.575	10.984	10.629	10.681	11.116	11.763	12.436	13.041	13.374
11	13.297	12.837	12.248	11.553	10.967	10.624	10.689	11.134	11.786	12.458	13.057	13.378
12	13.287	12.818	12.226	11.532	10.951	10.619	10.698	11.153	11.808	12.479	13.073	13.383
13	13.277	12.799	12.203	11.510	10.935	10.615	10.708	11.172	11.831	12.501	13.089	13.387
14	13.266	12.779	12.181	11.489	10.919	10.612	10.718	11.192	11.853	12.522	13.104	13.390
15	13.256	12.760	12.158	11.467	10.904	10.609	10.728	11.211	11.876	12.543	13.119	13.393
16	13.244	12.740	12.136	11.446	10.889	10.606	10.739	11.231	11.898	12.565	13.133	13.395
17	13.233	12.720	12.113	11.425	10.874	10.604	10.750	11.250	11.921	12.586	13.148	13.397
18	13.220	12.700	12.090	11.404	10.859	10.602	10.762	11.270	11.943	12.607	13.162	13.399
19	13.208	12.679	12.068	11.383	10.845	10.601	10.773	11.290	11.966	12.628	13.175	13.400
20	13.195	12.659	12.045	11.362	10.831	10.600	10.786	11.311	11.989	12.648	13.189	13.400
21	13.182	12.638	12.023	11.341	10.818	10.599	10.798	11.331	12.011	12.669	13.202	13.401
22	13.169	12.617	12.000	11.321	10.805	10.600	10.811	11.352	12.034	12.689	13.214	13.400
23	13.155	12.596	11.977	11.300	10.792	10.600	10.825	11.372	12.057	12.710	13.227	13.399
24	13.141	12.575	11.955	11.280	10.780	10.601	10.838	11.393	12.079	12.730	13.238	13.398
25	13.126	12.554	11.932	11.260	10.767	10.603	10.852	11.414	12.102	12.750	13.250	13.396
26	13.111	12.533	11.910	11.240	10.756	10.605	10.867	11.435	12.124	12.769	13.261	13.394
27	13.096	12.511	11.887	11.221	10.744	10.607	10.881	11.457	12.147	12.789	13.272	13.391
28	13.081	12.490	11.864	11.201	10.734	10.610	10.896	11.478	12.169	12.808	13.282	13.388
29	13.065		11.842	11.182	10.723	10.613	10.911	11.499	12.192	12.828	13.292	13.385
30	13.049		11.819	11.163	10.713	10.617	10.927	11.521	12.214	12.847	13.302	13.381
31	13.033		11.797		10.703		10.943	11.542		12.866		13.376
Averag	13.229	12.764	12.135	11.461	10.901	10.624	10.754	11.238	11.888	12.560	13.114	13.377

Table 5.3 Possible sunshine hours for Makhado Rabali station.

n	Jan	Feb	Mar	Apr	May	Jun	Jul	Aug	Sep	Oct	Nov	Dec
1	13.409	13.044	12.481	11.768	11.120	10.658	10.583	10.930	11.552	12.243	12.909	13.347
2	13.403	13.027	12.459	11.745	11.101	10.648	10.588	10.947	11.575	12.266	12.927	13.356
3	13.397	13.010	12.437	11.722	11.082	10.640	10.594	10.964	11.597	12.289	12.946	13.365
4	13.391	12.992	12.414	11.699	11.063	10.631	10.599	10.982	11.620	12.312	12.965	13.373
5	13.384	12.974	12.391	11.677	11.045	10.624	10.606	10.999	11.642	12.335	12.983	13.380
6	13.376	12.955	12.369	11.654	11.026	10.616	10.613	11.017	11.665	12.358	13.001	13.387
7	13.369	12.937	12.346	11.631	11.008	10.609	10.620	11.035	11.688	12.380	13.018	13.394
8	13.360	12.918	12.323	11.609	10.990	10.603	10.627	11.054	11.711	12.403	13.036	13.401
9	13.352	12.899	12.301	11.586	10.973	10.597	10.635	11.073	11.734	12.425	13.053	13.406
10	13.342	12.880	12.278	11.563	10.956	10.591	10.644	11.091	11.757	12.448	13.070	13.412
11	13.333	12.860	12.255	11.541	10.939	10.586	10.653	11.111	11.780	12.470	13.086	13.417
12	13.323	12.841	12.232	11.519	10.922	10.581	10.662	11.130	11.803	12.492	13.103	13.421
13	13.312	12.821	12.209	11.497	10.905	10.577	10.672	11.149	11.826	12.514	13.119	13.425
14	13.302	12.801	12.186	11.474	10.889	10.573	10.682	11.169	11.849	12.537	13.134	13.429
15	13.290	12.781	12.162	11.453	10.873	10.570	10.693	11.189	11.872	12.558	13.150	13.432
16	13.279	12.760	12.139	11.431	10.858	10.567	10.704	11.209	11.895	12.580	13.165	13.434
17	13.267	12.740	12.116	11.409	10.843	10.565	10.715	11.230	11.919	12.602	13.180	13.436
18	13.254	12.719	12.093	11.387	10.828	10.563	10.727	11.250	11.942	12.623	13.194	13.438
19	13.241	12.698	12.070	11.366	10.813	10.562	10.739	11.271	11.965	12.645	13.208	13.439
20	13.228	12.677	12.046	11.344	10.799	10.561	10.752	11.292	11.988	12.666	13.222	13.439
21	13.215	12.656	12.023	11.323	10.785	10.561	10.765	11.313	12.012	12.687	13.235	13.439
22	13.201	12.634	12.000	11.302	10.772	10.561	10.778	11.334	12.035	12.708	13.248	13.439
23	13.187	12.613	11.977	11.281	10.759	10.561	10.792	11.355	12.058	12.729	13.261	13.438
24	13.172	12.591	11.954	11.260	10.746	10.562	10.806	11.377	12.081	12.750	13.273	13.437
25	13.157	12.569	11.930	11.240	10.733	10.564	10.820	11.398	12.105	12.770	13.285	13.435
26	13.142	12.547	11.907	11.219	10.721	10.566	10.835	11.420	12.128	12.791	13.296	13.433
27	13.127	12.526	11.884	11.199	10.710	10.568	10.850	11.442	12.151	12.811	13.307	13.430
28	13.111	12.503	11.861	11.179	10.698	10.571	10.866	11.463	12.174	12.831	13.318	13.427
29	13.095		11.838	11.159	10.688	10.575	10.881	11.486	12.197	12.851	13.328	13.423
30	13.078		11.814	11.140	10.677	10.579	10.897	11.508	12.220	12.870	13.338	13.419
31	13.061		11.791		10.667		10.914	11.530		12.889		13.414
Averag	13.263	12.785	12.138	11.446	10.871	10.586	10.720	11.217	11.885	12.575	13.145	13.415

Table 5.4 Possible sunshine hours for Makhado Mulima station

n	Jan	Feb	Mar	Apr	May	Jun	Jul	Aug	Sep	Oct	Nov	Dec
1	13.363	13.011	12.466	11.776	11.149	10.701	10.629	10.965	11.567	12.235	12.879	13.303
2	13.358	12.994	12.444	11.753	11.130	10.692	10.634	10.981	11.588	12.258	12.898	13.312
3	13.352	12.977	12.422	11.731	11.112	10.684	10.639	10.998	11.610	12.280	12.916	13.320
4	13.346	12.960	12.401	11.709	11.093	10.676	10.645	11.015	11.632	12.302	12.933	13.328
5	13.339	12.942	12.379	11.687	11.075	10.668	10.651	11.032	11.654	12.324	12.951	13.335
6	13.332	12.925	12.357	11.665	11.058	10.661	10.658	11.049	11.676	12.346	12.968	13.342
7	13.324	12.907	12.335	11.643	11.040	10.654	10.665	11.067	11.698	12.368	12.985	13.349
8	13.316	12.888	12.313	11.621	11.023	10.648	10.672	11.084	11.720	12.390	13.002	13.355
9	13.308	12.870	12.291	11.599	11.006	10.642	10.680	11.102	11.742	12.412	13.019	13.361
10	13.299	12.851	12.269	11.578	10.989	10.637	10.688	11.121	11.765	12.433	13.035	13.366
11	13.290	12.833	12.247	11.556	10.973	10.632	10.697	11.139	11.787	12.455	13.051	13.371
12	13.280	12.814	12.224	11.534	10.957	10.627	10.706	11.158	11.809	12.476	13.067	13.375
13	13.270	12.794	12.202	11.513	10.941	10.623	10.715	11.177	11.832	12.498	13.083	13.379
14	13.259	12.775	12.180	11.491	10.925	10.620	10.725	11.196	11.854	12.519	13.098	13.382
15	13.248	12.755	12.157	11.470	10.910	10.616	10.735	11.215	11.876	12.540	13.113	13.385
16	13.237	12.736	12.135	11.449	10.895	10.614	10.746	11.235	11.899	12.562	13.127	13.387
17	13.226	12.716	12.112	11.428	10.880	10.612	10.757	11.254	11.921	12.583	13.141	13.389
18	13.214	12.696	12.090	11.407	10.866	10.610	10.769	11.274	11.944	12.603	13.155	13.391
19	13.201	12.675	12.067	11.386	10.852	10.608	10.780	11.294	11.966	12.624	13.169	13.392
20	13.189	12.655	12.045	11.366	10.838	10.608	10.793	11.314	11.989	12.645	13.182	13.393
21	13.175	12.634	12.022	11.345	10.825	10.607	10.805	11.335	12.011	12.665	13.195	13.393
22	13.162	12.614	12.000	11.325	10.811	10.607	10.818	11.355	12.034	12.686	13.207	13.392
23	13.148	12.593	11.978	11.304	10.799	10.608	10.831	11.376	12.056	12.706	13.220	13.392
24	13.134	12.572	11.955	11.284	10.786	10.609	10.845	11.397	12.079	12.726	13.231	13.390
25	13.120	12.551	11.933	11.264	10.774	10.611	10.859	11.417	12.101	12.746	13.243	13.388
26	13.105	12.530	11.910	11.245	10.763	10.613	10.873	11.438	12.124	12.765	13.254	13.386
27	13.090	12.509	11.888	11.225	10.752	10.615	10.887	11.460	12.146	12.785	13.265	13.384
28	13.075	12.487	11.865	11.206	10.741	10.618	10.902	11.481	12.168	12.804	13.275	13.380
29	13.059		11.843	11.186	10.730	10.621	10.917	11.502	12.191	12.823	13.285	13.377
30	13.043		11.820	11.167	10.720	10.625	10.933	11.524	12.213	12.842	13.294	13.373
31	13.027		11.798		10.710		10.949	11.545		12.861		13.368
Aver	13.222	12.759	12.134	11.464	10.907	10.632	10.761	11.242	11.888	12.557	13.108	13.369

Table 5.5 Possible sunshine hours for Makhado Alldays station

5.2.4 Discussion of computed possible sunshine hours, N

It is observed from the tables that for all the stations in the study, the average possible sunshine hours decrease from January to June and thereafter show an increasing trend. The longest sunshine hours are noticed during November, December and January and the shortest during the winter month namely May, June and July.

Comparing Tables 5.1 – 5.5, the highest and lowest monthly average possible sunshine hours are noticed at Makhado Mulima station with those values read as 13.415 hours and 10.586 hours respectively. For the corresponding days and months, all stations have approximately the same number of possible sunshine hours. This is due to where the stations are situated, recalling that the stations are very close to each other and in the same region.

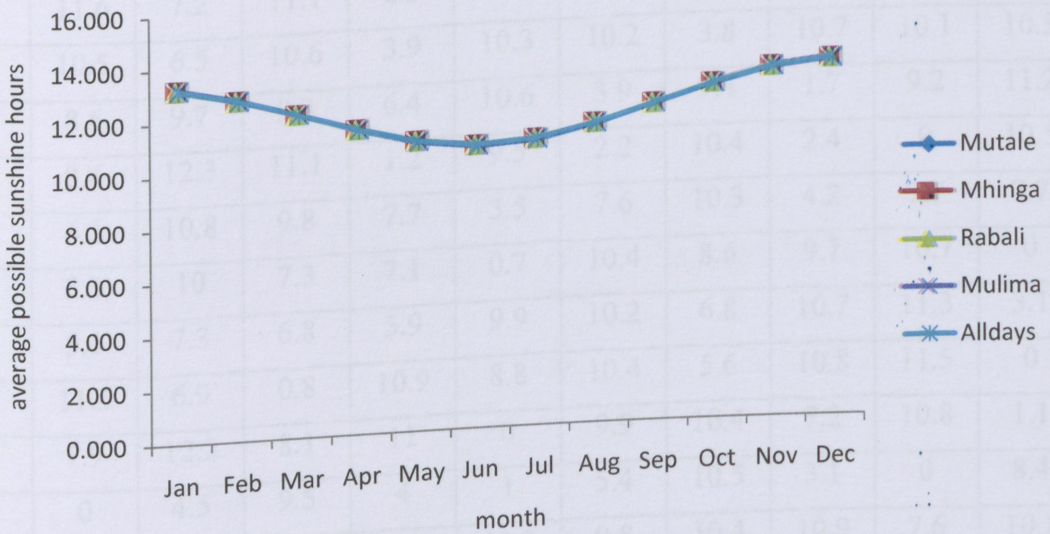

Figure 5.3 Variation of monthly average possible sunshine hours

For a further comparison of possible sunshine hours of the selected stations a graph represents the monthly average daily possible sunshine hours versus the month of the year was drawn. The monthly average daily possible sunshine hours versus the month of the year is represented in Figure 5.3.

5.3 ACTUAL SUNSHINE HOURS, N_o

As explained in Chapter 4, section 4.3.2, the results of the daily actual sunshine hours, N_o data measured by SAWS are presented in Table 5.6.

Day	JAN	FEB	MAR	APR	MAY	JUN	JUL	AUG	SEP	OCT	NOV
1	12.7	11.9	8.9	6.7	8.9	10	2.4	10.5	10.7	10.5	10.6
2	12.2	8.1	10.9	6	2.8	9.9	0	6.6	10.8	10.9	7.6
3	1.5	7.6	5.4	0	9.1	9.8	8.9	10.7	7.7	11.8	11.9
4	2.5	8.1	4	3.6	10.4	10.3	2.6	7.5	7.3	5.2	9.2
5	0	6.2	5.4	1.5	10.8	11.4	3.9	8.7	10.5	0.7	***
6	1.6	10.2	7	6.4	10.8	10	10.5	10.4	4	0.9	9.7
7	9.8	12.5	9.6	9.5	6.7	10.3	9.1	4	0.8	0.2	0.6
8	11.6	7.2	11.1	2.3	2.8	10.2	4.7	10.3	1.5	8.9	6.8
9	10.5	6.5	10.6	3.9	10.3	10.2	3.8	10.7	10.1	10.3	1.6
10	8.6	9.7	9.3	6.4	10.6	3.9	9.4	1.7	9.2	11.2	7.7
11	8.6	12.3	11.1	1.2	9.5	2.2	10.4	2.4	0	10.5	0
12	6.2	10.8	9.8	7.7	3.5	7.6	10.3	4.2	7.7	7.7	10.1
13	8.3	10	7.3	7.1	0.7	10.4	8.6	9.7	10.7	0	***
14	5.1	7.3	6.8	5.9	9.9	10.2	6.8	10.7	11.3	3.1	0
15	11.5	6.9	0.8	10.9	8.8	10.4	5.6	10.8	11.5	0	0
16	7.9	12.2	8.1	11	0	9.9	10.4	7.2	10.8	1.1	9.5
17	0	4.5	9.5	4	1	5.4	10.5	3.1	0	8.4	0.4
18	4.7	0.4	2.7	11.9	10.2	9.8	10.4	10.9	7.6	10.1	0
19	11.4	1.8	4	3.2	10.4	9	3.7	10.3	10.9	11.4	0.8
20	6.9	1.1	8.1	3.4	2.1	10.3	2.4	0	10.8	11	8.4
21	3.1	10.9	0	0.5	0.2	10.4	7.8	10.6	10	11.9	5
22	9	2.3	5.4	6.6	0	10.2	1.6	10.4	10.1	11.8	11.9
23	12.2	8	10.6	0.3	9.5	10.4	10.2	10.1	4.4	5.2	10.8
24	10.6	5.9	6.3	0	10.6	7.3	10.2	***	10.1	8.5	0
25	6.3	7.1	8.8	0	10.4	10.2	8.9	0.7	8.1	11.4	0

26	2.8	6.8	10.9	2.9	9.2	10.3	7.8	10	9.9	4.1	2.3
27	0	0.6	10.6	0	10	3.1	10	10.3	10	5.1	9.2
28	5.3	1.8	9.4	9.1	10.5	0.3	***	7.2	0	4.4	***
29	0	***	3.8	10.9	0	1.8	9.5	10.5	8.8	2.6	0
30	0.1	***	10.8	4.8	0	1.5	0	6.5	10.5	6.1	0.3
31	6.3	***	0.6	***	2.4	***	9	***	***	2.8	***

Table 5.6 Daily Actual sunshine hours, in hours as measured by the SAWS

The symbol *** shows that there is no data recorded during that respective day. No explanation was given for data with zero readings.

5.3.1 Comparison between $\overline{N}$ and $\overline{N_o}$

It is observed in Figure 5.3 that the average monthly possible sunshine hours of the stations in study are almost identical. The average monthly possible sunshine hours of Malamulele Mhinga station are compared to the average monthly actual sunshine hours in Table 5.6 graphically.

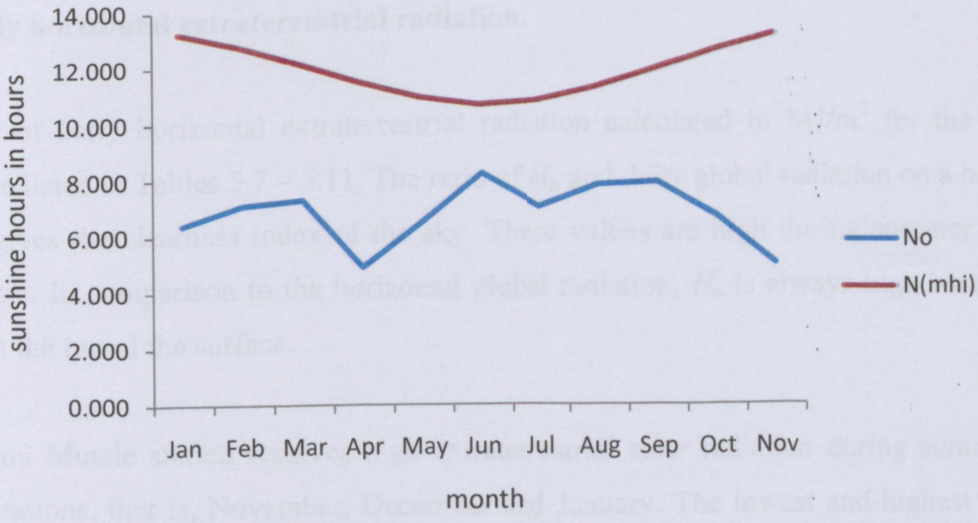

Figure 5.4 Average monthly possible and actual sunshine hours.

Referring to Figure 5.4, N_o and N have the same decreasing trend of sunshine hours during mid-March to mid-April and mid-June to July. The actual sunshine hour data show that there is a need for the calibration of the measuring instrument and/or training of the personnel.

5.4 EXTRATERRESTRIAL SOLAR RADIATION (H_o) ON THE HORIZONTAL SURFACE

H_o is one of the important parameters to be calculated for the determination of solar regression coefficients. The daily extraterrestrial solar radiation on a horizontal surface is computed using Equation 3.5 and converted to MJ/m^2. Daily extraterrestrial solar radiation is computed and thereafter these values were used to determine the monthly average daily extraterrestrial radiation. H_o depends on the declination angles that change with seasons, latitude of the study area and eccentricity correction factor of the Earth's orbit E_o given by the expression [35]:

$$E_o = 1 + 0.033\cos\frac{360n}{365} \qquad 5.2$$

5.4.1 Daily horizontal extraterrestrial radiation.

The results of daily horizontal extraterrestrial radiation calculated in MJ/m^2 for the selected stations are listed in Tables 5.7 – 5.11. The ratio of H_o and daily global radiation on a horizontal surface H gives the clearness index of the sky. These values are high during summer and low during winter. In comparison to the horizontal global radiation, H_o is always high because it is measured at the top of the surface.

Thohoyandou Mutale station receives high extraterrestrial solar radiation during summer time like other stations, that is, November, December and January. The lowest and highest daily H_o are 22.727 and 42.661 MJ/m^2 respectively. In comparison to the station's daily possible sunshine hours, as the possible sunshine hour increases the corresponding extraterrestrial radiation also increases. The minimum and maximum monthly average daily extraterrestrial radiation on the horizontal surface of Malamulele Mhinga, Makhado Mulima, Makhado Rabali and Makhado

Alldays are 22.693 MJ/m^2 - 42.673 MJ/m^2 , 22.389 – 42.779 MJ/m^2, 22.653 – 42.687 MJ/m^2 and 22.775 – 42.651 MJ/m^2 respectively. The difference between the stations' average H_0 lies between 0.092-0.118 MJ/m^2 and 0.264-0.338 MJ/m^2 for maximum and minimum respectively.

n	Jan	Feb	Mar	Apr	May	Jun	Jul	Aug	Sep	Oct	Nov	Dec
1	42.708	41.356	38.305	33.010	27.398	23.353	22.666	25.527	30.841	36.280	40.375	42.362
2	42.692	41.279	38.161	32.819	27.228	23.274	22.704	25.670	31.029	36.443	40.472	42.399
3	42.675	41.200	38.016	32.628	27.060	23.199	22.746	25.815	31.218	36.604	40.566	42.433
4	42.656	41.118	37.868	32.436	26.894	23.127	22.792	25.963	31.407	36.763	40.658	42.466
5	42.636	41.034	37.718	32.243	26.730	23.059	22.842	26.114	31.596	36.921	40.748	42.497
6	42.614	40.948	37.566	32.051	26.569	22.995	22.896	26.267	31.785	37.076	40.836	42.526
7	42.589	40.860	37.412	31.858	26.410	22.935	22.953	26.423	31.974	37.230	40.922	42.554
8	42.564	40.769	37.256	31.665	26.253	22.879	23.015	26.580	32.163	37.382	41.005	42.580
9	42.536	40.675	37.097	31.473	26.098	22.826	23.080	26.740	32.351	37.531	41.087	42.604
10	42.506	40.580	36.937	31.280	25.946	22.777	23.148	26.902	32.539	37.679	41.166	42.626
11	42.475	40.482	36.775	31.087	25.797	22.732	23.221	27.066	32.727	37.824	41.243	42.647
12	42.442	40.381	36.611	30.895	25.650	22.691	23.297	27.232	32.914	37.968	41.318	42.667
13	42.407	40.278	36.445	30.703	25.506	22.654	23.377	27.400	33.101	38.109	41.391	42.684
14	42.370	40.173	36.277	30.511	25.364	22.621	23.460	27.569	33.286	38.249	41.461	42.700
15	42.331	40.065	36.107	30.320	25.226	22.592	23.547	27.740	33.472	38.386	41.530	42.714
16	42.290	39.955	35.936	30.129	25.090	22.567	23.637	27.913	33.656	38.521	41.597	42.727
17	42.247	39.842	35.763	29.939	24.957	22.546	23.731	28.088	33.839	38.653	41.661	42.738
18	42.203	39.727	35.588	29.750	24.828	22.528	23.828	28.264	34.022	38.784	41.724	42.748
19	42.156	39.610	35.412	29.562	24.701	22.515	23.929	28.442	34.203	38.912	41.784	42.755
20	42.107	39.490	35.235	29.375	24.577	22.506	24.033	28.620	34.384	39.038	41.843	42.762
21	42.056	39.368	35.056	29.188	24.457	22.500	24.141	28.800	34.563	39.162	41.900	42.766
22	42.003	39.243	34.875	29.003	24.340	22.499	24.251	28.982	34.741	39.284	41.954	42.769
23	41.948	39.116	34.693	28.819	24.226	22.502	24.365	29.164	34.918	39.403	42.007	42.770
24	41.891	38.987	34.510	28.636	24.115	22.508	24.482	29.347	35.093	39.520	42.058	42.770
25	41.832	38.855	34.326	28.454	24.008	22.519	24.603	29.532	35.267	39.635	42.107	42.768
26	41.771	38.721	34.141	28.274	23.904	22.534	24.726	29.717	35.440	39.747	42.154	42.764
27	41.707	38.584	33.955	28.096	23.803	22.552	24.852	29.903	35.611	39.857	42.199	42.759
28	41.641	38.446	33.767	27.918	23.706	22.575	24.981	30.089	35.781	39.965	42.243	42.752
29	41.573		33.579	27.743	23.613	22.601	25.113	30.276	35.949	40.071	42.284	42.743
30	41.503		33.390	27.569	23.523	22.632	25.248	30.464	36.115	40.175	42.324	42.733
31	41.431		33.200		23.436		25.386	30.652		40.276		42.721
Averag	42.212	40.041	35.870	30.248	25.207	22.727	23.776	27.976	33.533	38.434	41.487	42.661

Table 5.6 Daily extraterrestrial radiation in MJ/m^2 (Thohoyandou Mutale)

n	Jan	Feb	Mar	Apr	May	Jun	Jul	Aug	Sep	Oct	Nov	Dec
1	42.719	41.361	38.298	32.990	27.369	23.320	22.632	25.496	30.818	36.268	40.377	42.373
2	42.704	41.283	38.154	32.799	27.199	23.241	22.671	25.639	31.007	36.432	40.474	42.409
3	42.687	41.204	38.008	32.607	27.031	23.166	22.713	25.785	31.196	36.593	40.569	42.444
4	42.668	41.122	37.860	32.415	26.865	23.094	22.759	25.933	31.385	36.753	40.661	42.477
5	42.647	41.038	37.710	32.222	26.701	23.026	22.809	26.084	31.575	36.911	40.752	42.508
6	42.625	40.951	37.557	32.029	26.539	22.962	22.862	26.238	31.764	37.067	40.840	42.538
7	42.600	40.862	37.402	31.836	26.379	22.901	22.920	26.393	31.953	37.221	40.926	42.565
8	42.574	40.771	37.246	31.643	26.222	22.845	22.981	26.551	32.143	37.373	41.010	42.591
9	42.547	40.677	37.087	31.450	26.068	22.792	23.046	26.711	32.331	37.523	41.091	42.616
10	42.517	40.581	36.926	31.257	25.916	22.743	23.115	26.873	32.520	37.671	41.171	42.638
11	42.485	40.482	36.764	31.064	25.766	22.699	23.188	27.037	32.708	37.817	41.248	42.659
12	42.452	40.381	36.599	30.871	25.619	22.658	23.264	27.203	32.895	37.961	41.323	42.679
13	42.417	40.278	36.433	30.679	25.475	22.620	23.344	27.371	33.082	38.103	41.397	42.696
14	42.380	40.172	36.264	30.487	25.333	22.587	23.427	27.541	33.268	38.243	41.468	42.712
15	42.340	40.064	36.094	30.295	25.194	22.558	23.514	27.713	33.454	38.380	41.537	42.727
16	42.299	39.954	35.923	30.105	25.059	22.533	23.605	27.886	33.638	38.516	41.604	42.739
17	42.256	39.841	35.749	29.914	24.926	22.512	23.699	28.061	33.822	38.649	41.668	42.750
18	42.211	39.725	35.574	29.725	24.796	22.494	23.796	28.237	34.005	38.780	41.731	42.760
19	42.164	39.607	35.398	29.536	24.669	22.481	23.897	28.415	34.187	38.908	41.792	42.768
20	42.115	39.487	35.220	29.349	24.545	22.472	24.001	28.594	34.368	39.035	41.851	42.774
21	42.064	39.364	35.040	29.162	24.425	22.467	24.109	28.774	34.547	39.159	41.908	42.778
22	42.011	39.239	34.859	28.976	24.307	22.465	24.219	28.956	34.726	39.281	41.963	42.781
23	41.956	39.112	34.677	28.792	24.193	22.468	24.333	29.138	34.903	39.401	42.016	42.783
24	41.898	38.982	34.494	28.609	24.082	22.475	24.451	29.322	35.079	39.518	42.067	42.782
25	41.839	38.850	34.309	28.427	23.975	22.485	24.571	29.506	35.253	39.634	42.116	42.780
26	41.777	38.715	34.123	28.247	23.871	22.500	24.694	29.692	35.426	39.747	42.164	42.777
27	41.713	38.578	33.937	28.068	23.770	22.518	24.821	29.878	35.598	39.857	42.209	42.771
28	41.647	38.439	33.749	27.890	23.673	22.541	24.950	30.065	35.768	39.966	42.253	42.764
29	41.579		33.560	27.715	23.580	22.567	25.082	30.252	35.937	40.072	42.295	42.756
30	41.508		33.371	27.541	23.490	22.598	25.217	30.440	36.103	40.176	42.335	42.745
31	41.436		33.181		23.403		25.355	30.629		40.277		42.733
Averag	42.221	40.040	35.857	30.223	25.175	22.693	23.743	27.949	33.515	38.429	41.494	42.673

Table 5.7 Daily extraterrestrial radiation in MJ/m^2 (Malamulele Mhinga)

n	Jan	Feb	Mar	Apr	May	Jun	Jul	Aug	Sep	Oct	Nov	Dec
1	42.824	41.399	38.234	32.810	27.109	23.021	22.329	25.220	30.610	36.165	40.390	42.466
2	42.807	41.319	38.086	32.616	26.936	22.941	22.367	25.364	30.802	36.332	40.491	42.504
3	42.789	41.236	37.937	32.421	26.766	22.865	22.410	25.512	30.994	36.497	40.589	42.540
4	42.769	41.151	37.784	32.225	26.599	22.793	22.456	25.662	31.187	36.661	40.685	42.575
5	42.747	41.063	37.630	32.029	26.433	22.724	22.506	25.814	31.379	36.823	40.779	42.607
6	42.723	40.973	37.474	31.833	26.269	22.659	22.561	25.969	31.572	36.983	40.870	42.638
7	42.698	40.881	37.315	31.637	26.108	22.599	22.619	26.127	31.764	37.141	40.959	42.667
8	42.670	40.786	37.155	31.441	25.949	22.542	22.681	26.286	31.956	37.297	41.046	42.694
9	42.641	40.689	36.992	31.245	25.793	22.489	22.746	26.448	32.148	37.451	41.131	42.719
10	42.609	40.589	36.827	31.048	25.639	22.440	22.816	26.612	32.340	37.603	41.214	42.743
11	42.576	40.487	36.661	30.853	25.488	22.394	22.889	26.778	32.531	37.753	41.294	42.765
12	42.541	40.383	36.492	30.657	25.340	22.353	22.966	26.946	32.722	37.900	41.372	42.785
13	42.504	40.276	36.322	30.462	25.194	22.316	23.046	27.116	32.913	38.046	41.448	42.803
14	42.465	40.166	36.150	30.267	25.051	22.282	23.130	27.288	33.102	38.190	41.522	42.820
15	42.424	40.054	35.976	30.073	24.911	22.253	23.218	27.462	33.291	38.331	41.594	42.835
16	42.380	39.940	35.800	29.879	24.774	22.228	23.310	27.637	33.479	38.470	41.664	42.848
17	42.335	39.823	35.623	29.686	24.640	22.206	23.404	27.814	33.667	38.607	41.731	42.860
18	42.288	39.704	35.444	29.494	24.509	22.189	23.503	27.993	33.853	38.742	41.797	42.869
19	42.239	39.582	35.264	29.303	24.381	22.176	23.605	28.173	34.038	38.874	41.860	42.877
20	42.187	39.458	35.082	29.113	24.256	22.166	23.710	28.354	34.223	39.005	41.921	42.884
21	42.134	39.332	34.899	28.924	24.134	22.161	23.818	28.537	34.406	39.133	41.981	42.888
22	42.078	39.203	34.715	28.736	24.016	22.160	23.930	28.721	34.588	39.259	42.038	42.891
23	42.020	39.072	34.529	28.549	23.901	22.162	24.045	28.906	34.769	39.382	42.093	42.892
24	41.960	38.938	34.342	28.363	23.789	22.169	24.164	29.092	34.949	39.503	42.147	42.892
25	41.898	38.802	34.153	28.179	23.681	22.180	24.285	29.280	35.127	39.622	42.198	42.889
26	41.833	38.663	33.964	27.997	23.576	22.195	24.410	29.468	35.304	39.739	42.247	42.885
27	41.767	38.523	33.774	27.816	23.474	22.214	24.538	29.656	35.479	39.853	42.295	42.879
28	41.698	38.380	33.583	27.636	23.376	22.236	24.668	29.846	35.653	39.965	42.341	42.872
29	41.627		33.391	27.458	23.282	22.263	24.802	30.036	35.825	40.075	42.384	42.862
30	41.553		33.198	27.283	23.191	22.294	24.938	30.227	35.996	40.182	42.426	42.851
31	41.477		33.004		23.104		25.078	30.418		40.287		42.839
Aver	42.299	40.031	35.736	30.001	24.893	22.389	23.450	27.702	33.356	38.383	41.550	42.779

Table 5.8 Daily extraterrestrial radiation in MJ/m^2 (Makhado Mulima)

n	Jan	Feb	Mar	Apr	May	Jun	Jul	Aug	Sep	Oct	Nov	Dec
1	42.733	41.366	38.290	32.967	27.335	23.281	22.592	25.460	30.791	36.255	40.379	42.385
2	42.718	41.288	38.145	32.775	27.164	23.202	22.631	25.603	30.980	36.419	40.476	42.422
3	42.700	41.208	37.999	32.583	26.996	23.126	22.673	25.749	31.170	36.581	40.571	42.457
4	42.681	41.126	37.850	32.390	26.830	23.054	22.719	25.898	31.359	36.741	40.664	42.490
5	42.660	41.041	37.699	32.197	26.666	22.986	22.769	26.049	31.549	36.900	40.755	42.521
6	42.638	40.954	37.546	32.004	26.504	22.922	22.823	26.202	31.739	37.056	40.844	42.551
7	42.613	40.865	37.391	31.810	26.344	22.862	22.880	26.358	31.929	37.211	40.930	42.579
8	42.587	40.773	37.234	31.617	26.187	22.805	22.942	26.516	32.118	37.363	41.015	42.605
9	42.559	40.679	37.075	31.423	26.032	22.752	23.007	26.676	32.307	37.514	41.097	42.629
10	42.529	40.582	36.914	31.230	25.879	22.704	23.076	26.839	32.496	37.663	41.177	42.652
11	42.498	40.483	36.750	31.036	25.730	22.659	23.148	27.003	32.685	37.809	41.254	42.673
12	42.464	40.382	36.585	30.843	25.582	22.618	23.225	27.170	32.873	37.954	41.330	42.693
13	42.428	40.278	36.418	30.650	25.438	22.580	23.305	27.338	33.060	38.096	41.404	42.711
14	42.391	40.172	36.250	30.458	25.296	22.547	23.388	27.508	33.247	38.236	41.475	42.727
15	42.352	40.063	36.079	30.266	25.157	22.518	23.475	27.680	33.432	38.374	41.544	42.741
16	42.310	39.952	35.907	30.075	25.021	22.493	23.566	27.853	33.618	38.510	41.612	42.754
17	42.267	39.838	35.733	29.884	24.888	22.472	23.660	28.028	33.802	38.644	41.677	42.765
18	42.222	39.723	35.557	29.695	24.758	22.454	23.757	28.205	33.985	38.775	41.740	42.775
19	42.174	39.604	35.380	29.506	24.631	22.441	23.858	28.383	34.168	38.904	41.801	42.782
20	42.125	39.483	35.202	29.318	24.507	22.432	23.963	28.562	34.349	39.031	41.861	42.789
21	42.073	39.360	35.022	29.131	24.387	22.426	24.070	28.743	34.529	39.156	41.918	42.793
22	42.020	39.235	34.840	28.945	24.269	22.425	24.181	28.925	34.708	39.278	41.973	42.796
23	41.964	39.107	34.658	28.760	24.155	22.428	24.296	29.108	34.886	39.399	42.026	42.797
24	41.907	38.976	34.474	28.577	24.044	22.434	24.413	29.292	35.062	39.517	42.078	42.797
25	41.847	38.844	34.289	28.394	23.936	22.445	24.533	29.477	35.237	39.632	42.127	42.795
26	41.785	38.709	34.103	28.214	23.832	22.460	24.657	29.663	35.411	39.746	42.175	42.791
27	41.720	38.571	33.915	28.035	23.731	22.478	24.784	29.849	35.583	39.857	42.221	42.786
28	41.654	38.432	33.727	27.857	23.634	22.501	24.913	30.036	35.753	39.966	42.265	42.779
29	41.585		33.538	27.681	23.540	22.527	25.046	30.224	35.922	40.072	42.307	42.770
30	41.514		33.348	27.507	23.450	22.558	25.181	30.413	36.089	40.177	42.347	42.759
31	41.441		33.158		23.364		25.319	30.601		40.279		42.747
Avera	42.231	40.039	35.841	30.194	25.138	22.653	23.705	27.917	33.494	38.423	41.501	42.687

Table 5.9 Daily extraterrestrial radiation in MJ/m^2 (Makhado Rabali)

n	Jan	Feb	Mar	Apr	May	Jun	Jul	Aug	Sep	Oct	Nov
1	42.698	41.352	38.310	33.027	27.422	23.381	22.694	25.552	30.860	36.289	40.373
2	42.682	41.276	38.167	32.836	27.252	23.302	22.732	25.695	31.048	36.452	40.470
3	42.665	41.197	38.022	32.645	27.084	23.227	22.774	25.841	31.237	36.613	40.564
4	42.647	41.115	37.875	32.453	26.919	23.155	22.820	25.989	31.426	36.771	40.656
5	42.626	41.032	37.725	32.261	26.755	23.087	22.870	26.139	31.614	36.929	40.746
6	42.604	40.946	37.574	32.069	26.594	23.023	22.924	26.292	31.803	37.084	40.833
7	42.580	40.858	37.420	31.877	26.435	22.963	22.981	26.447	31.992	37.237	40.919
8	42.555	40.767	37.264	31.684	26.278	22.907	23.042	26.605	32.180	37.388	41.002
9	42.527	40.674	37.106	31.491	26.124	22.854	23.107	26.764	32.368	37.538	41.083
10	42.498	40.579	36.946	31.299	25.972	22.805	23.176	26.926	32.556	37.685	41.162
11	42.466	40.481	36.784	31.107	25.822	22.760	23.248	27.090	32.743	37.830	41.238
12	42.433	40.381	36.621	30.915	25.676	22.719	23.324	27.255	32.930	37.973	41.313
13	42.399	40.278	36.455	30.723	25.532	22.682	23.404	27.423	33.116	38.114	41.386
14	42.362	40.173	36.287	30.531	25.390	22.649	23.487	27.592	33.302	38.253	41.456
15	42.323	40.066	36.118	30.340	25.252	22.620	23.574	27.764	33.486	38.390	41.525
16	42.282	39.956	35.947	30.150	25.116	22.595	23.664	27.936	33.670	38.525	41.591
17	42.240	39.844	35.775	29.961	24.984	22.574	23.758	28.111	33.854	38.657	41.655
18	42.195	39.729	35.600	29.772	24.854	22.557	23.856	28.287	34.036	38.787	41.718
19	42.149	39.612	35.424	29.583	24.728	22.543	23.956	28.464	34.217	38.915	41.778
20	42.100	39.492	35.247	29.396	24.604	22.534	24.060	28.642	34.397	39.041	41.836
21	42.049	39.370	35.068	29.210	24.484	22.529	24.168	28.822	34.576	39.164	41.893
22	41.997	39.246	34.888	29.025	24.367	22.527	24.278	29.003	34.753	39.285	41.947
23	41.942	39.120	34.707	28.841	24.253	22.530	24.392	29.185	34.930	39.404	42.000
24	41.885	38.990	34.524	28.658	24.142	22.537	24.509	29.368	35.105	39.521	42.050
25	41.826	38.859	34.340	28.477	24.035	22.547	24.629	29.552	35.279	39.636	42.099
26	41.765	38.725	34.155	28.297	23.931	22.562	24.752	29.737	35.451	39.748	42.146
27	41.702	38.589	33.969	28.119	23.830	22.580	24.878	29.923	35.622	39.858	42.191
28	41.636	38.451	33.783	27.942	23.733	22.603	25.007	30.109	35.791	39.965	42.235
29	41.569		33.595	27.767	23.640	22.629	25.139	30.296	35.959	40.071	42.276
30	41.499		33.406	27.593	23.550	22.660	25.274	30.484	36.125	40.174	42.316
31	41.427		33.217		23.464		25.412	30.671		40.275	

Table 5.10 Daily extraterrestrial radiation in MJ/m^2 (Makhado Alldays)

5.4.2 Monthly average daily extraterrestrial radiation

The monthly average daily extraterrestrial radiation computed from Tables 5.7-5.11 is listed in Table 5.11.

	Mutale	Mhinga	Rabali	Alldays	Mulima
Jan	42.212	42.221	42.231	42.204	42.299
Feb	40.041	40.040	40.039	40.041	40.031
Mar	35.870	35.857	35.841	35.881	35.736
Apr	30.248	30.223	30.194	30.268	30.001
May	25.207	25.175	25.138	25.233	24.893
Jun	22.727	22.693	22.653	22.755	22.389
Jul	23.776	23.743	23.705	23.803	23.450
Aug	27.976	27.949	27.916	27.999	27.702
Sep	33.533	33.515	33.494	33.547	33.356
Oct	38.434	38.429	38.423	38.438	38.383
Nov	41.487	41.494	41.501	41.481	41.550
Dec	42.661	42.673	42.687	42.651	42.789

Table 5.11 Monthly average daily extraterrestrial radiations in MJ/m^2

It is evident from Table 5.11 that the computed H_o values for the stations in a given month are very close to each other. There is a slight variation of monthly average daily extraterrestrial solar radiation. The highest values are observed during November, December, January and February with 40 MJ/m^2 and above for all the selected stations. The lowest monthly average global radiation of these stations is obtained in May, June and July ranging from 22.389 – 25.207 MJ/m^2 during winter.

This is clearly indicated by the graph drawn in Figure 5.4 below. The graphs overlap, indicating that the selected stations receive almost the same magnitude of horizontal extraterrestrial radiation above the surface of the earth. The minimum value is about 22.309 MJ/m^2 while maximum extraterrestrial radiation is observed during summer which ranges from 41.487 to 42.789MJ/m^2.

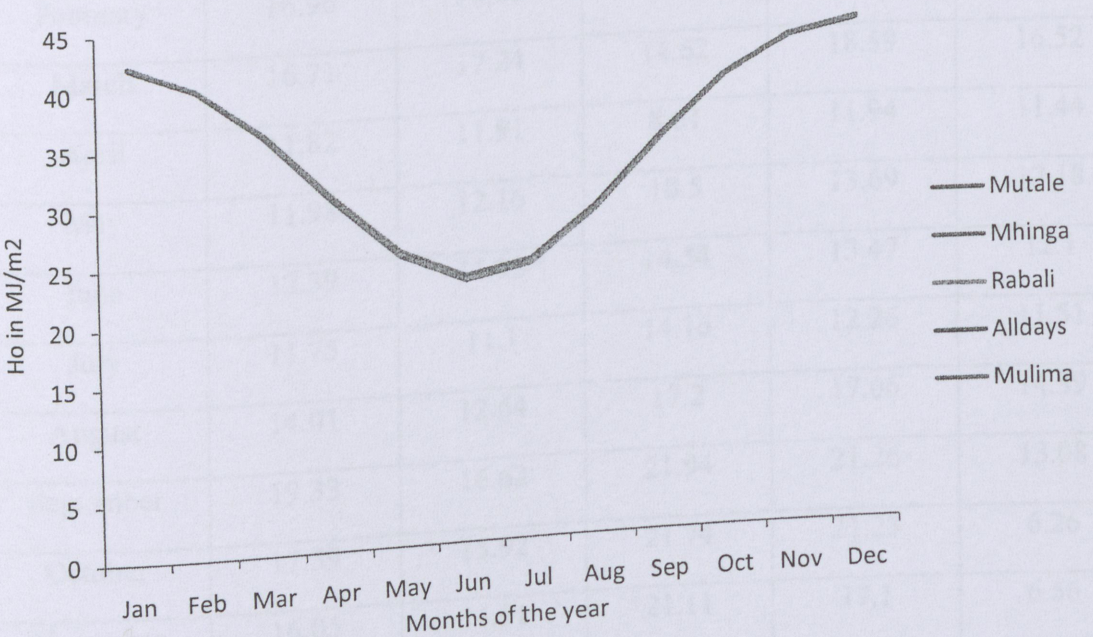

Figure 5.5 Variation of monthly average daily extraterrestrial radiation

It may also be seen in Figure 5.5 that the horizontal extraterrestrial solar radiation decreases in winter.

5.5 DAILY GLOBAL SOLAR RADIATION (*H*)

The monthly average daily global radiation is another parameter found in Angstrom-Prescott linear equation [5.1]. In order to determine the monthly average H, daily ground global measurements are essential. The monthly average daily global radiation of the five selected stations is listed in Table 5.12. December is excluded in each station. During computation of regression coefficients, the month of December has been excluded since there is no daily actual sunshine hour data for this month.

Station	Mutale	Mhinga	Rabali	Alldays	Mulima
January	17.8	18.15	20.77	18.92	16.53
February	16.96	18.06	21.47	19.32	17.97
March	16.71	17.24	14.62	18.59	16.52
April	11.82	11.91	8.61	11.94	11.44
May	11.98	12.16	10.5	13.69	12.18
June	12.39	11.95	14.54	13.47	12.1
July	11.75	11.1	14.16	12.26	11.51
August	14.01	12.64	17.2	17.06	14.39
September	19.33	16.62	21.94	21.26	13.08
October	17.59	15.92	21.74	21.23	6.26
November	16.05	14.91	21.11	17.1	6.56

Table 5.12 Monthly average daily global solar radiation in MJ/m^2

Environmental conditions and the geographic positions of the stations determine the amount of global radiation received per day. It could be noticed from Table 5.12 that the Rabali location receives higher global radiation than any other station selected except during March, April and May. Rabali is surrounded by shrubs and it is a semi-desert with no industrial companies nearby that releases unwanted gas. As stated in Section 5.1, the rocky ground gives more scattering that increases the horizontal global solar radiation. One can predict therefore that there could be some errors that might have occurred during measurements or it could be due to the rainfall in that location. The trend of increasing and decreasing of global radiation data is the same with some exceptions during April.

About 40% of the days on which daily global radiation was measured, data was recorded as zero during October and November at Mulima station which eventually contributes to a lesser value of daily global radiation. Hence these two months are excluded during computation of regression coefficients.

The monthly average daily global solar radiations listed in Table 5.12 are translated into a graphical representation in Figure 5.6.

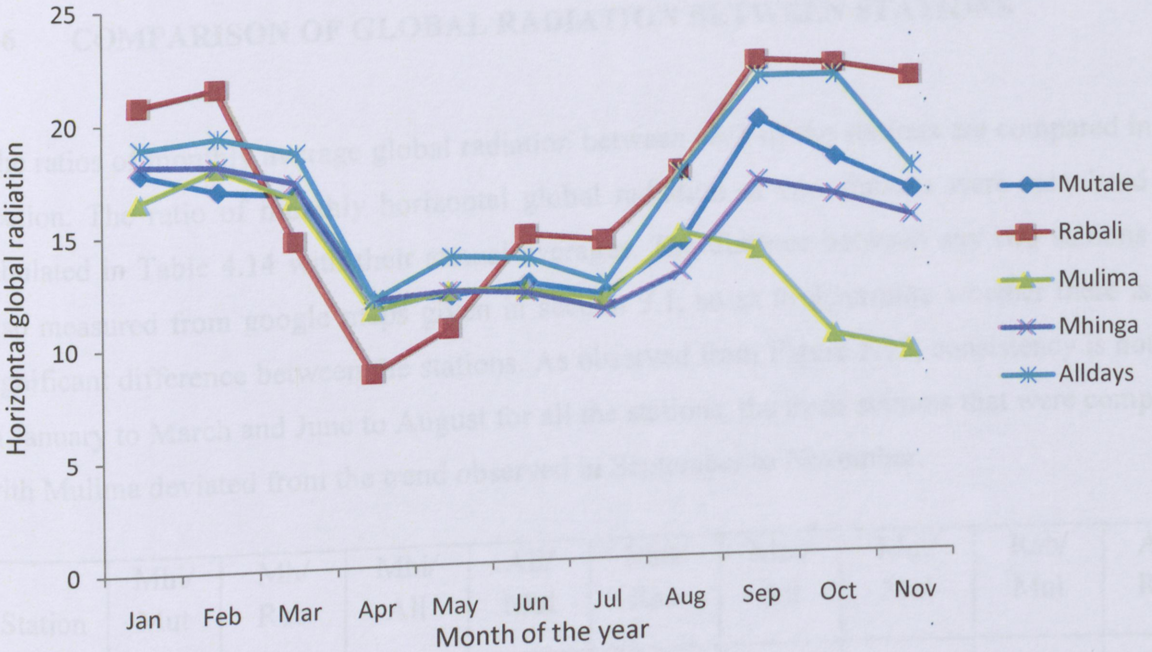

Figure 5.6 Annual horizontal global radiations of the five stations

It is clearly observed from the graph that Mulima station recorded the lowest monthly average daily global radiation in September to November. Makhado Rabali recorded the highest global radiation in January and dropped in February to mid-April. The lowest horizontal global radiation was measured from mid-April to mid-July with an exception of Makhado Mulima station. Thohoyandou Mutale; Malamulele Mhinga and Makhado Alldays station have the same pattern from January to July and differ slightly in the remaining months. The amount of global radiation measured on the horizontal surface is mostly affected by geographical parameters such as type of buildings around the station.

It may be observed from the map (Figure 3.6) that Mulima station is situated closer to the gravel road and surrounded by 3D-buildings. Radiometers that were used to record data in this station need great care. It is noticed from Table 4.13 that November and December have low average monthly radiations; this might have been caused by dust and shades. During these months, trees grow high since it is summer season and hot.

5.6 COMPARISON OF GLOBAL RADIATION BETWEEN STATIONS

The ratios of monthly average global radiation between each of the stations are compared in this section. The ratio of monthly horizontal global radiation of two stations were calculated and tabulated in Table 4.14 with their annual averages. The distance between any two stations was also measured from google maps given in section 3.1, so as to determine whether there is any significant difference between the stations. As observed from Figure 5.13, consistency is noticed in January to March and June to August for all the stations, the three stations that were compared with Mulima deviated from the trend observed in September to November.

Station	Mhi/ Mut	Mh/ Rab	Mhi/ All	All/ Mul	Mut/ Rab	Mut/ All	Mut/ Mul	Rab/ Mul	All/ Rab
X (km)	34.6	78.11	178.26	116.94	47.88	145.61	87.74	53.51	102.1
Jan	1.020	0.874	0.959	1.145	0.857	0.941	1.077	1.257	0.911
Feb	1.065	0.841	0.935	1.075	0.790	0.878	0.944	1.195	0.900
Mar	1.032	1.179	0.927	1.125	1.143	0.899	1.012	0.885	1.272
Apr	1.008	1.383	0.997	1.044	1.373	0.990	1.033	0.753	1.387
May	1.015	1.158	0.888	1.124	1.141	0.875	0.984	0.862	1.304
Jun	0.964	0.822	0.887	1.113	0.852	0.920	1.024	1.202	0.926

Jul	0.945	0.784	0.905	1.065	0.830	0.958	1.021	1.230	0.866
Aug	0.902	0.735	0.741	1.186	0.815	0.821	0.974	1.195	0.992
Sep	0.860	0.758	0.782	1.625	0.881	0.909	1.478	1.677	0.969
Oct	0.905	0.732	0.750	3.391	0.809	0.829	2.810	3.473	0.977
Nov	0.929	0.706	0.872	2.607	0.760	0.939	2.447	3.218	0.810
Aver.	0.968	0.907	0.877	1.500	0.932	0.905	1.346	1.541	1.028

Table 5.13 Comparison of H of different stations

Key: Mut – Mutale, Mhi – Mhinga, Rab – Rabali, All – Alldays and Mul – Mulima.

The results tabulated in Table 5.13 are represented graphically in Figure 5.7

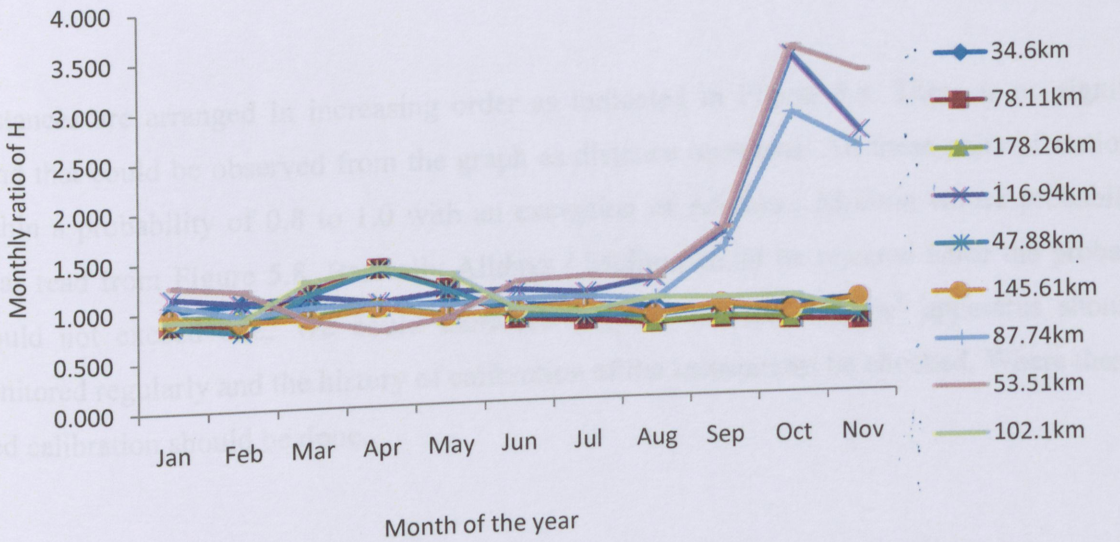

Figure 5.7 The monthly average ratio for global solar radiation

With an assumption that the larger deviations may be due to a suspect data flagging for sun-obscured days, only ratios within ± 10% of the annual average monthly global radiation was calculated for each pair of the station in Table 5.13. A column diagram was then drawn to represent the data graphically as displayed in Figure 5.7.

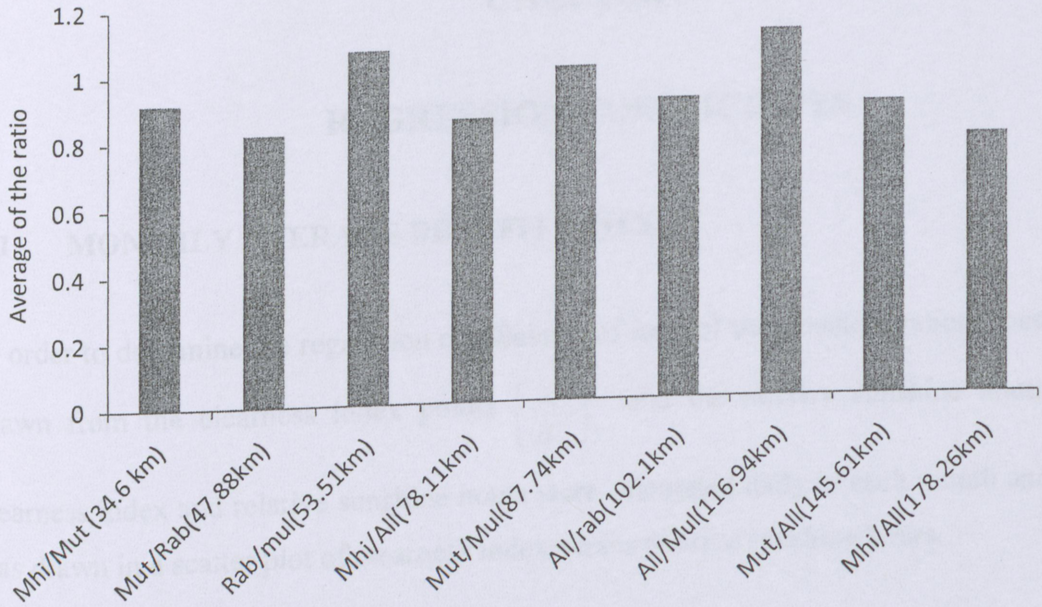

Figure 5.8 Average ratio of H versus distance

Distances are arranged in increasing order as indicated in Figure 5.8. There is no significant trend that could be observed from the graph as distance increases. All these pairs of stations lie within a probability of 0.8 to 1.0 with an exception of Alldays / Mulima whose probability is 1.1as read from Figure 5.8. Basically Alldays / Mulima could be rejected since the probability should not exceed one. We could therefore suggest that the stations' apparatus should be monitored regularly and the history of calibration of the instruments be checked. Where there is a need calibration should be done.

CHAPTER 6

REGRESSION COEFFICIENTS

6.1 MONTHLY AVERAGE BEST FIT LINES

In order to determine the regression coefficients of each of the selected stations, best fit lines are drawn from the clearness index points $\left(\frac{H}{H_o}\right)$ and the relative sunshine hours $\left(\frac{N_o}{N}\right)$. The clearness index and relative sunshine hours were calculated daily in each month and best fit line was drawn in a scatter plot of clearness index versus relative sunshine hours.

6.2 THOHOYANDOU MUTALE STATION

The monthly best fit lines of Thohoyandou Mutale station are drawn below. A scatter plot of the daily coordinates of $\left(\frac{\overline{H}}{\overline{H_o}}\right)$ and $\left(\frac{\overline{N_o}}{\overline{N}}\right)$ is drawn for the determination of the monthly average regression coefficients. It is noticed from the best fit lines that there is a relationship between the clearness index and the relative sunshine hours since the R-squared statistic (R^2) ranges from 88.4% to 96.7%. The best fit lines are represented by Figures 6.1.1 – 6.1.11 .

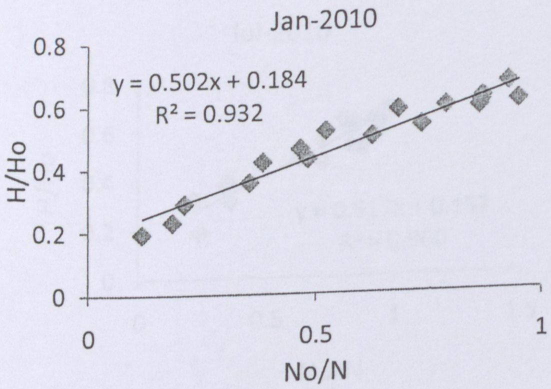

Figure 6.1. 1

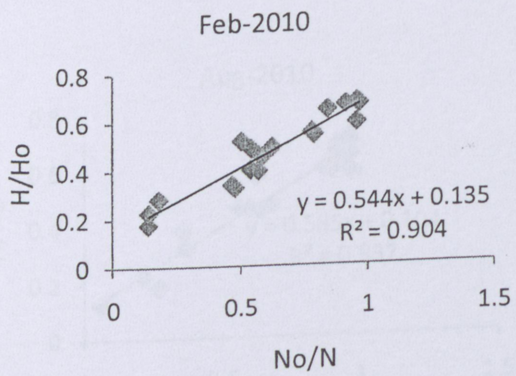

Figure 6.1.2

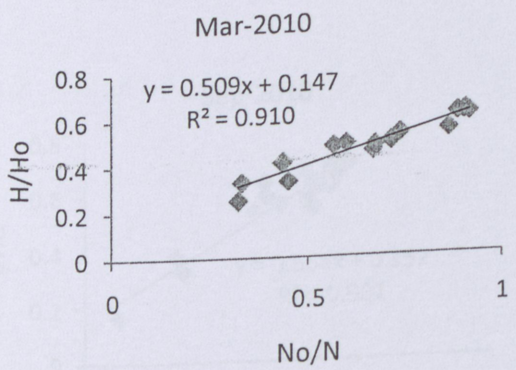

Figure 6.1. 3

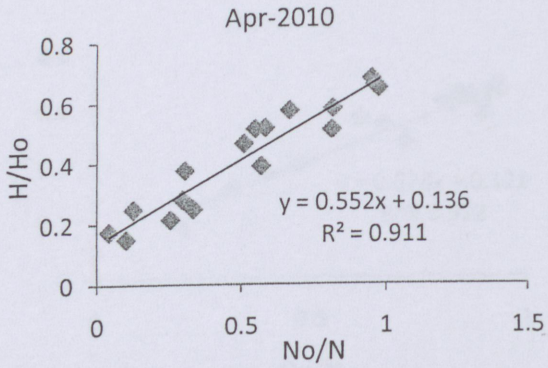

Figure 6.1. 4

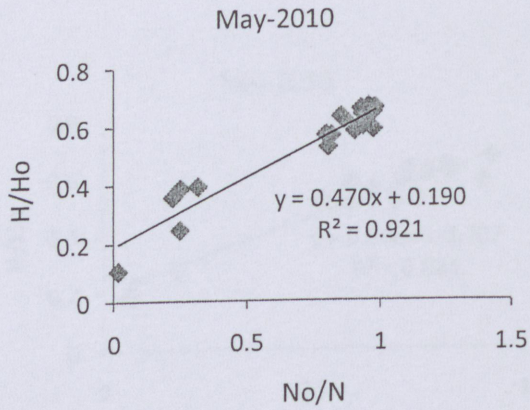

Figure 6.1. 5

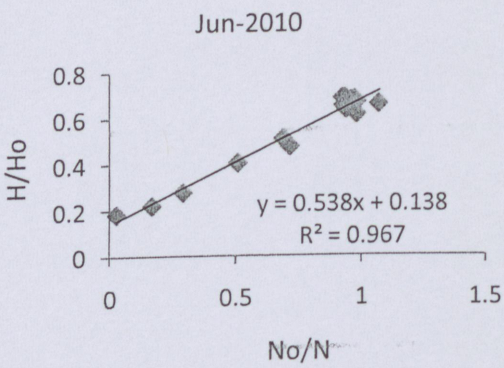

Figure 6.1. 6

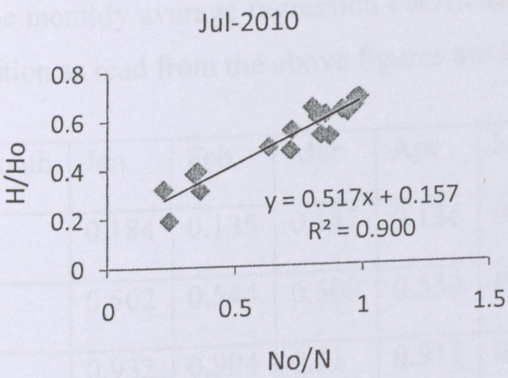

Figure 6.1 .7

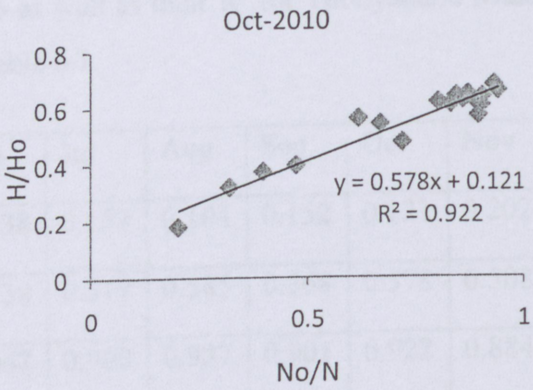

Figure 6.1..10

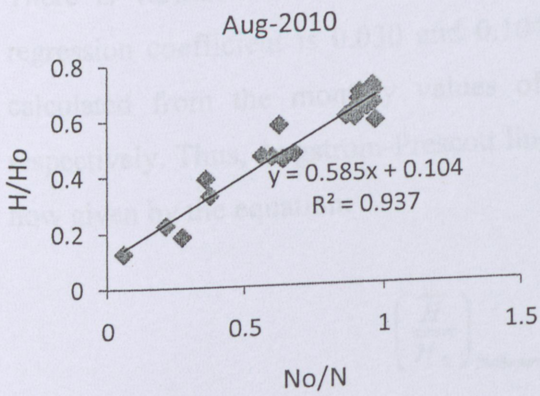

Figure 6.1. 8

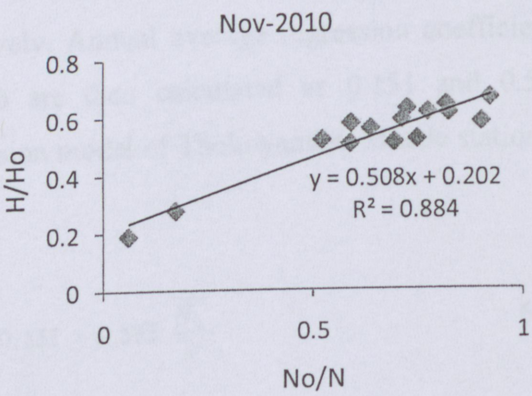

Figure 6.1. 11

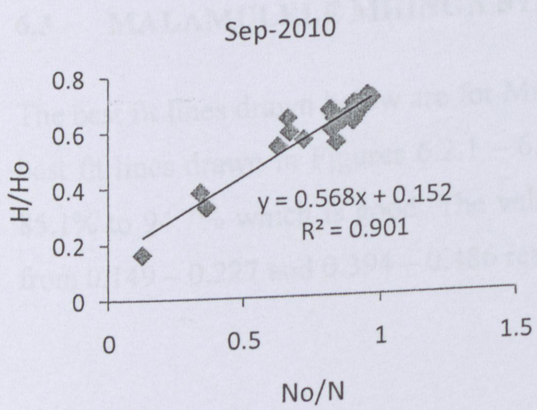

Figure 6.1 .9

The monthly average regression coefficients a and b as well as their R^2 for Thohyandou Mutale station as read from the above figures are listed in Table 6.1.

Month	Jan	Feb	Mar	Apr	May	Jun	Jul	Aug	Sep	Oct	Nov
a	0.184	0.135	0.147	0.136	0.190	0.138	0.157	0.104	0.152	0.121	0.202
b	0.502	0.544	0.509	0.552	0.470	0.538	0.517	0.585	0.568	0.578	0.508
R^2	0.932	0.904	0.91	0.911	0.921	0.967	0.900	0.937	0.901	0.922	0.884

Table 6.1 Regression coefficients of Thohoyandou Mutale Station

There is variation of the regression coefficients a and b. The standard deviation of each regression coefficient is 0.030 and 0.104 respectively. Annual average regression coefficients calculated from the monthly values of a and b are then calculated as 0.151 and 0.533 respectively. Thus, Angstrom-Prescott linear regression model of Thohoyandou Mutale station is now given by the equation:

$$\left(\frac{\overline{H}}{H_0}\right)_{Thohoyando\ umutale} = 0.151 + 0.533\frac{\overline{N_o}}{N} \qquad 6.1$$

Where $a = 0.151$ is the intersection on the $\left(\frac{\overline{H}}{H_o}\right)$ axis and 0.533 the slope of the straight line.

6.3 MALAMULELE MHINGA STATION

The best fit lines drawn below are for Malamulele Mhinga station. It is noticed from the monthly best fit lines drawn in Figures 6.2.1 – 6.2.11 that the correlation of coefficient CC ranges from 85.1% to 94.7% which is good. The values of a and b the regression coefficients vary monthly from 0.149 – 0.227 and 0.394 – 0.486 respectively.

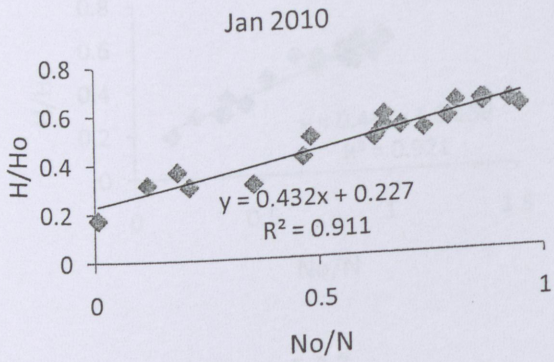

Figure 6.2. 1

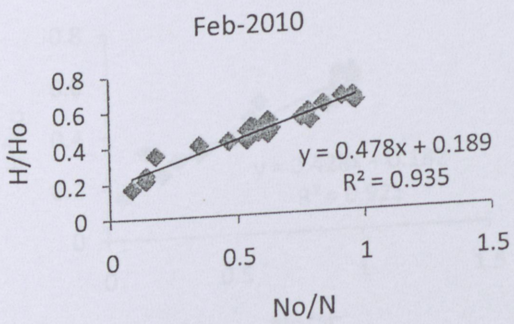

Figure 6.2. 2

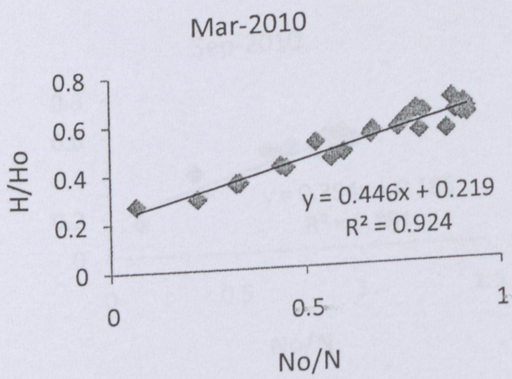

Figure 6.2. 3

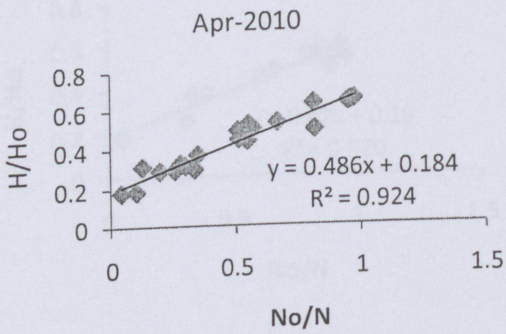

Figure 6.2. 4

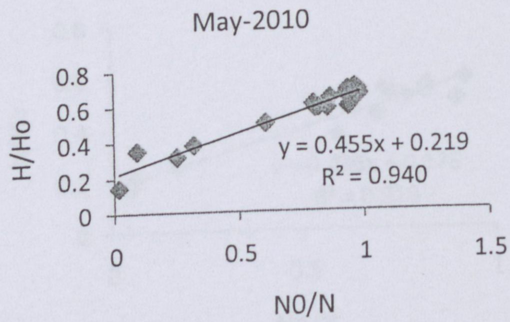

Figure 6.2. 5

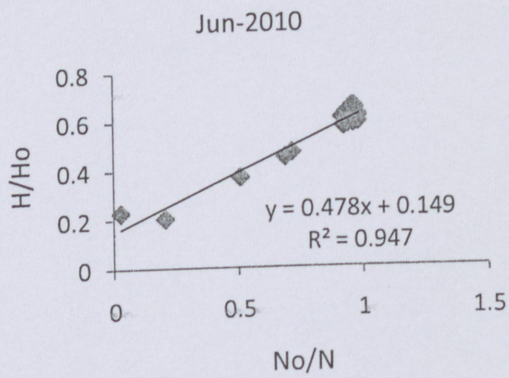

Figure 6.2. 6

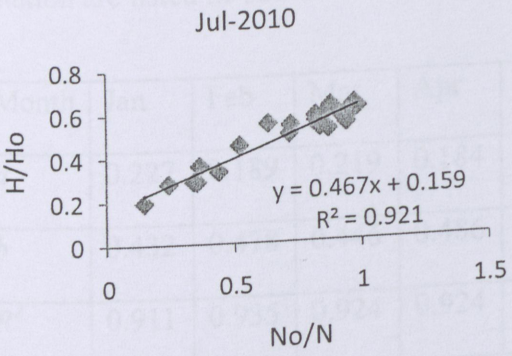

Figure 6.2.7

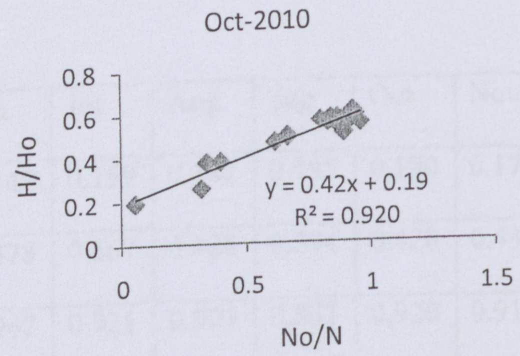

Figure 6.2 .10

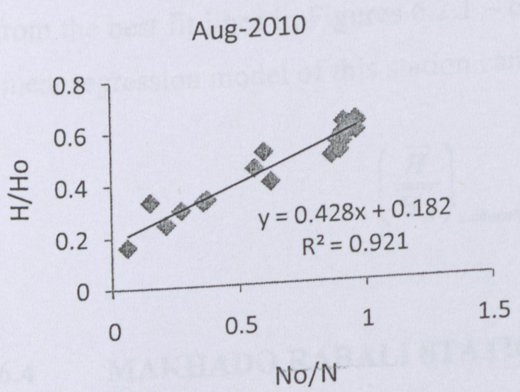

Figure 6.2.8

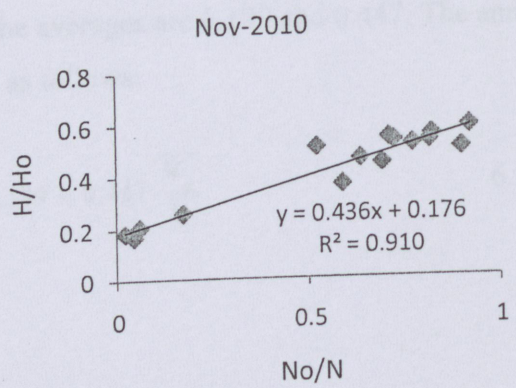

Figure 6.2 .11

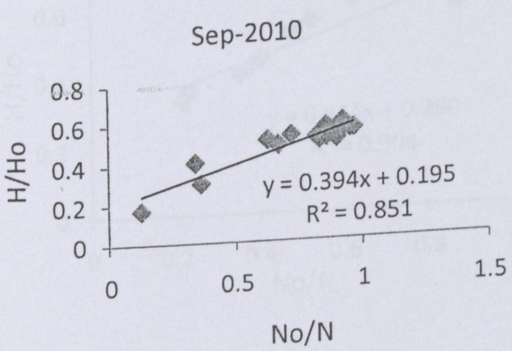

Figure 6.2. 9

The monthly regression coefficients and correlation of coefficients of Malamulele Mhinga station are listed in Table 6.2.

Month	Jan	Feb	Mar	Apr	May	Jun	Jul	Aug	Sep	Oct	Nov
a	0.227	0.189	0.219	0.184	0.219	0.149	0.159	0.182	0.195	0.190	0.176
b	0.432	0.478	0.446	0.486	0.455	0.478	0.467	0.428	0.394	0.420	0.436
R^2	0.911	0.935	0.924	0.924	0.940	0.947	0.921	0.921	0.851	0.920	0.910

Table 6.2 Monthly regression coefficients of Malamulele Mhinga Station

The average annual regression coefficients are calculated from the monthly values that were read from the best fit lines in Figures 6.2.1 – 6.2.11 and the averages are 0.189 and 0.447. The annual linear regression model of this station can be written as follows:

$$\left(\frac{\overline{H}}{\overline{H_0}}\right)_{malamulele\ lmhinga} = 0.189 + 0.447\frac{\overline{N_o}}{\overline{N}} \qquad 6.2$$

6.4 MAKHADO RABALI STATION

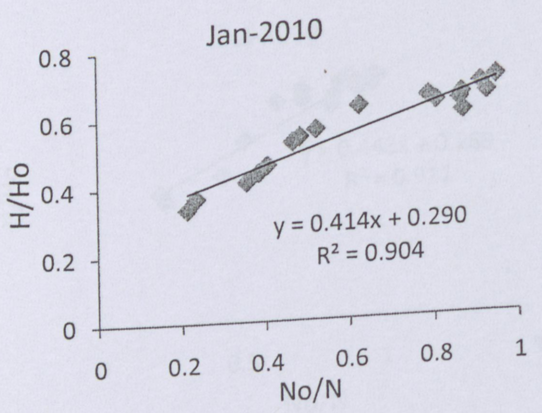

Figure 6.3.1

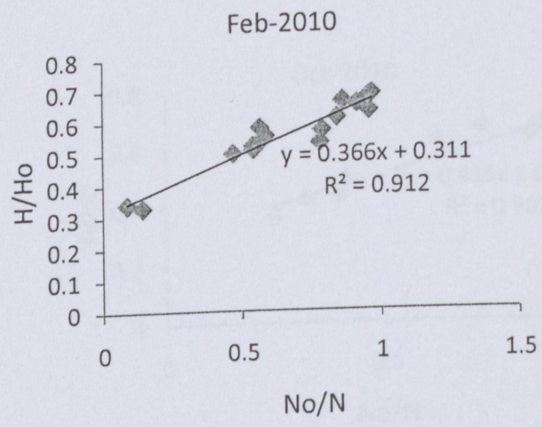

Figure 6.3. 2

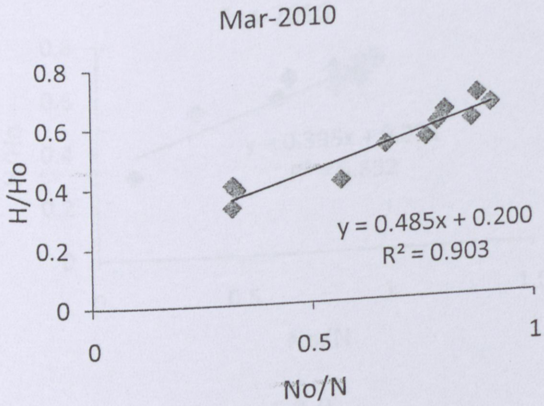

Figure 6.3 .3

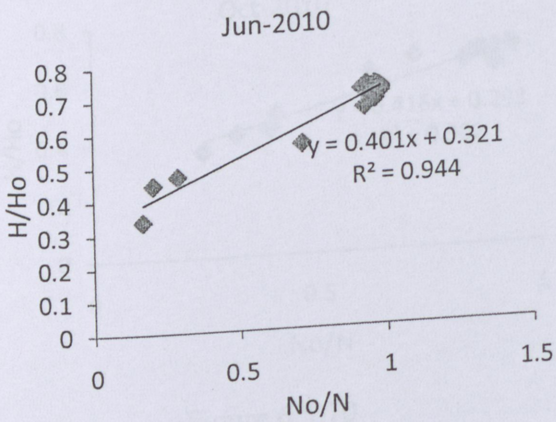

Figure 6.3 .4

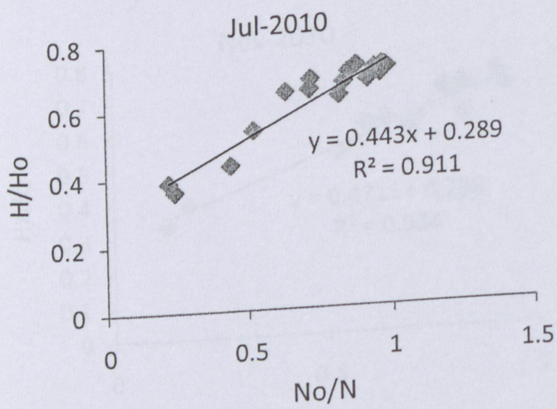

Figure 6.3 .5

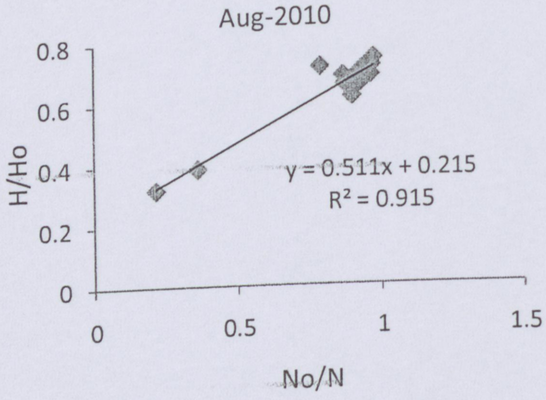

Figure 6.3 .6

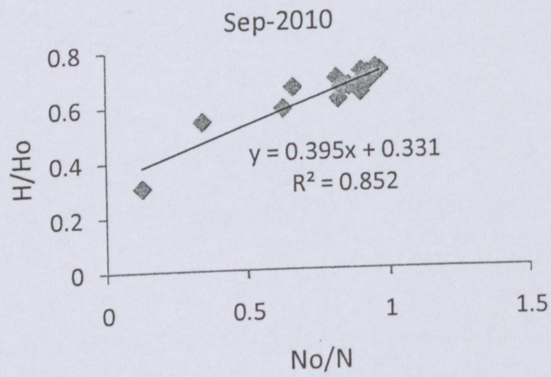

Figure 6.3 .7

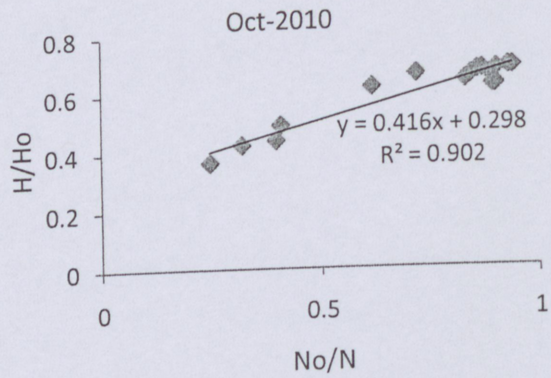

Fig ure 6.3 .8

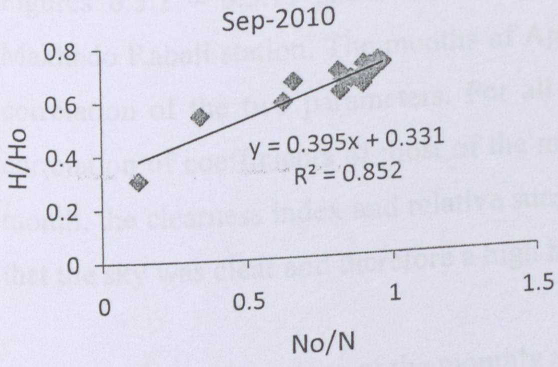

Figure 6.3.9

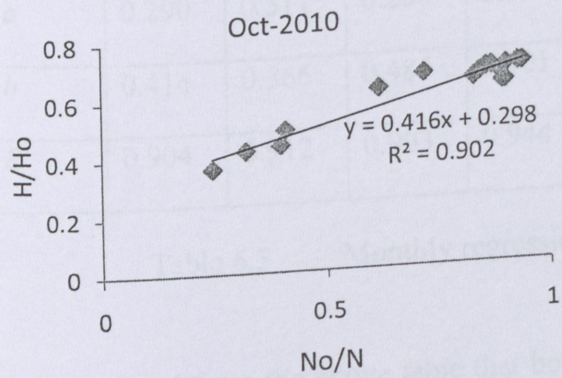

Figure 6.3.10

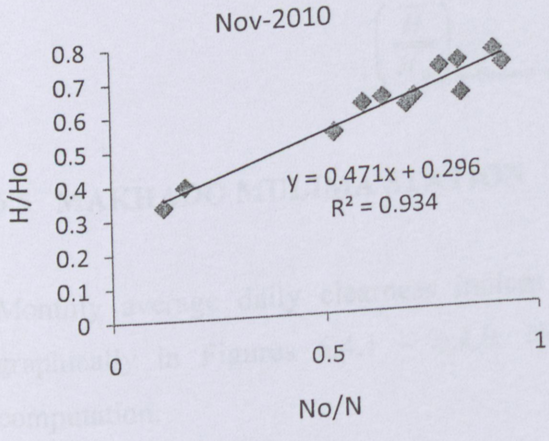

Figure 6.3.11

Figures 6.3.1 – 6.3.11 show the correlation of clearness index and relative sunshine hours Makhado Rabali station. The months of April and May are excluded since there was a very low correlation of the two parameters. For all these months, a good correlation is observed since correlation of coefficients of most of the months is higher than 90.0%. During most days of the month, the clearness index and relative sunshine hours are greater than 0.500. It clearly indicates that the sky was clear and therefore a high horizontal global radiation was recorded

Table 6.3 shows the values of the monthly regression coefficients and correlation coefficients.

Month	Jan	Feb	Mar	Jun	Jul	Aug	Sep	Oct	Nov
a	0.290	0.311	0.200	0.321	0.289	0.215	0.331	0.298	0.296
b	0.414	0.366	0.485	0.401	0.443	0.511	0.395	0.416	0.471
R^2	0.904	0.912	0.903	0.944	0.911	0.915	0.852	0.902	0.934

Table 6.3 Monthly regression coefficients of Makhado Rabali Station

It is observed from the above table that both values of a and b vary throughout the month. The average of the regression coefficients a and b are calculated from the monthly values as 0.283 and 0.433 respectively. Thus Angtrom-Prescott annual linear equation can be written as:

$$\left(\frac{\overline{H}}{\overline{H_0}}\right)_{makhadorab\ ali} = 0.283 + 0.433\,\frac{\overline{N_o}}{\overline{N}} \qquad 6.3$$

6.5 MAKHADO MULIMA STATION

Monthly average daily clearness indices versus relative sunshine duration are represented graphically in Figures 6.4.1 – 6.4.9. November and December are excluded during this computation.

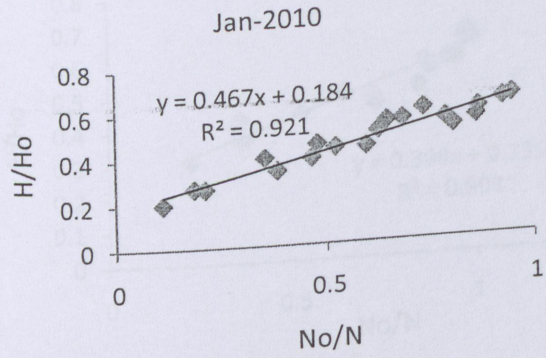

Figure 6.4. 1

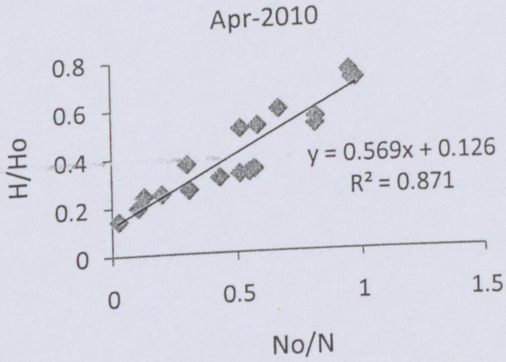

Figure 6.4. 4

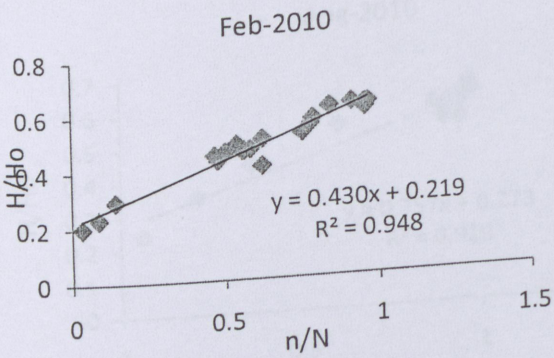

Figure 6.4.2

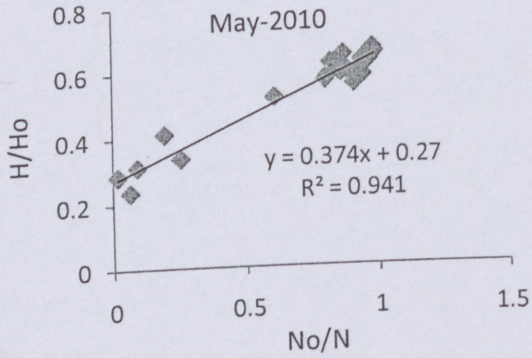

Figure 6.4.5

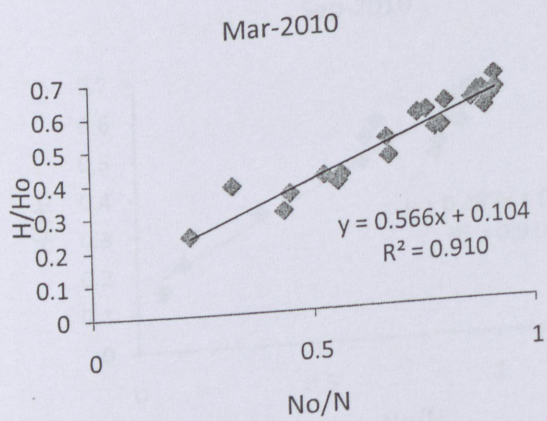

Figure 6.4. 3

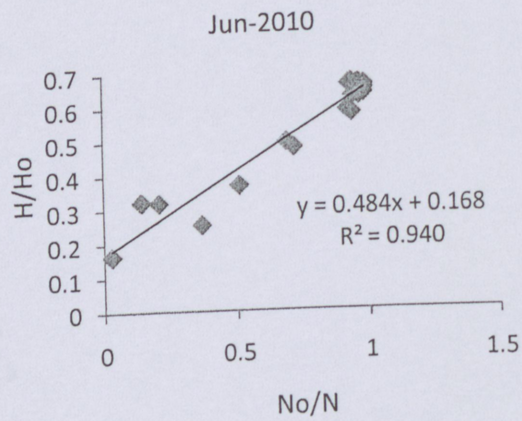

Figure 6.4.6

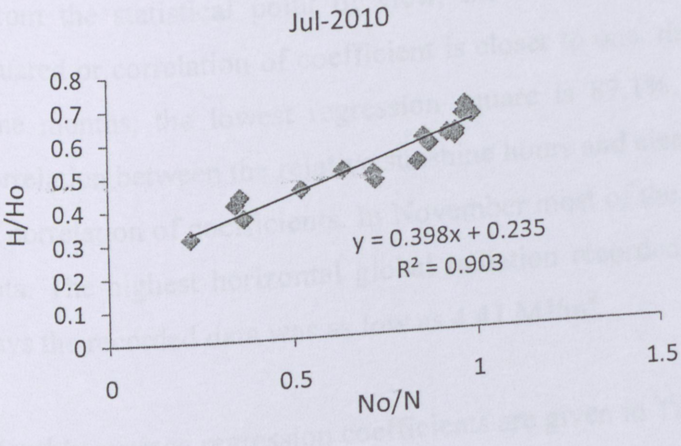

Figure 6.4.7

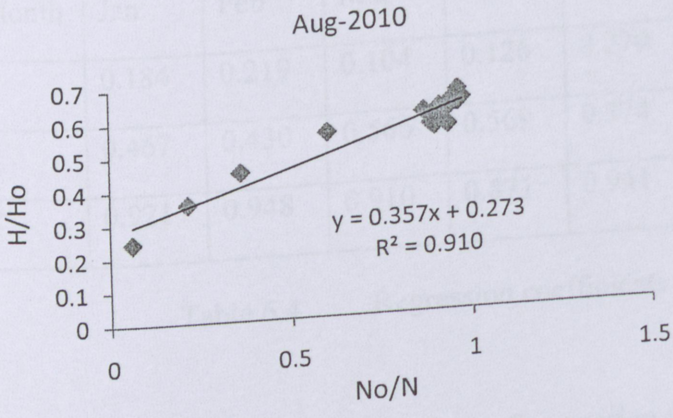

Figure 6.4.8

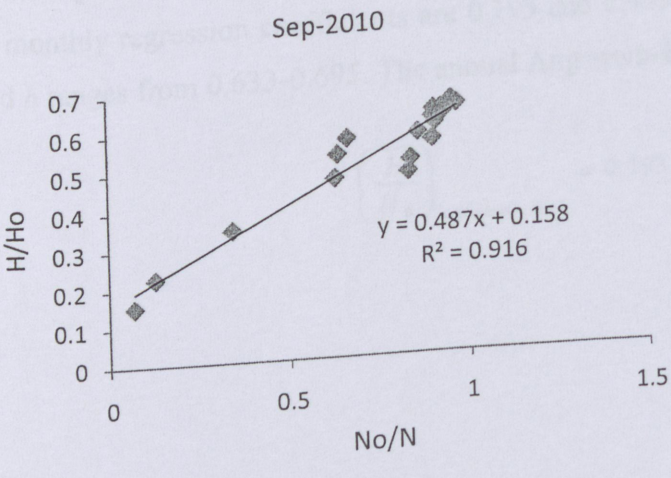

Figure 6.4.9

From the statistical point of view, the best correlation determined provided the regression squared or correlation of coefficient is closer to one, that is about hundred percent. Out of these nine months, the lowest regression square is 87.1%. One could notice that there is a good correlation between the relative sunshine hours and clearness index because there are high values of correlation of coefficients. In November most of the days had zero horizontal global radiation data. The highest horizontal global radiation recorded was 22.21 MJ/m^2 whilst in most of the days the recorded data was as low as 4.41 MJ/m^2.

Monthly average regression coefficients are given in Table 6.4.

Month	Jan	Feb	Mar	Apr	May	Jun	Jul	Aug	Sep
a	0.184	0.219	0.104	0.126	0.270	0.168	0.235	0.273	0.158
b	0.467	0.430	0.566	0.569	0.374	0.484	0.398	0.357	0.487
R^2	0.921	0.948	0.910	0.871	0.941	0.940	0.903	0.910	0.916

Table 6.4 Regression coefficients of Makhado Mulima station

There is a variation of the coefficients of regression throughout the year. The standard deviation of the regression coefficients a and b are 0.060 and 0.076 respectively, while the annual average of monthly regression coefficients are 0.193 and 0.459 respectively. The sum of the values of a and b ranges from 0.633-0.695. The annual Angstrom-Prescott linear equation can be written as

$$\left(\frac{\overline{H}}{H_0}\right)_{makhadomu\ \lim a} = 0.193 + 0.459\frac{\overline{N_o}}{\overline{N}} \qquad 6.4$$

6.6 MAKHADO ALLDAYS

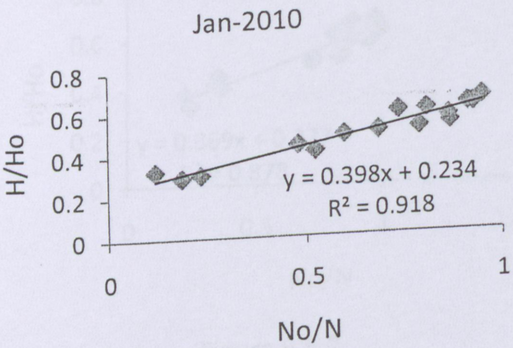

Figure 6.5.1

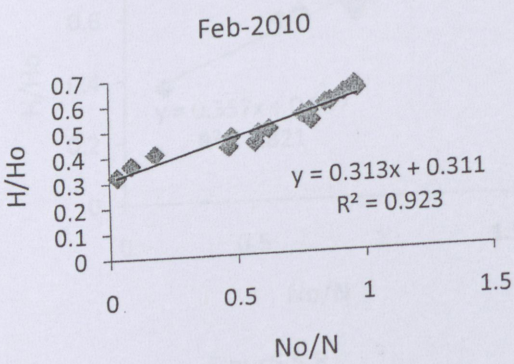

Figure 6.5. 2

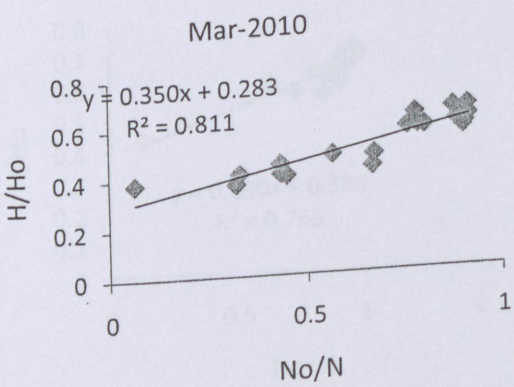

Figure 6.5. 3

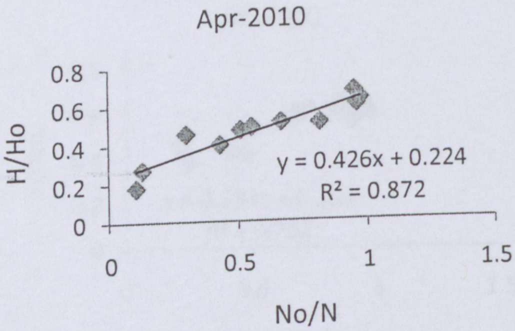

Figure 6.5. 4

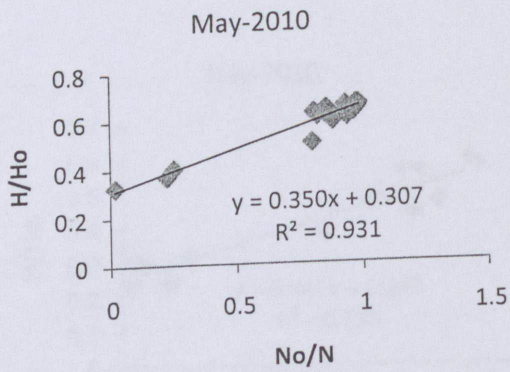

Figure 6.5. 5

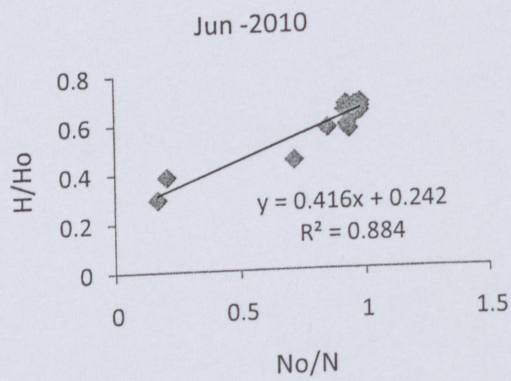

Figure 6.5.6

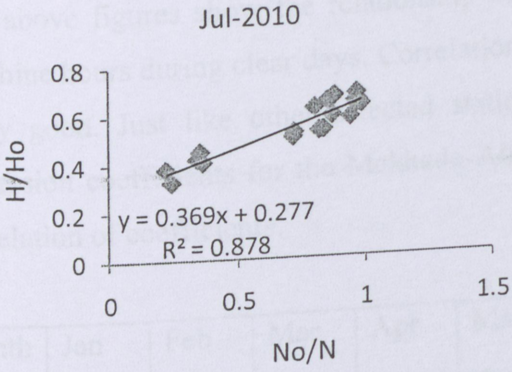

Figure 6.5.7

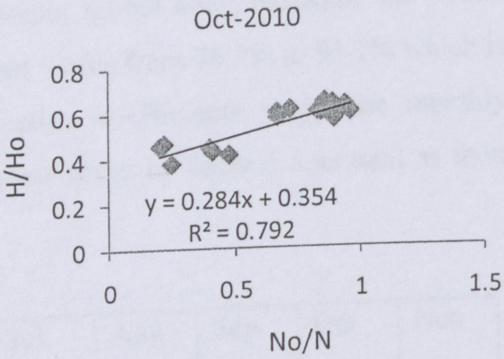

Figure 6.5.10

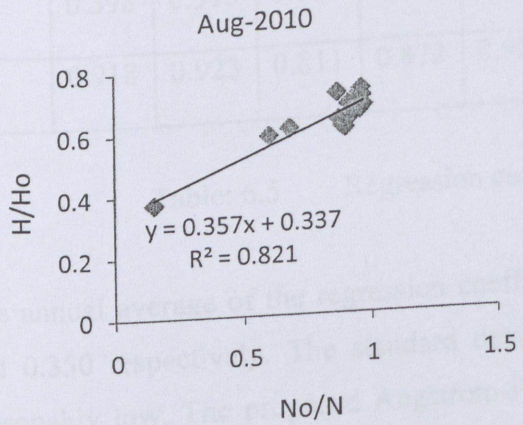

Figur6.5.8

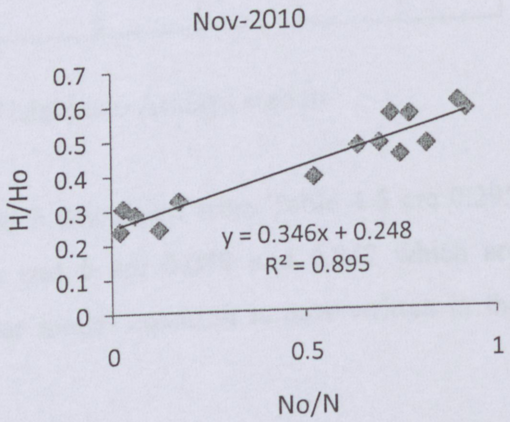

Figure 6.5.11

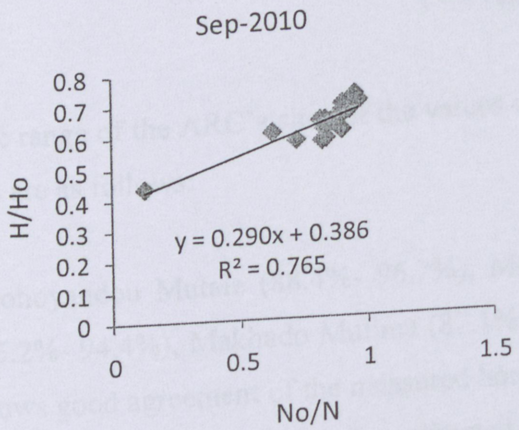

Figure 6.5.9

The above figures show the relationship between horizontal global solar radiation and actual sunshine hours during clear days. Correlation of coefficient varies from 76.5% to 93.1% which is fairly good. Just like other selected station, the regression coefficients vary. The monthly regression coefficients for the Makhado Alldays station are listed in Table 6.5 as well as their correlation of coefficients.

Month	Jan	Feb	Mar	Apr	May	Jun	Jul	Aug	Sep	Oct	Nov
a	0.234	0.311	0.283	0.224	0.307	0.284	0.277	0.337	0.386	0.354	0.248
b	0.398	0.313	0.350	0.426	0.350	0.373	0.369	0.357	0.290	0.284	0.346
R^2	0.918	0.923	0.811	0.872	0.931	0.838	0.878	0.821	0.765	0.792	0.895

Table: 6.5 Regression coefficients of Makhado Alldays station

The annual average of the regression coefficients a and b calculated from Table 4.6 are 0.295 and 0.350 respectively. The standard deviations of a and b are 0.050 and 0.042 which are reasonably low. The proposed Angstrom-Prescott linear model equation is now written in the form:

$$\left(\frac{\overline{H}}{H_0}\right)_{makhadoall\ \ days} = 0.295 + 0.350\frac{\overline{N_0}}{N} \qquad 6.7$$

The range of the ARC's sites of the values of R^2 of the proposed model as read from Table 6.1 - 6.5 are as follows:

Thohoyandou Mutale (88.4%- 96.7%); Malamulele Mhinga (85.1%-94.7%); Makhado Rabali (85.2%- 94.4%), Makhado Mulima (87.1%-94.8%) and Makhado Alldays (79.2%- 93.1%). This shows good agreement of the measured horizontal global radiation and the actual sunshine hours. For further analysis, monthly estimated global radiations on the horizontal surface were computed.

6.7 VUWANI STATION – UNIVEN SITE

This station is included in order to make comparison with the ARC horizontal global solar radiation data. Solar parameters such as N and H_o were calculated and these values are reasonably compared to the computed values of the five selected stations from ARC. Taking into consideration the standard deviation of the variation of the values of a and b, the monthly regression coefficients were determined, i.e. a = 0.161 and b = 0.382. The correlations of coefficients were above 80.0% which is quite good. This simply gives an idea that sunshine hours play an important role to the global solar radiation falling on the horizontal surface. During clear days H measured values are high like in the ARC selected stations in this study.

6.8 ANNUAL REGRESSION COEFFICIENTS

In order to calculate the monthly horizontal global solar radiation of each of the selected station, the annual average values of the regression coefficients a and b were computed from Tables 6.1-6.5 and listed in Table 6.6 below:

Station	Malamulele Mhinga	Thohoyandou Mutale	Makhado Rabali	Makhado Alldays	Makhado Mulima
Latitude	22.797° S	22.735° S	22.87° S	22.683° S	23.356° S
Longitude	30.842° E	30.522° E	30.081° E	29.105° E	29.989° E
Altitude (m)	460	550	720	842	1032
a	0.189	0.151	0.283	0.295	0.193
b	0.447	0.533	0.433	0.350	0.459

Table 6.6 Annual regression coefficients of the selected stations

From the results in Table 6.6, it can be concluded that neither a or b vary with latitude or altitude in any systematic manner. However the sum of the regression coefficients $a + b$; which represent the clearness index provided the relative sunshine hour ($\frac{N_0}{N} = 1$) averaged over the period of recording data were found to be almost the same. Those values were 0.684, 0.716, 0.687, 0.636 and 0.652 for Mhinga, Mutale, Rabali, Alldays and Mulima respectively. The sum of the regression coefficients did not vary with an increase of latitude, longitude or altitude as it does in other countries like in Nigeria [65]

6.9 SEASONAL TRENDS

The graphical representations of a and b versus month of the year were drawn in order to observe whether there was any seasonal trend. Regression coefficients of the station in this study were grouped together. Three stations were considered since Mulima and Rabali missed two month. Figures 6.6 and 6.7 represent the relationship of a and b values respectively.

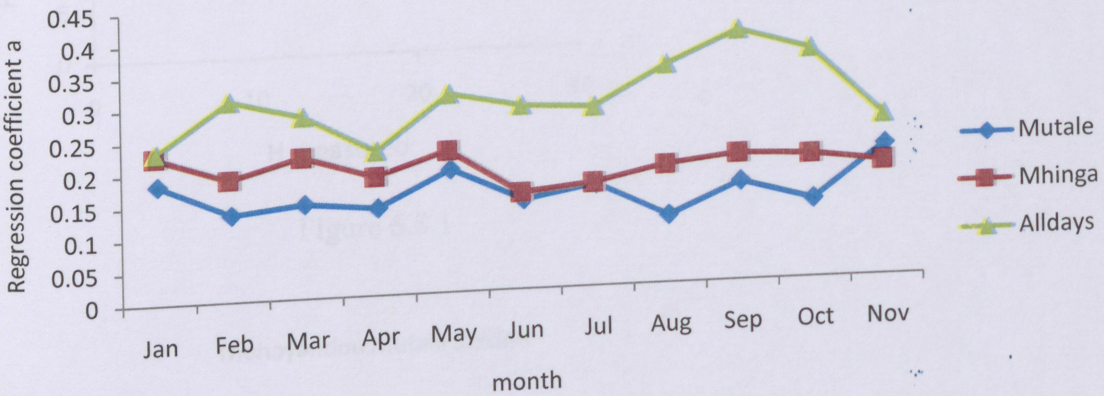

Figure 6.6 Month of the year versus a

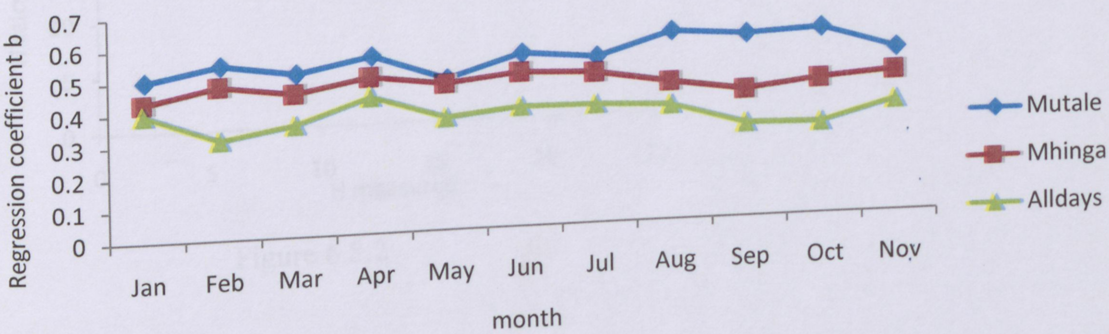

Figure 6.7 Month of the year versus b

6.10 REPRESENTATIVE REGRESSION COEFFICIENTS FOR VHEMBE REGION

An attempt has been made to determine a representative pair of coefficients for Vhembe Region. Malamulele Mhinga's regression coefficients, from Equation 6.2 were used to compute horizontal global radiation for each of the other stations. The Figures 6.8.1 – 6.8.4 represent the correlation between *H* measured versus *H* estimated of the stations in this study.

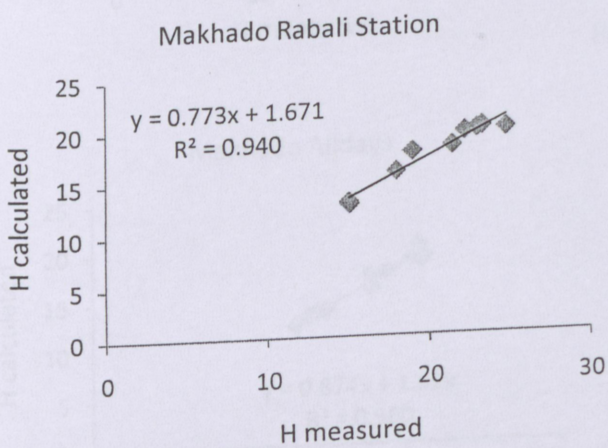

Figure 6.8.1

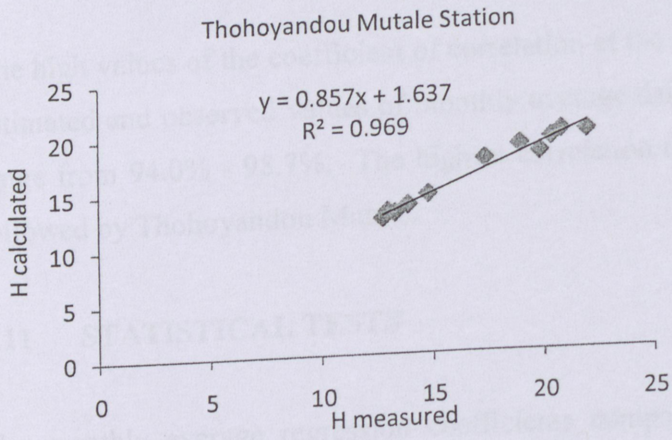

Figure 6.8.2

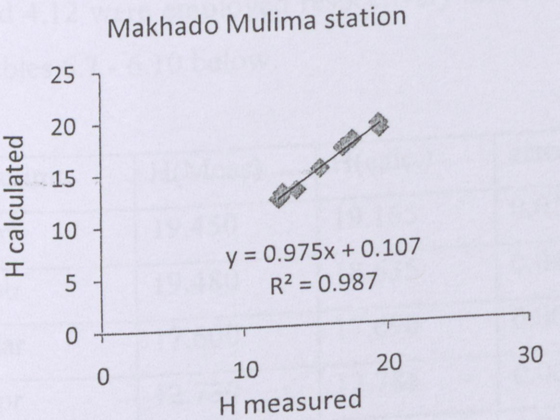

Figure 6.8.3

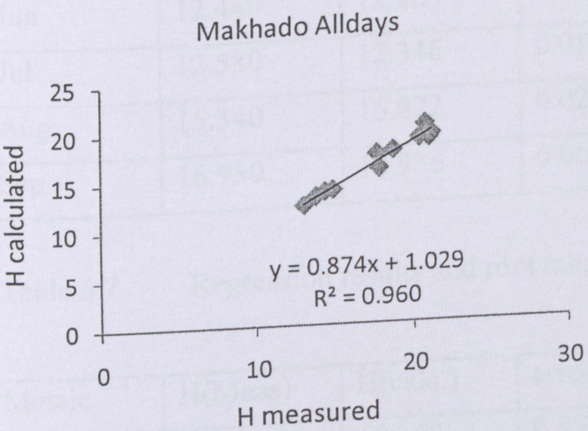

Figure 6.8.4.

The high values of the coefficient of correlation of the proposed model give a good agreement of estimated and observed values of monthly average daily global solar irradiation. The R^2 values range from 94.0% - 98.7%. The highest correlation coefficient is read from Makhado Mulima followed by Thohoyandou Mutale.

6.11 STATISTICAL TESTS

The monthly average regression coefficients computed has been employed to calculate the annual regression coefficients which are then used to determine the monthly estimated global solar radiation. In this study, three statistical tests, the root mean square error (RMSE), mean bias error (MBE) and t-test are used to evaluate the accuracy of the correlations. Equations 4.10; 4.11

and 4.12 were employed respectively and the values of RMSE; MBE and t-test are recorded in Tables 6.7 - 6.10 below.

Mulima	H(Meas)	H(calc.)	error	RMSE	MBE	t
Jan	19.450	19.165	0.015	0.070	0.015	0.936
Feb	19.480	18.635	0.043	0.189	0.042	1.000
Mar	17.600	17.690	0.005	0.020	-0.004	1.000
Apr	12.730	12.785	0.004	0.013	-0.003	0.986
May	13.700	13.017	0.050	0.159	0.028	0.873
Jun	12.440	12.224	0.017	0.043	0.009	1.000
Jul	12.580	12.346	0.019	0.054	0.012	0.947
Aug	15.340	15.022	0.021	0.075	0.017	0.945
Sep	16.930	16.936	0.000	0.001	0.000	1.000

Table 6.7 Regression results and root mean square error, mean bias error and *t*-statistic

Mutale	H(Meas)	H(calc.)	error	RMSE	MBE	t
Jan	20.330	19.168	0.057	0.209	0.068	1.387
Feb	18.910	18.613	0.016	0.068	0.017	1.059
Mar	17.340	17.418	0.005	0.020	-0.005	1.000
Apr	12.970	12.900	0.005	0.017	0.004	1.000
May	13.880	13.412	0.034	0.100	0.021	1.000
Jun	13.300	12.711	0.044	0.118	0.024	1.000
Jul	12.750	12.259	0.038	0.107	0.023	1.000
Aug	14.790	14.341	0.030	0.092	0.019	1.000
Sep	19.810	17.892	0.097	0.400	0.087	1.048
Oct	20.780	19.780	0.048	0.243	0.056	0.941
Nov	21.930	19.718	0.101	0.571	0.147	1.000

Table 6.8 Regression results and root mean square error, mean bias error and *t*-statistic of Thohoyandou Mutale.

Rabali	H(Meas)	H(calc.)	Error	RMSE	MBE	t
Jan	23.280	19.843	0.148	0.810	0.202	1.063
Feb	22.220	19.430	0.126	0.697	0.174	1.000
Mar	18.980	17.588	0.073	0.420	0.127	1.000
Jun	15.040	12.911	0.142	0.444	0.093	1.000
Jul	15.090	12.727	0.157	0.528	0.118	1.026
Aug	17.980	15.730	0.125	0.530	0.125	1.000
Sep	21.440	18.079	0.157	0.771	0.177	1.106
Oct	22.960	19.634	0.145	0.831	0.208	1.000
Nov	24.770	19.657	0.206	1.476	0.426	1.000

Table 6.9 Regression results and root mean square error, mean bias error and *t*-statistic of Makhado Rabali.

Alldays	H(Meas)	H(calc.)	Error	RMSE	MBE	t
Jan	20.780	20.200	0.028	0.150	0.039	1.000
Feb	20.400	18.810	0.078	0.397	0.099	1.000
Mar	18.720	17.629	0.058	0.244	0.055	1.000
Apr	14.360	13.667	0.048	0.209	0.063	1.000
May	14.880	13.814	0.072	0.245	0.056	1.000
Jun	13.800	13.208	0.043	0.123	0.026	1.000
Jul	13.030	12.305	0.056	0.162	0.036	1.000
Aug	17.830	15.845	0.111	0.468	0.110	0.970
Sep	21.030	18.760	0.108	0.521	0.119	0.972
Oct	21.190	19.187	0.095	0.448	0.100	1.000
Nov	17.670	17.333	0.019	0.090	0.024	0.920

Table 6.10 Regression results and root mean square error, mean bias error and *t*-statistic of Makhado Alldays

The following observations are made from a study of the results presented in Tables 6.7 -6.10. The RMSE and MBE values vary. A.A El-Sebaii and A.A Trabea [57] in one of their published papers indicated that low RMSE is desirable since it gives a remarkable agreement between the measured and calculated values of horizontal global solar radiation. The positive MBE shows overestimation while a negative MBE indicates underestimation [62]. It is noticed from Tables 6.7 – 6.10, that there are negative and positive MBE values.

6.12 SUMMARY

The regression coefficients a and b for Angstrom- Prescott equation are listed in Tables 6.1 – 6.5. In each of the selected stations there is a monthly variation of the regression coefficients a and b. This can be explained as the consequence of periodic climatologically variations in the atmosphere. In South Africa, during summer (November- February), high temperatures are predicted but this is the period wherein rainfall is received and hence this variation. Windy days are observed in spring (August- October). It is rare to receive rainfall during the winter season.

The statistical tests of RMSE, MBE, R^2 and t-test were determined for the entire period of study. The observations made from the study of the results are presented in Tables 6.7 – 6.10. The RMSE values, which are the measure of the accuracy of estimation, vary in each station as follows: Thohoyandou Mutale (0.02-0.571); Makhado Mulima (0.001 - 0.189). The MBE values obtained from the selected station are positive and negative as noticed from the presented tables and this shows that Angstrom- Prescott model vary above and below the estimated of the average horizontal global radiation.

The use of the additional t-statistic is used to achieve more statistical reliable result. This is because it is possible to have large RMSE values at the same time very small MBE (Table 6.7-6.10). The smaller the t-calculated value, the better the model's performance. To determine whether the model's estimates are statistically significant, we determined the critical t-value ($t_{critical}$ = 1.96) from the standard statistical tables at α level of confidence $\alpha = 95\%$. In order to analyse the model's estimates at $(1 - \alpha)$ confidence level the calculated value must be within the interval defined by - $t_{critical}$ and $t_{critical}$. This is the accepted region under normal distribution curve. The low values of t-calculated demonstrate the excellent performance of the proposed linear model for estimating the monthly mean daily global solar radiation on a horizontal surface for different stations in Vhembe District of Limpopo, South Africa.

CHAPTER 7

CALIBRATION OF SOLAR RADIOMETERS

7.1 INTRODUCTION

It is of vital importance to this study to understand and know how to calibrate solar radiometers. Parameters that are employed in this study found in Angstrom-Prescott linear equation are measured using solar radiometers. That is, horizontal global solar radiation is measured using a pyranometer or a pyrheliometer with a shading mechanism. In collaboration with CSIR, gave the researcher an opportunity to attend the Eleventh International Pyrheliometer Comparison at Davos Switzerland as well some hands-on training at DWD, Germany to gain skills in the calibration of radiometers.

7.2 THE IMPORTANCE OF CALIBRATING MEASURING INSTRUMENTS.

Calibration can be defined as the setting of a device with another instrument whose measurements are known. The instrument with known correctness is called a standard reference. It is of vital importance to calibrate the measuring instruments like solar radiometry (pyranometer, pryheliometer, pyrgeometer, e.t.c.), barometers, and others. Calibration can be done before the instrument's scheduled time due to the following conditions:

- If the measurements are out of uncertainty range assigned by the manufacturer or a body assigned to standardize such an instrument.
- When the scheduled period specified by the manufacturer has elapsed.
- If the equipment is new and one is not quite sure that it has been calibrated i.e when calibration schedule is not indicated.
- Sudden change of climate (temperature rises or falls extremely).
- Change of position as this can change the optical design of the instrument due to shifting.

Calibration of solar radiometers must be in accordance with the specifications given in the International Organization for Standardization (ISO) 9060 standards or the revised standardization and Guide to the expression of Uncertainty in Measurement (GUM) for evaluating and expressing uncertainty in measurement.

7.3 TERMS INVOLVED IN CALIBRATION OF RADIOMETERS

There are terms and parameters that the calibrator has to understand when calibrating solar radiometers like pyrheliometer, pyranometer. Pyrgeometer, e.t.c [53].

i. Calibration of a radiometer is defined as the determination of the responsivity of a radiometer under well-defined measurement conditions. Well-defined measurement conditions defined by the World Meteorological Organization (WMO) are:
   a. Clear sky conditions- this reduces the variance in the results.
   b. Tolerable clouds at large angular distance greater than 15 degrees.
   c. Range of solar elevation

   The reciprocal of responsivity is the calibration factor of the calibrated radiometer.
ii. Field –of- view: This is a full angle of the cone which is defined by the center of the receiver surface and the border of the aperture. Field-of-view of absolute cavity of pyrheliometer is discussed in 7.7.1
iii. Solar tracker or sun tracker: The power-driven or manual operated support which is employed to direct a pyrheliometer to the sun. Automated sun trackers are now available from EPLAB manufacturers as well EKO and BRUSAG. The steps for operation of solar tracker are found in information and guideline manual of a respective company.
iv. Sun-shading device: Device which allows movement of a disc in such a way that the receiver of the radiometer is shaded from the sun. This is mostly applied to a pyranometer for diffuse radiation measurement. It is also applicable during calibration of pyranometers where pyrheliometers are refered to as references, i.e. calibration of pyranometer with reference pyrheliometer.

7.4 WORLD RADIOMETRIC REFERENCE (WRR)

World Meteorological Organization (WMO) realized that several radiation references were used in the past in meteorology. Such references include Angstrom scale of 1905 and IPS 1936. In order to control the standardization of meteorological instruments on national and international scale, WMO adopted a system of national and international standards [54]. In order to guarantee the long-term stability of the new reference (WRR), a group of several absolute pyrheliometers of different design from different companies are used as World Standard Group (WSG). For these instruments to meet the stability criteria, they must fulfill the following specifications:

1. Long-term stability has to be better than 0.2 % of the measured value.
2. The 95% uncertainty of the series of measurements with instrument has to lie within the limits of the uncertainty of the WRR.
3. The instrument must have a different design from other WSG instruments.

The World Radiation Centre (WRC) at Davos is responsible for maintaining the basic reference, the WSG of instruments, which is used to establish the WRR. International comparison of solar radiometric instruments takes place every five years. During this comparison, the standards of the regional centers are compared with the WSG, and their calibration factors are adjusted to the WRR. During international Pyrheliometer comparisons (IPCs) the WRR value is calculated from the mean of at least three participating instruments of the WSG. Instruments that had an opportunity of being calibrated at PMOD WRC are in turn used to tranfer the WRR periodically to national centers.

7.5 CALIBRATION FACTOR

Determination of calibration factor involves the transfer of calibration from one radiometer to another of similar type of instrument [53]. The intercomparison of these radiometers is always done in the sunlight on a very clear day. One of the instruments has to be a standard or reference instrument from which the calibration is transferred. In this case a reference radiometer is the one that participated during recent International Pyrheliometer Comparisons.

The reference radiometer and the one to be calibrated should be mounted on the same solar tracking device or exposed to the same solar intensity on different trackers. The solar tracker has to be aligned properly with the sun [16]. Both instruments must be allowed to stabilize before taking data. At least three clear days' data must be collected for calibration purposes and direct radiation data must be above or equal to 800W/m^2 [53, 54]. A set of one day data with a number of series are compared, if these values differ, a calibration factor is calculated.

For each reading *i* within a measurement series *j*, the ratio is calculated using the formula:

$$F(i;j)=\frac{E_{SP}(i,j)}{V_{FP}(i,j)} \tag{7.1}$$

where $E_{SP}(i,j)$ is the irradiance of direct solar radiation given by the reference pyrheliometer and $V_{FP}(i,j)$ is the signals of the field pyranometer.

In order to find the final calibration factor *F* of the field pyranometer from the total number k of the measuring series, the following formula is used:

$$F(j)=\frac{1}{k}\sum_{j=1}^{k}F(j) \tag{7.2}$$

where

$$F(j)=\frac{\sum E_{SP}(i,j)}{\sum V_{FP}(i,j)} \tag{7.3}$$

In general, one can say that the calibration factor is calculated by dividing the sum of the corresponding series of the reference radiometers by the one to be calibrated.

7.6 HIERARCHY OF CALIBRATION OF PYRHELIOMETERS

Primary standard pyrheliometers are referred to the WRR by comparison of well-maintained group of primary standards [53]. Primary standard pyrheliometers are used as reference for calibration of secondary standard pyrheliometer, first class and second class pyrheliometer. The reference for calibration of each pyrheliometer of a certain category is a pyrheliometer of the same category. That is, the reference pyrheliometer for the calibration of absolute cavity pyrheliometer is the absolute cavity. It is recommended that more than one reference pyrheliometer of the same category must be used for calibrating test pyrheliometers.

7.7 ABSOLUTE CAVITY PYRHELIOMETER (AHF 31117)

Absolute cavity pryheliometer AHF 31117 participated in the Eleventh International Pyrheliometer Comparison in September 2010 at the World Radiation Centre in Davos Switzerland, the coordinates are 46°48’ N (latitude); 9°50’ E (longitude) and at the elevation is 1560 m (5.118 ft). Davos has an area of 283.99 km^2. The instrument also participated in the IPC-xi in 2000. Specifications of AHF 31117 are listed in this work where its calibration had been done.

7.7.1 Description and operation of the AHF31117 pryheliometer.

The literature and operation of this instrument is well outlined in the *Eplab- instruction and information manual* [55] and J. Hickey developed a software program to be used during calibration. The manual instruction of this program is found in *Hickey J.R., Program* [56]. The instrument is also described by Lysko [57]. The AHF 31117 pyrheliometer is a self-calibrating instrument.

A description of the absolute cavity radiometers is also found in the *World Climate Research Programme operation manual version 2.1*. The AHF cavity radiometer has been a reference standard device for quite number of years. Sensor consists of a balanced cavity receiver pair attached to a circular wirewound and plated thermopile. The blackened cavity receivers are fitted with heater windings. These windings allow for absolute operation using the electrical substitution method, which relates radiant power in SI units. AHF cavity consists of two cavities. The forward cavity views the direct solar beam by a 5° full field of view and a slope of 0.8° through a precision aperture whose area is 50 mm^2. The rear receiver views an ambient temperature blackbody. The model AHF has an automatic shutter attached to the outer tube. A separate mounted window is supplied with each unit for continuous operation of the radiometer, but at reduced accuracy.

The operation of the cavity radiometer and the measurement of the required parameter are performed using the appropriate control box. The control box functions include setting of the calibration heater power level, activation of the calibration heater, selection of the signals to be measured and control of the meter measurement functions and ranges. The measured parameters include the thermopile signal, the heater voltage and the heater current. The control box operates one radiometer in the measurement mode. Since, AHF 31117 cavity is automatic, the automatic operation allows for computer control of all shuttering, calibration heating and measurements functions.

7.7.2 Specifications of AHF cavity radiometers

The sensor consists of sixty junction circular wirewounds and plated thermopiles with balanced cavity receivers of approximately three hundred and fifty ohms. An inverted cone within a cylinder coated with specular black paint has an emissivity greater than 0.999 [55]. The heater resistance is approximated one hundred and fifty ohms whereas the irradiance sensitivity is approximately $1\mu VW^{-1}m^{2}$. The diameter of the base of the instrument is 5.5 inch, the outer tube has a diameter of 3.5 inch, shutter housing is 7 inch x 5 inch and its length is 13.32 inch without an adaptor. The size, weight and power required by the control box are 7 inch high x 17 inch wide x 16 inch deep, 23 lb and 115 VAC @ or 230VAC 50 Hz selectable respectively.

7.8 CALIBRATION OF AHF31117 PYRHELIOMETER

International Pyrheliometer Comparison's (IPC) calibration procedure was e-mailed to each participant in advance and it was revised each day before calibration. This is called IPC protocol.

7.8.1 Calibration procedure during IPC-xi

1. Mount the participating reference pyrheliometer on a solar tracker and keep it aligned to the sun throughout the measurement runs for the day.
2. Computer control systems are synchronized to the timing of the IPC's measurement series, i.e.
   - (i) Measurement is taken in series of 21 minutes duration with 90-seconds base cadence
   - (ii) A 30-seconds sub-cadence is evaluated for HF
3. Participants maintain log-book (either electronic or on paper) of all the readings.
4. Data acquisition (DAQ) system warm-up for at least 30 minutes.
5. Real time or by file upload to the dedicated FTP directory by the end of each series or day for comparison with WSG

7.8.2 Computation of direct solar irradiance

The series of direct irradiance S_m is submitted daily during calibration for direct comparison with the WSG. The calculation of IPC-xi and general operation of AHF radiometers is by Primary Absolute Cavity Radiometer (PACRAD) mode the data reduction and equation used are as described by Lysko [57] below.

The instrument has power (P_s) assigned to the solar irradiance which is effective in heating the front cavity during exposure to the Sun and the electrical power (P_e). The Power and solar irradiance relation is given by the equation:

$$P_s = S_m \alpha_c A \gamma \tag{7.4}$$

where α_c is the absorptivity ; A is the area of the precision aperture; γ is the stray light factor for the view tube and S_m is the solar irradiance. The Electrical power is calculated from the measured voltage and current V_1 and I_1 and the equation is:

$$P_e = I_1(V_1 - V_c) \quad 7.5$$

where $V_c = I_1R_c$ is the resistance drop with R_c being the lead correction resistance between the four wire connection points and the cavity heater .

The thermopile output signals are proportional the power dissipated in the cavity, i.e.

$$E_s = K_s P_s \quad 7.6$$

$$E_e = K_e P_e \quad 7.7$$

where K_s and K_e the proportionality constants that are not equal due to the existence of non-equivalence L between the radiant and the electrical heating such that

$$K_e = LK_s \quad 7.8$$

Combining Equations 7.5 to 7.8, the solar irradiance is obtained using the following equation:

$$S_m = \left(\frac{E_s}{E_e}\right)\left(\frac{P_e L}{\alpha_c A \gamma}\right) \quad 7.9$$

If the instrument's constants are combined to a single correction factor C_f, then Equation 7.9 can now be written as

$$S_m = \left(\frac{E_s}{E_e}\right)[C_f I_1(V_1 - I_1R_c)] \quad 7.10$$

where $C_f = \frac{L}{\alpha_c A \gamma}$

When solar irradiance is stable over the measuring period, thermopile outputs are approximately equal during electrical calibration such that solar irradiance S_m reduces to

$$S_m = [C_f I_1(V_1 - I_1R_c)] \quad 7.11$$

Equation 7.11 assumes that an equilibrium temperature has been achieved before measurement period and that the radiative loss from the front cavity to the surroundings has been the same between measurements and calibration.

7.8.3 Traceability to the World Radiometric Reference

The absolute cavity NIP, AHF31117, has participated in the 11th International Pyrheliometer Comparison (IPC XI) in October 2010. The AHF31117 therefore has direct traceability to the WRR. The World Meterological Organisation (WMO) will publish the results from the IPC XI within 2011. As an indication of the performance of the AHF31117, a set of its WRR factors from the IPC XI is given in Figure 7.1. The final WMO report will show a mean correction factor to the WRR by using at least four of the World Standard Group of instruments.

For the purposes of this report, the AHF31117 correction factor is set to unity given the close to unity mean in Figure 7.1.

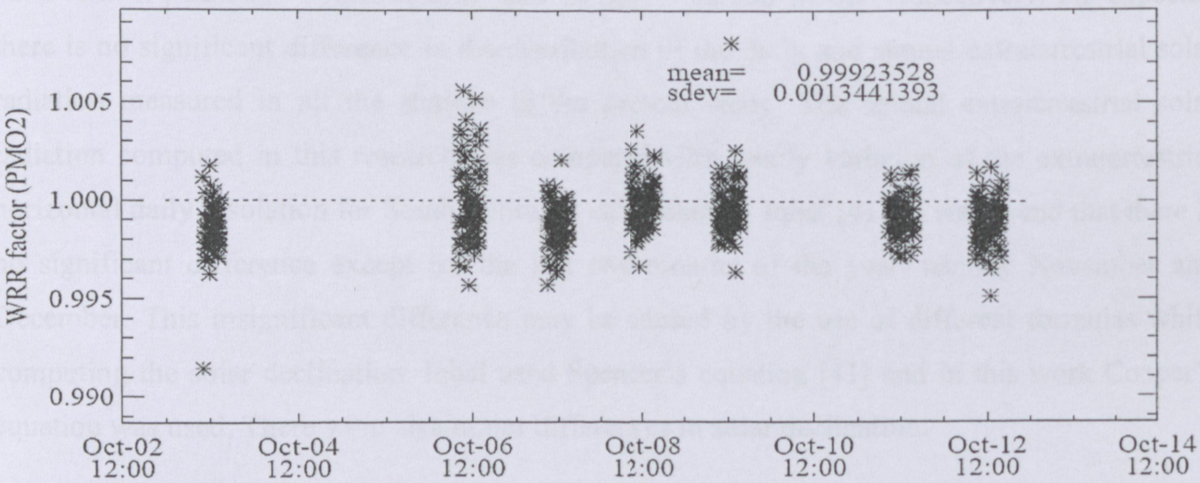

Figure 7.1: Preliminary results of AHF31117 to the World Radiometric Reference

As stated in section 7.5, a series of measurements was recorded daily so as to compare direct solar radiation in W/m^2 of the calibrated instrument AHF 31117 with WSG reference pryheliometers.

CHAPTER 8

SUMMARY AND CONCLUSIONS

8.1 SUMMARY

This study was geared towards the collection and analysis of the solar radiation data and hence to the computation of H (global solar radiation) and H_o (extraterrestrial solar radiation). The daily and monthly average values obtained were used to compute the values of regression coefficients for the North-Eastern region of the Limpopo province, i.e. Vhembe Region. The method of determining the regression coefficients was described in Chapter 4.

The results in Tables 5.6 – 5.10 indicate that the daily extraterrestrial radiation on the horizontal surface in Thohoyandou Mutale, Malamulele Mhinga, Makhado Rabali, Makhado Mulima and Makhado Alldays are in the range of 22.499 – 42.770 MJ/m^2, 22.465 – 42.783 MJ/m^2, 22.425 – 42.797MJ/m^2, 22.160 – 42.892MJ/m^2 and 22.527 – 42.760 MJ/m^2 respectively. As expected there is no significant difference in the distribution of the daily and annual extraterrestrial solar radiation measured in all the stations in the present study. The annual extraterrestrial solar radiation computed in this research was compared with yearly variation of the extraterrestrial horizontal daily insolation for South Latitudes calculated by Iqbal [41]. It was found that there is no significant difference except for the last two months of the year, namely November and December. This insignificant difference may be caused by the use of different formulas while computing the solar declination. Iqbal used Spencer's equation [41] and in this work Cooper's equation was used. There were also minor differences in solar declination.

According to the statistical test results, it can be seen that the regressions equation of the selected stations in this study gave reasonably good results. Tables 6.1 – 6.4 show the values of the Angstrom model parameters, a and b. It is observed from these tables that the values vary throughout the year. In the development of the models, the values of the coefficient a varies from 0.104 to 0.386 while those for b vary from 0.284 to 0.511. The overall mean and deviation of the five values of a, b and $a + b$ were found as 0.222 ± 0.042, 0.445 ± 0.038 and 0.670 ± 0.025

respectively. Analysis does not show any significant seasonal variation. The correlation of the stations in study gave averages of 91.8% (Malmulele Mhinga), 85.8% (Makhado Alldays), 91,7% (Thohoyandou Mutale), 91,9% (Makhado Rabali) and 91.8% (Mulima).

In order to check the variation of the regression coefficients in this study, graphs of *a* versus months of the year and that of *b* versus months of the year were drawn. They are given in Figures 6.8 and 6.9. The variation of *a* and *b* are similar in Thohoyandou Mutale and Malamulele Mhinga while for Makhado Alldays the trend was not like in the other two stations.

Computation of Angstrom-Prescott linear regressions coefficients is found extensively in literatures. The regression coefficients determined in this study are consistent with the values reported in Toledo [66] where $a = 0.2170$ and $b = 0.5453$, in Comilla [67] where $a = 0.2315$ and $b = 0.5473$, Rwanda [68] and Lesotho [69], $a = 0.266$ and $b = 0.512$, Bulawayo [63], $a = 0.304$ and $b = 0.440$. However, in general Periera has recommended the values of *a* and *b* to be 0.250 and 0.50 respectively [70].

Estimated monthly average daily global solar radiation on horizontal surface was calculated using Malamulele Mhinga Angstrom's regression coefficients. The corresponding measured value obtained from ARC was compared with the calculated values and discussed in section 5.8. The calculated and measured values of the monthly mean daily global solar irradiation intensity were analysed using statistical tests per month. The accuracy of the estimated and measured values of the horizontal global solar radiation was tested by calculating MBE, RMSE and *t*-statistic. Linear regression graphs were drawn with *H*-measured versus *H*-calculated and it is noticed that there is good correlation since *CC* is greater than 90.0% for each station. The statistical values as well as *H*-calculated and *H*- measured are tabulated in Tables 6.7 – 6.10. The values of *t*-calculated are all less than *t*-critical; this shows that there is statistical significance between *H*-calculated and *H*- measured.

Furthermore horizontal global solar radiation data obtained from ARC is analysed graphically. The ratio of monthly horizontal global solar radiation for the ARC stations are calculated and averaged. The average and its 10% were then summed up so that a graph in Figure 5.7 could be drawn. It has been observed that the distance between two stations do not give any significance although the distances are arranged in an increasing order. No normal distribution curve could be fitted. This gives one an idea that ground measurements of global solar radiation are more important than interpolation of data. The stations are within the probability of 0.8 to 1.0 as observed from Figure 5.8. This gives one a prediction that the history of calibration of the radiometer in each station can be checked and if there is a need for calibration of the instruments, this must be done with immediate effect. Monitoring of the equipment regularly helps to reduce unnecessary errors.

Angstrom linear regression coefficients for the Vhembe Region can now be taken as $a = 0.262$ and $b = 0.483$. Thus the specific Angstrom's equation [4.1] that can be used generally over the Vhembe Region may be given as:

$$\frac{\bar{H}}{\bar{H}_0} = 0.262 + 0.483\,\frac{\bar{N}_0}{\bar{N}} \qquad 8.1$$

8.2 CONCLUSIONS

Regression coefficients for the Vhembe Region were computed using a linear regression method, whereby plots of the ratio of monthly mean daily global solar radiation and extraterrestrial solar radiation on a horizontal surface and relative sunshine hours were drawn. These values are expressed in Equation 8.1. More accurate can be obtained if we can get the recording of solar parameters from regularly calibrated instruments as well as other models such as the Angstrom quadratic model, the third degree model and the exponential model. Due to the limited scope of this study, the other models like quadratic model, the third degree model and the exponential model were not considered.

The values obtained from the present study can be taken as a first step for future investigations. Also, the regression coefficients we have obtained are for the Vhembe Region. Hence there is a wide scope to extend the study to outer regions of South Africa in order to obtain the values of the regression coefficients for the entire country. It should be borne in mind that South Africa is a country with abundant solar radiation and studies to harness this freely available energy is crucial to tackle the energy crisis in the country, particularly in rural areas.

8.3 REFERENCES

1. UNDP, 2001: Energy for Poverty Reduction: The concept of the multi-functional platform (MFP) as a regional project. www.undp.gov.org.
2. D Elliot, 1997. Energy, Society and Environment: technology for sustainable future, Routledge, London.
3. V Sankaran, 2002. Renewable energy, Chapter in Green Chemistry in Africa, Interuniversity Consortium "Chemistry for the environment", Viale della, Italy. ISBN : 8888214070
4. R A Hinrichs, 1992. Energy. Renewable Energy Series. Pergamon Press. Oxford
5. H.Cohen,2003:From Coreto Corona.www.fusedweb.pppl.gov/CPEP/chartpages/5.pasmas/sunlayers .html.
6. J May, 2000: Growth Development, Poverty and Inequality; in A Clark and S Drimie, 2002. Energy Sustainability for South Africa's poor: Weigh up the Alternatives. Human Science Research Council (HSRC) publishers. Cape Town.
7. B Cousin. 2001: Not Rural Development but Agrarian reform; in Clark, A and Drimie S. 2002. Energy Substitution for South Africa's Poor: Weighing the Alternatives. HSRC Publishers. Cape Town.
8. J May, I Woolard and S Klasen, 2002. The Nature and measurement of poverty and inequality, in Clark, A and Drimie S. Energy Sustainability for South Africa: Weighing the Alternative. HSRC publishers. Cape Town.
9. M Aliber, 2002. Poverty-Eradication and Sustainable Development; in A Clark and S Drimie. Energy Sustainability for South Africa. Weighing the Alternative. HSRC Publishers. Cape Town.
10. J May and A Vaughan, 1999. Mistaken Identity: Markets and the Strategy for Poverty Alleviation in South Africa; in A Clark and S Drimie, S, 2002. Sustainability for South Africa: Weighing the Alternative. HSRC Publishers. Cape Town.

11. M Orkin,. *et.al,* 1999. Census 96: Key finding for Development Planning indicator for South Africa; in A Clark and S Drimie, 2002. Energy Sustainability for South Africa: Weighing the Alternative HSRC Publishers. South Africa.
12. L Bin, L Wang, B Kang, P Wang and Y Qiu, 2006. Review of recent progress in solid-state dye-sensitized solar cells, Solar Energy Materials & Solar Cells, Vol. 90: 549-573.
13. A Clark and S Drimie, 2002. Energy Sustainability for South African's Poor, Integrated Rural and Regional Development Research Programme, Occasional Paper 2, HRC publisher.
14. F C Treble and A A M Sayingh., 1991. Generating electricity from the sun, Pergamon press, Oxford.
15. J C Mc Veigh, 1983. Sun power, An introduction to the application of solar energy, Pergamon Press, Oxford.
16. H P Garg and J Prakash, 1992. Solar Energy Fundamentals and Applications, Tata McGraw-Hill Publishing Company Limited, New Delhi.
17. P Valizedh, Amorphous Silicon Solar Cells: Efficiency and Stability Issues, Electrical Engineering and Computer Science Department, University of Michigan 1301 Beal Ave, Ann Arbor, MI 48109, http://www.personal.engin.umich.edu/~pvalizad/amorphours.pdf
18. A Jacobson, D R Duke and D M Kammen, 2000. Amorphous Silicon PV Panels are they a good value for money? Htt://ist-socrates.berkeley.edu/`kamen/Solarnet.pdf
19. Y Ichikawa, M Tanda and H Sakai, 1996. Analyses of Field test data for Amorphous Silicon PV array, WREC, pp 318-389.
20. N Larr, L Lewis, J Spivack, S Gasaway and D Eric, 2006. Williams, John Y. Gui, Venkatesan Manivannan, Oltea P. Siclovan, A novel UV-mediated low-temperature sintering of TiO_2 for dye-sensitized solar cells, Solar Energy Materials & Solar Cells Vol. 90: 1041-1051.
21. L Schmidt-Mende and M Gratzel, 2006. TiO_2 pore-filling and its effect on the efficiency of solid-state dye-sensitized solar cells, Thin Solid Films Vol. 500, p 296-301. Thomas Stergiopoulos, Marie-Claude Bernard, Anne Hugot-Le Goff, Polycarpos Falaras, 2004. Resonance micro-Raman spectrophotoelectrochemistry on nanocrystalline TiO_2 thin film electrodes sensitized by Ru(II) complexes, Coordination Chemistry Reviews 248: 1407-1420.

22. T Stergiopoulos, e.t.c.,2004. Resonance micro-Raman spectrophotoelectrochemistry on nanocrystalline TiO_2 thin film electrodes sentisized by Ru(II) complexes, Coordination Chemistry Reviews 248: 1407-1420.
23. D Gutierrez-Tauste, I Zumeta, E Vigil, M A Hernandez-Fenollosa, X Domenech and J A. Ayllon, 2005. New low-temperature preparation method of TiO_2 porous photoelectrode for dye–sensitized solar cells using UV irradiation, Journal of Photochemistry and Photobiology, A: Chemistry, Vol.175: 165-171.
24. M Rusop, T Shirata, P M Sirimanne, T Soga, T Jimbo and M Umeno, 2005. Study on the properties and charge generation in dye-sensitised n-TiO_2/dye/ p-CuI solid state photovoltaic solar cells, Applied Surface Science.
25. Titanium and Titanium Alloys http://www.key-to- metals.com/printArticle.asp? ID=20
26. http://www.rti-intl.com/tag/intro.html
27. www.facts-about-solar-energy.com/solar-energy-advantages-disadvantages.html
28. R.G. Allen, L.S.Pereira, D.Raes and M. Smith, 1998. Crop Evapotranspiration. Guidelines for computing crop water requirement. FAO Irrigation and drainage paper 56. Rome.
29. http://rredc.nrel.gov/solar/old_data/nsrdb/redbook/atlas/
30. http://www.solarfeedintariff.net/germanymap.html
31. http://www.bom.gov.au/sat/solrad.shtml
32. H P Garg and J Prakash, 2002. Solar Energy fundamentals and applications. Tata McGraw-Hill Publishing Company Limited, New Delhi.
33. G D Rai, 2009. Solar Energy Utilization. Khanna Publishers
34. B Brooke, R E Train, 1992. Introduction of Solar energy. 1st Edition, Chelsea House Publishers New York Philadelphia.
35. J A Duffie and W A Beckman, 1991. Solar engineering of thermal processes.
36. H P Garg, 1982. Treatise on solar Energy. John Wiley.
37. C Frohlich and R W Brusa, 1981. Solar radiation and its variation in time. Sol Physics, Vol. 74: 209-215.
38. F C Treble, 1991. Generating Electricity from the sun. Renewable Energy, Vol. 2: 59-61.
39. S Wieder, 1982. Introduction to solar energy for scientists and engineers.
40. G N Tiwari, 2002. Solar Energy Fundamentals, Design, Modelling and Applications. ISBN 81-7319-450-5

41. M Iqbal, 1983. Introduction to solar radiation. New York: Academic Press.

42. B Y H Liu and R C Jordan, 1960. The interrelationship and characteristic distribution of direct, diffuse and total solar radiation. Solar Energy, Vol. 4 (1).

43. http://www.southafrica.info/travel/advice/climate.htm

44. http://en.wikipedia.org/wiki/Pyrheliometer

45. User Manual for DL2e Data Logger Hardware Reference, 2000 Delta-T Devices Ltd., Cambridge UK.

46. A. Angstrom, 1924. Solar and terrestrial radiation. Q.J.R.Meteorol. Soc, Vol. 50: 121-125.

47. M. A Wohab, 1993. New approach to estimate Angstrom coefficients. Solar Energy, Vol. 51: 241-245.

48 B G Akinnoglu and A Ecevit, 1990. Construction of a quadratic model using modified Angstrom coefficients to estimate global solar radiation. Solar Energy, Vol. 45: 85-92

49. C Ertekin, O Yaldiz, 2000. Comparison of some existing models for estimating global solar radiation for Antalya(Turkey). Energy Conversion Mgmt, Vol. 41: 311-330.

50 D B Ampratwum, A S S Dorvlo, 1990. Estimation of solar radiation from the number of sunshine hours. Applied Energy , Vol 62: 161-167

51. M Cheggar and A Chibani, 2001. Global solar radiation estimation in Algeria. Energy Conversion Mgt, Vol. 42: 967-973.

52. R J Stone and M Iqbal, 1993. Improved statistical procedure for the evaluation of solar radiation models. *Solar Energy,* Vol. 51: 289–29. *An introduction to solar radiation*, Academic Press (1983).

53. Guide to meteorological instruments and methods of observation. WMO No.8, seventh edition, 2008.

54. International Organization for standardization 1993. Solar energy- calibration of pyrheliometers.

55. Eplab- instruction and information manual for model AHF self-calibrating Cavity Pyrheliometer and Model 409 Radiometer Control Unit, The Eppley Laboratory, Inc., October 1998.

56. J R Hicky, 2000. Program IPC HF117.BAS 09/20/2000 for single operation of AHF s/n 31117 at IPC, Eplab.

57. M D Lysko, 2006. Doctoral Thesis. Measurement and models of solar irradiance.

58. A A El-Sebaii and A A Trabea, 2005. Estimation of global solar radiation on horizontal surfaces over Egypt. J.Solids, Vol. 28 (1).

59. F Odendaal, H Suich and V Rojas, Richtersveld: The land and its people. 2008/2009

60. P I Cooper, 1969. The absorption of solar radiation in solar stills. Solar Energy, Vol. 12 (3): 333-346.

61. A Whillier, Solar radiation 5 91965n, 164-16n graphs. Solar Energy, Vol. 9 (3).

62. R.E Walpole and R H Myers, 1989. The probability and statistics for engineers and scientists. 4th Edition. New York: Macmillan.

63. I T Togrul, 1998. Comparison of statistical performance of seven sunshine-based models for Elazig, Turkey, Chemica Acta Turuca, 26, 37.

64 R J Stone, 1993. Improved statistical procedure for the evaluation of solar radiation estimation models. Solar Energy Vol. 51: 289.

65. E O Ogolo, 2010. Evaluating the performance of some predictive models for estimating global solar radiation across varying climate conditions in Nigeria. Indian Journal, Vol. 39: 121 – 131.

66. J Almor4ox and C Hontoria, 2004. Global solar radiation estimation using sunshine duration in Spain. Energy conservation and management, Vol. 45: 1529 – 1535. Elsevier.

67. A S Bhuiyan Mohammad. Computation of solr radiation and regression coefficients for Comilla. Southern University. Bangladesh.

68 B Safari and J Gasore, 2009. Estimation of global solar radiation in Rwanda using empirical models. Asian Journal of scientific research, Vol. 2 (2): 68-75.

69. K K Gopinathan, 1988. A general formula for computing the coefficients of the correlation connecting global solar radiation to sunshine duration. Solar Energy, Vol. 41(6): 499-502.

70. R G Allen, L S Pereira, D Raes and M Smith, 1988. Crop Evapotranspiration. Guidelines for computing crop water requirement. FAO Irrigation and drainage paper 56. Rome.